

CHAPTER 5

POLYMERIC MATERIALS

Take a minute to look at the room and furnishings around you. Virtually everything you will see is at least partially comprised of organic-based building blocks. From the plastics that surround electronic components to individual carpet fibers, no other type of material is as heavily **utilized** in our society as organic-based polymers. As first defined by Staudinger in 1920, a *polymer* is any material that is comprised of an extended structure of small chemical repeat units, known as *monomers*.^[1] For simplicity, the monomeric unit is almost always clearly identified within the polymer name (*i.e.*, “poly(*monomeric unit*)”, Figure 5.1). A polymer is generally comprised of more than 100 repeat units; structures with lower numbers of chemical repeat units are known as *oligomers*. Strictly speaking, all solid-state materials with an infinite structural array are classified as polymers – even inorganic structures such as metals, ceramics, and glasses. However, since we have described inorganic-based materials in previous chapters, we will focus our present discussion on polymeric materials that feature a carbon-containing backbone.

Organic-based materials are generally associated with “soft” characteristics – *i.e.*, relatively low-melting and facile plastic deformation. Though this is generally the case for popular commercial polymers such as plastics and rubbers, there are numerous other polymer classes that exhibit hardness and thermal stabilities that even rival inorganic ceramics. Polymeric materials have long been used in packaging and other consumer product applications; however, recent developments have extended the utility range to now include microelectronics, photovoltaics, self-healing materials, and drug-delivery agents that were not envisioned a short time ago. As a testament to the importance of polymers in our world, the current volume of polymers used for commercial and industrial applications already exceeds the volume of steel and aluminum combined. In our era of soaring gas prices, automobile manufacturers are also scrambling to add more plastics to their vehicles.^[2] In addition to fabrication cost savings and enhanced design flexibility relative to steel, it is estimated that every 10% of weight reduction will yield a 5% increase in fuel economy. This chapter will delve into various polymer classes, with a detailed examination of the structural influence on resultant properties.

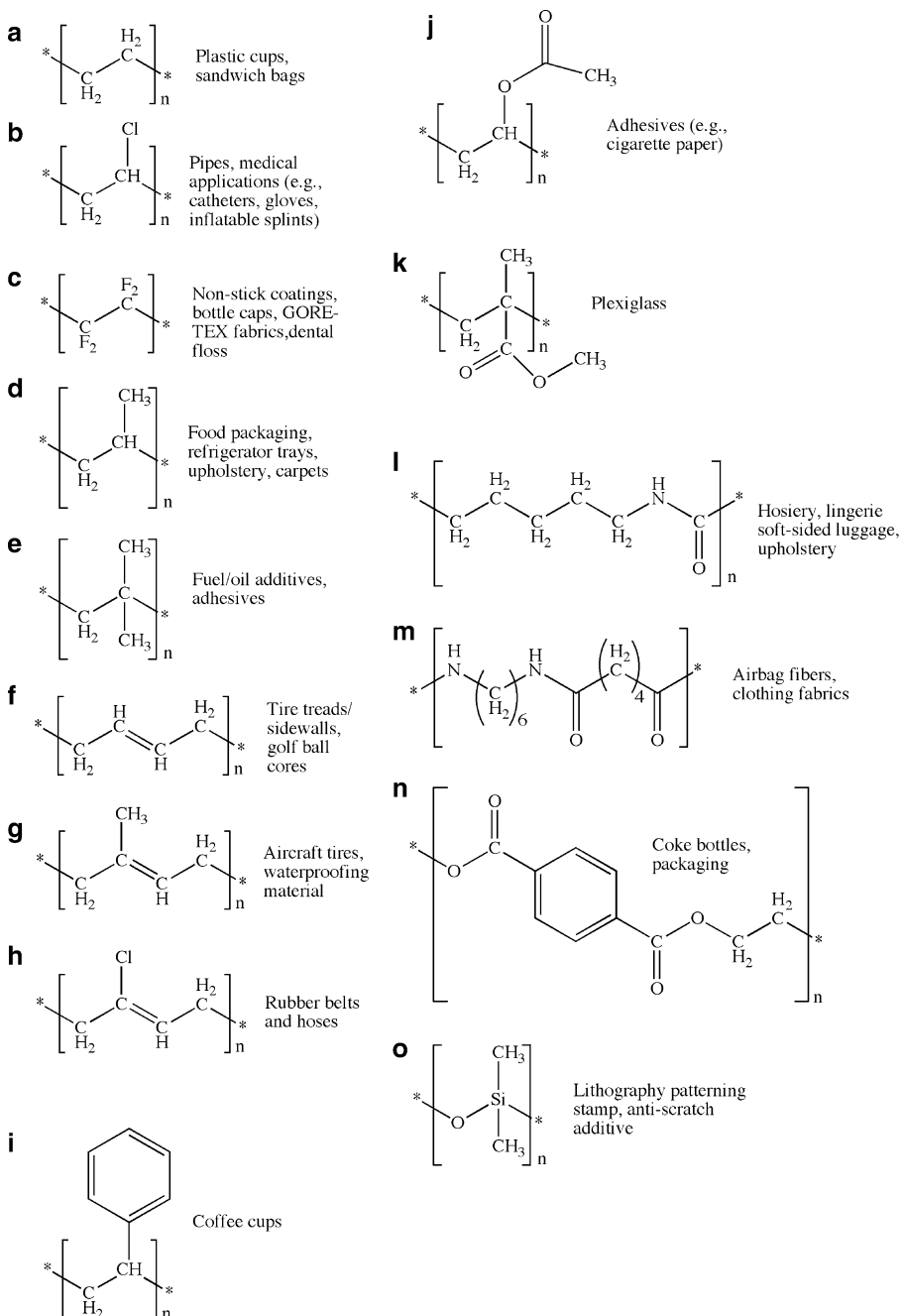


Figure 5.1. Molecular structures of the chemical repeat units for common polymers. Shown are (a) polyethylene (PE), (b) poly(vinyl chloride) (PVC), (c) polytetrafluoroethylene (PTFE), (d) polypropylene (PP), (e) polyisobutylene (PIB), (f) polybutadiene (PBD), (g) *cis*-polyisoprene (natural rubber), (h) *trans*-polychloroprene (Neoprene® rubber), (i) polystyrene (PS), (j) poly(vinyl acetate) (PVAc), (k) poly(methyl methacrylate) (PMMA), (l) polycaprolactam (polyamide – nylon 6), (m) nylon 6,6, (n) poly(ethylene teraphthalate), (o) poly(dimethyl siloxane) (PDMS).

5.1. POLYMER CLASSIFICATIONS AND NOMENCLATURE

The most fundamental classification of polymers is whether they are **synthetic** or naturally-occurring. Common synthetic polymers (Figure 5.1) are pervasive in commercial applications; for example, Table 5.1 lists some synthetic polymers used for automotive applications. In contrast, natural polymers include macromolecules such as polysaccharides (*e.g.*, starches, sugars, cellulose, gums, *etc.*), proteins (*e.g.*, enzymes), fibers (*e.g.*, wool, silk, cotton), polyisoprenes (*e.g.*, natural rubber), and nucleic acids (*e.g.*, RNA, DNA). Accordingly, these polymer classes are often referred to as **biopolymers**, of which some recent materials applications will be discussed later in this chapter.

Synthetic polymers may be classified under two general umbrellas: **thermoplastics** and **thermosets**. As their names imply, this definition is illustrative of the properties exhibited by these materials under elevated temperatures. For instance, **thermoplastics** consist of long molecules with side chains or groups that are not connected to neighboring molecules (*i.e.*, not *crosslinked*). Hence, both amorphous and crystalline thermoplastics are glasses at low temperature, and transform to a rubbery **elastomer** or flexible plastic at an elevated temperature known as the **glass-transition temperature** (T_g ; Figure 5.2). The T_g is the most important property of polymers, being analogous to the melting point of low molecular weight compounds.^[10] In contrast to thermoplastics, **thermosets** are initially liquids and become hardened by a thermally induced crosslinking process known as *curing*. Also, unlike thermoplastics, since the crosslinking process yields a stable 3D network, thermosets may not be re-melted/re-processed. Thermoset polymers are usually synthesized within a mold to yield a desired shape/part; once the polymer cures, the only way to reshape the material is through machining processes (*e.g.*, drilling, grinding). The most common type of thermosetting polymer is epoxy resin, widely used

Table 5.1. Polymers Used for Automotive Applications

Polymer	Application
Poly(ethylene), PE	Fuel tanks, windshield washer bottles
Poly(propylene), PP	Bumpers, external trim
Poly(vinyl chloride), PVC	Interior trim
Poly(acrylonitrile) (PAN) + poly(styrene) (PS) blend + Poly(butadiene) = ABS	Exterior and interior trim, wheel covers
Nylon-6,6	Intake manifolds, rocker cover/air cleaner, ^[3] hubcaps ^[4]
Polyester	Grill opening panel, ^[5] sunroof frame, passenger-side airbag doors ^[6]
Poly(methylmethacrylate), PMMA	Lenses
Polycarbonate, PC	Headlamp lenses, trim
Polyurethane, PU	Foam, bumpers
Poly(butylene terephthalate), PBT	Headlamp bezel ^[7]
Poly(vinyl butyral), PVB	Laminated safety glass ^[8]
Poly(ethylene terephthalate), PET	Windshield wiper brackets ^[9]

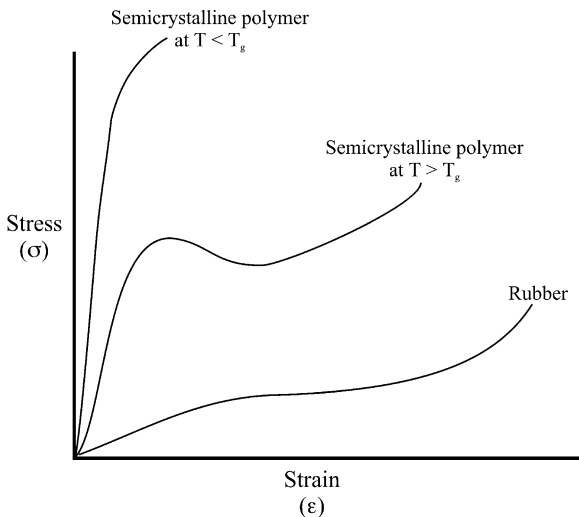


Figure 5.2. Stress *vs.* strain curves for various polymers around its glass-transition temperature. The maximum in the curve that occurs at T_g is referred to as the *yield point* (onset of plastic deformation).

for adhesives and paints/coatings, which harden through crosslinking reactions with a curing agent such as primary and secondary polyamines (*i.e.*, containing reactive $-\text{NH}_2$ groups; Figure 5.3).^[11]

Regarding the overall **structure** of polymers, there are five classes of macromolecular architectures, ranging from simple linear arrays to *megamers* – complex structures built from ordered hyperbranched (dendritic) polymers (Figure 5.4). As you might imagine, **linear** chains are best able to pack into a regular crystalline array; however, as the degree of chain branching increases, only amorphous phases are formed. Due to the pronounced length of polymer chains, it should be noted that regions of crystallinity generally form where only a portion of the polymer chains are regularly organized, while others remain disordered. This structural diversity directly affects physical properties such as tensile strength, flexibility, and opacity of the bulk polymer.

As a more general structural definition, a polymer synthesized from only one type of monomer is referred to as a *homopolymer*. In contrast, a polymer that is formed from more than one type of monomer is known as a **copolymer**. The terms terpolymer, tetrapolymer, pentapolymer, *etc.* are used to designate a polymer derived from three, four, five, *etc.* co-monomers. Although homopolymers contain only one repeating chemical unit in their structure, this distinction is not always clear. For instance, polyethylene polymers often contain short-chain branched impurities as a consequence of the polymerization process. However, since this unintentional structural deviation results from a polymerization process involving only one type of monomer, the term *homopolymer* is still most appropriate.

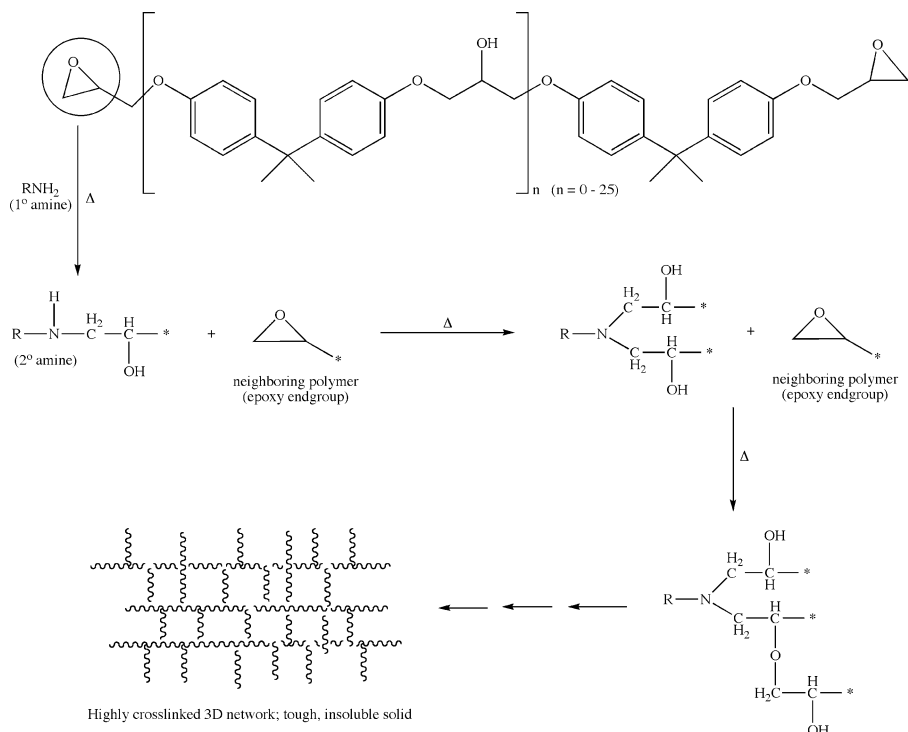


Figure 5.3. Illustration of a hardening mechanism responsible for epoxy resin curing.

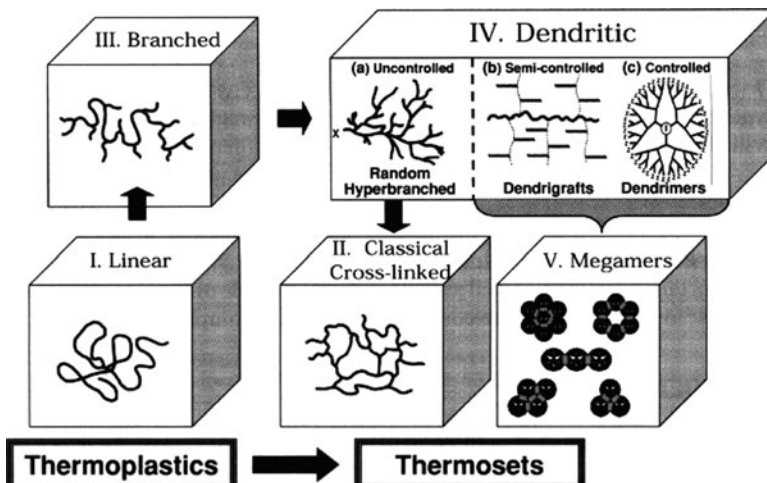


Figure 5.4. The five major structural classes of polymers. Reproduced with permission from Frechet, J. M. J.; Tomalia, D. A. *Dendritic Polymers*, Wiley: New York, 2001.

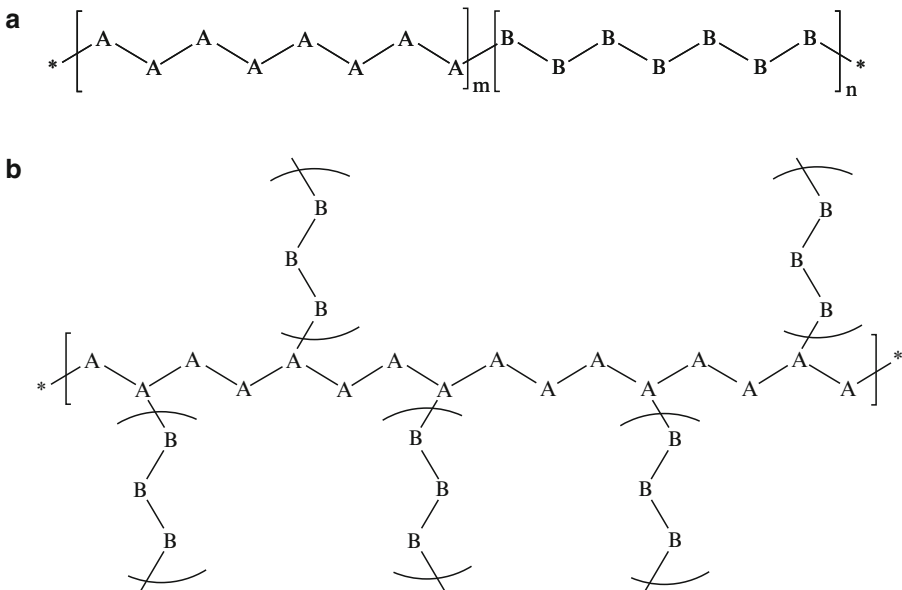


Figure 5.5. Illustration of (a) block copolymers and (b) graft copolymers.

There are four types of copolymers: *random*, *alternating*, *block*, and *graft*, each exhibiting varied physical properties. In contrast to block copolymers, which contain long adjacent sequences of A and B monomers, the chain of an alternating copolymer is comprised of the sequence $(-\text{A}-\text{B}-)_n$. A random copolymer is formed from the random linkages of A and B monomers along the chain (e.g., $-\text{AAABAABBBAAB}-$). Graft copolymers may be considered as another type of block copolymer, which feature one long chain of one monomer with offshoots of a second monomer emanating along its length (Figure 5.5). The structure, length, and placement of the copolymer units directly affect physical **properties** such as crystallinity, density, strength, brittleness, melting point, and electrical conductivity (for conductive polymers).

Each carbon within the polymer chain may be considered as a chiral center. As a result, a parameter referred to as the *tacticity* may be defined that describes the stereoregularity of adjacent carbon centers (Figure 5.6). A polymer that contains substituents on the same side of the polymer chain is referred to as *isotactic*, and often exhibits some degree of crystallinity. In contrast, if adjacent substituents are arranged on alternating sides of the polymer chain, a *syndiotactic* polymer is formed. Unless a polymerization scheme uses a catalyst that confines the nucleation/propagation site, the substituents will be randomly organized – either disordered throughout the entire polymer chain (*atactic*) or along every other repeat unit (*hemiisotactic*). Due to the structural randomness, atactic polymers are almost always entirely amorphous. Not surprisingly, the tacticity of a polymer significantly

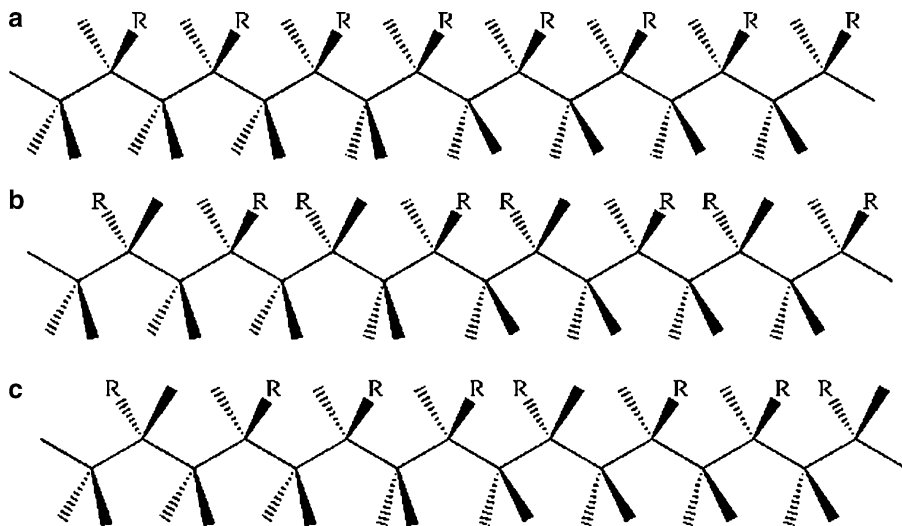


Figure 5.6. The tacticity of polymer chains. Illustrated are (a) isotactic, (b) syndiotactic, and (c) atactic polymers.

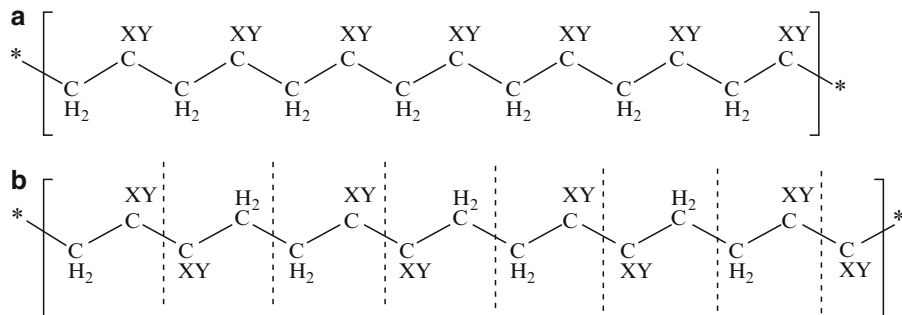


Figure 5.7. Illustration of sequence isomerization exhibited by polymer chains. Shown are (a) head-to-tail and (b) head-to-head/tail-to-tail sequencing.

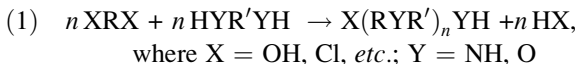
affects its mechanical properties. For instance, isotactic polypropylene has an elastic modulus and hardness of 1.09 GPa and 125 MPa, whereas atactic polypropylene has values of 0.15 GPa and 1.4 MPa, respectively.

Another form of isomerism that exists for polymers is the arrangement of adjacent repeat units. For an individual monomeric unit, the subsequent monomer may add in a head-to-tail or head-to-head/tail-to-tail fashion (Figure 5.7). The sequence is often determined by the substituents; for instance, sterically bulky groups (*e.g.*, phenyl) dictate a head-to-tail array for polystyrene. On the other hand, polymers that feature halide substituents (*e.g.*, poly(vinyl fluoride)) contain significant numbers of head-to-head/tail-to-tail sequences.

Thus far, we have considered the organization and composition of the main polymer chain, held together through covalent bonding of neighboring carbons. However, the physical properties of a particular polymer are more strongly affected by the intermolecular forces that exist between individual polymer chains. For instance, crosslinking through covalent bond formation is responsible for vulcanization of rubber (Figure 5.8a). In contrast, the greater flexibility of nylon is due to the relatively weaker interchain hydrogen bonding interactions (Figure 5.8b). Other types of inter- or intrachain interactions include dipole-dipole and van der Waals (induced dipole) forces (Figure 5.8c, d).

5.2. POLYMERIZATION MECHANISMS

Polymers may be synthesized by two general mechanisms: *step-growth* (condensation) and *chain* (addition) polymerizations. Step-growth is the least limiting designation, relative to condensation, since the former is also appropriate for polymerizations that do not eliminate water during the reaction (Eq. 1). Table 5.2 lists the important distinctions between addition and step-growth polymerization schemes. As its name implies, step-growth involves the reactions of functionalized monomers to build up polymer chains through dimers, trimers, etc., *en route* toward oligomers, and polymers. The acid/base-catalyzed synthesis of SiO₂ networks by sol-gel (Chapter 2) is a widely used application of step-growth polymerization. In contrast, addition polymerization involves the activation/addition of unsaturated monomers, yielding a much higher MW polymer in a relatively short period of time. Since step-growth proceeds through the reaction of neighboring complementary functional groups, small molecular byproducts such as HX, H₂O, etc. are generated; addition reactions do not yield such elimination products.



The molecular weight of a polymer may be generally described as the molecular weight of the monomer(s) multiplied by the *degree of polymerization* (DoP, Eq. 2) or the number of repeat units. Whereas oligomers have DoP values between 2 and 10 (e.g., polysaccharides, polypeptides), most commercial plastics are high-mass polymers with DoP values >1,000. If all of the individual polymer chains were equivalent in length and composition, this would yield an exact molecular weight value analogous to molecular or ionic solids. However, due to the variance in polymer chain lengths, the best we can attain is to assign a molecular weight distribution, characterized by using an empirical technique known as *gel-permeation chromatography* (GPC).^[12] A broad peak indicates that a greater variance in molecular weight is present, which is not desirable for most applications.

$$(2) \quad \text{DoP} = \frac{\text{M}_r}{\text{M}_R},$$

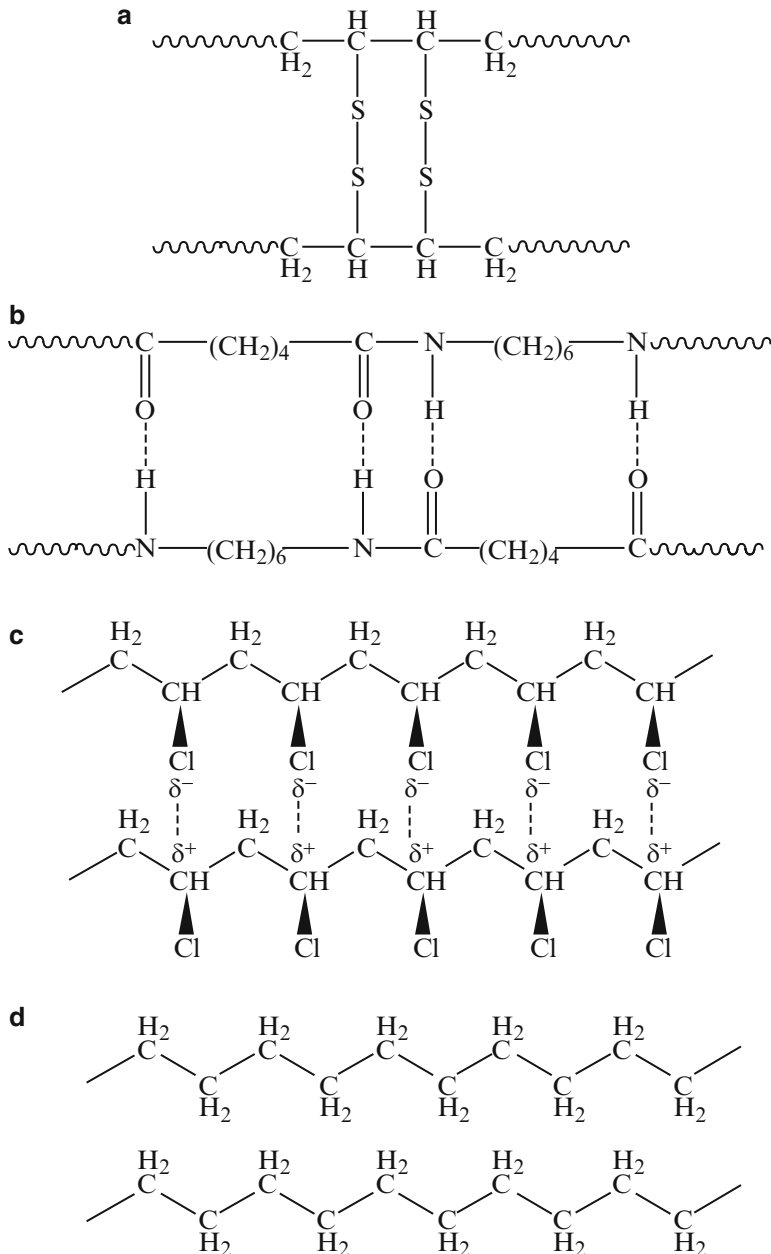


Figure 5.8. The intermolecular forces involved in adjacent polymer chains. Shown are (a) covalent crosslinking (vulcanized rubber), (b) hydrogen bonding (nylon 6,6), (c) dipole-dipole (PVC), and (d) van der Waal interactions (polyethylene).

Table 5.2. Features of Addition and Condensation Polymerization Schemes

Addition (chain growth)	Condensation (step-growth)
1. Unsaturated monomers	Monomers contain ≥ 2 functional groups
2. No products are eliminated	Elimination of H_2O , HCl , etc.
3. Only monomer and polymer are present during polymerization	Monomers and polymer are accompanied by dimers, trimers, and oligomeric species
4. Only monomers add to the growing polymer	All intermediate species are reactive, and contribute to the growing polymer
5. Mechanism involves reacting with double bond by active species like free radicals or ions	Involves simple elimination reaction between monomer functional groups
6. Rapidly yields a high MW polymer; crosslinking is achieved through use of monomers with two double bonds (e.g., divinylbenzene)	Molecular weight is typically lower than addition polymerization. The presence of small amounts of multifunctional monomers results in extensive crosslinking (gels)
7. Examples: polyolefins, polydienes, vinyl polymers, acrylic polymers	Examples: polyesters, polyamides, polycarbonates ^a , epoxies

^a(Fun fact) a polycarbonate layer is used between glass panels to absorb the energy of a bullet blast – “bullet-proof” glass.

where M_r = relative molar mass of the polymer, and M_R = relative molar mass of the monomer

The range of the molecular weight distribution is referred to as the *Polydispersity*, given by the polydispersity index (PDI). This value is calculated from the weight average molecular weight, \bar{M}_w , divided by the number average molecular weight, \bar{M}_n (Eq. 3). Whereas the number average molecular weight is experimentally determined by colligative properties (e.g., elevation of boiling point, depression of freezing point, osmotic pressure), weight average molecular weight is determined by light scattering, neutron scattering, or ultracentrifugation. Matrix-assisted laser desorption/ionization mass spectrometry (MALDI-MS) may also be used to determine number/weight average molecular weights.

The PDI for man-made polymers will always be > 1.0 ; however, as the polymer chains approach a uniform length, the PDI will approach unity. The type of polymerization used, as well as experimental conditions (e.g., temperature and nature of the catalyst), are paramount in generating a polymer with a narrow polydispersity. For instance, typical addition polymerization, results in PDI values of *ca.* 10–20, compared to two to three for step-growth polymerization. However, using precise temperature control to limit termination mechanisms, PDIs of < 1.5 may be generated for both techniques. Not surprisingly, nature is far ahead of human ingenuity – biopolymers (e.g., polypeptides) have PDI values very close or equal to one, indicating that only one length of polymer is present – directly responsible for the high specificity and efficiency of complex living systems.

$$(3) \quad PDI = \frac{\bar{M}_w}{\bar{M}_n},$$

where

$$\overline{M}_w = \frac{\sum_i N_i M_i^2}{\sum_i N_i M_i} \text{ and } \overline{M}_n = \frac{\sum_i N_i M_i}{\sum_i N_i}$$

(N_i is the number of molecules with molecular weight, M_i)

5.2.1. Addition Polymerization

Addition polymerization involves three steps: initiation, propagation, and termination. During initiation, either radicals (Figure 5.9) or ionic species are generated from the controlled decomposition of an initiator molecule. The reactive intermediates are then sequentially added to the C=C bonds of monomers to propagate the growing

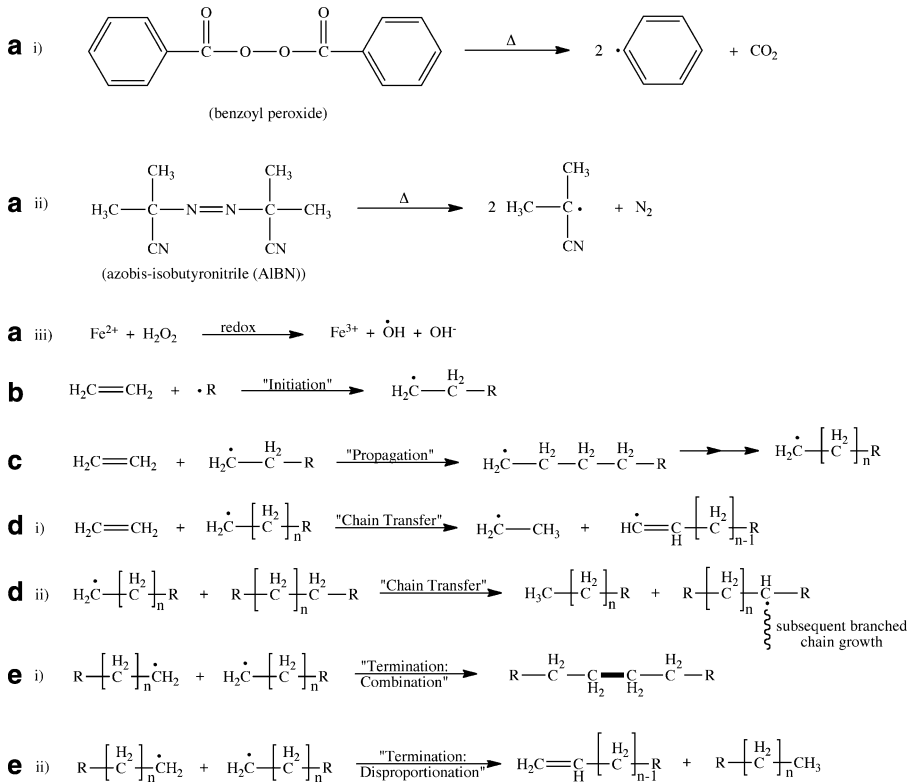


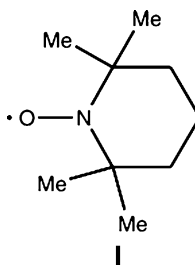
Figure 5.9. Reactions involved in free-radical addition polymerization. Shown are (a) (i)–(iii) generation of free radicals from a variety of initiators, (b) initiation of polymer chain growth through the combination of a free radical and unsaturated monomer, (c) propagation of the polymer chain through the combination of growing radical chains, (d) chain-transfer of free radicals between the primary and neighboring chains, and (e) termination of the polymer growth through either combination (i) or disproportionation (ii) routes.

polymer chain. Free-radical polymerization is the most common method currently used to synthesize polymers from vinyl-based monomers.

Due to the high reactivity of the radical fragments, facile *chain-transfer* may occur (Figure 5.9d, i, ii), whereby the radical end of the growing chain abstracts an atom from another molecule/chain. The second molecule may be monomer, solvent, initiator, or other polymers that exist in solution. As a result, the growth of the primary chain is terminated, and a new radical capable of propagation/polymerization is generated. Oftentimes, chain-transfer results in hydrogen abstraction from the second molecule, which causes branching (Figure 5.9d, ii). The second molecule may be totally unreactive or moderately reactive with the monomer (*i.e.*, relative to normal propagating radicals). Hence, a deliberate addition of these molecules may be used to inhibit or slow the polymerization process.

Although radical polymerization is highly susceptible to chain-transfer, it is possible to suppress these side reactions – resulting in *living polymerization*.^[13] By definition, a living process will result in a linear increase in the polymer molecular weight with monomer consumption. In order to gain strict control over the polymerization process, a number of **approaches** have recently been designed:

- (i) *Nitroxide-Mediated Polymerization* (NMP). A stable free radical (*e.g.*, I, 2,2,6,6-tetramethyl-1-piperidinyloxy (TEMPO)) is added to the solution, acting as a radical scavenger. The TEMPO radical is exceedingly stable due to the nearby methyl groups that supply electron density and help stabilize the unpaired electron that is delocalized over the N—O bond. The coupling of TEMPO with the polymeric radical is reversible, which allows one to control the molecular weight and polydispersity of the resultant polymer by varying the monomer:TEMPO ratio.



- (ii) *Atom-Transfer Radical Polymerization* (ATRP). A halogenated organic and metal complex^[14] are added to the solution, which generate a radical initiator (Figure 5.10). As the monomer reacts with the initiator, the halide moiety preferentially terminates the chain. This process is considered redox-controlled polymer growth, since the polymer chain may grow only as additional atom-transfer reagents are added to the solution.
- (iii) *Reversible Addition Fragmentation Chain-Transfer Polymerization* (RAFT).^[15] This process features the addition of a thiocarbonylthio-based RAFT agent (*e.g.*, dithioesters, thiocarbamates, xanthates). The reaction of radicals with

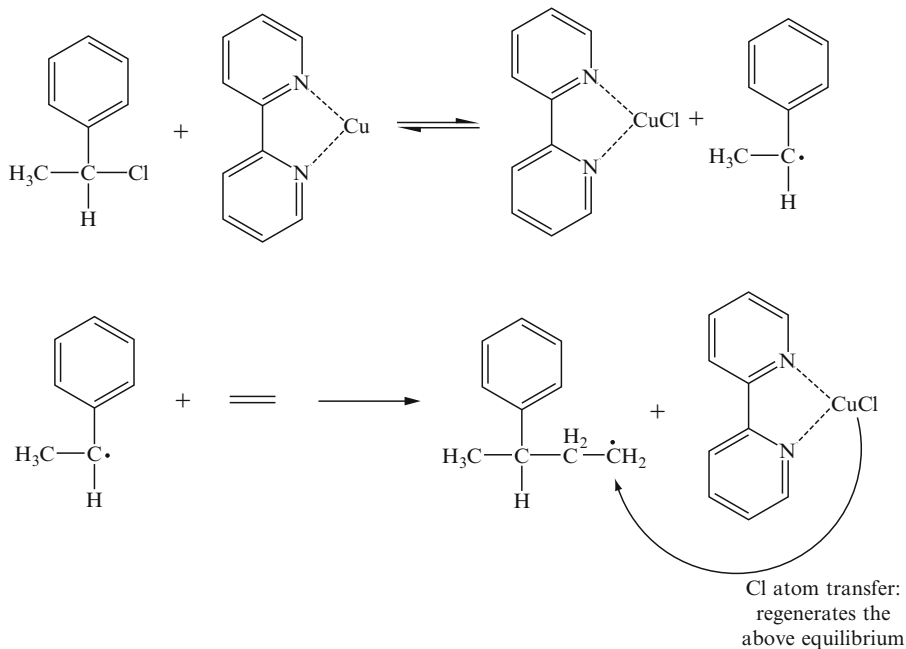


Figure 5.10. Mechanism of atom-transfer radical living polymerization. In this process, addition of atom-transfer agents results in initiating radicals that react with monomers. Rather than terminating polymer growth, halogenated end units are formed that are capable of propagating chain growth when additional monomer is added.

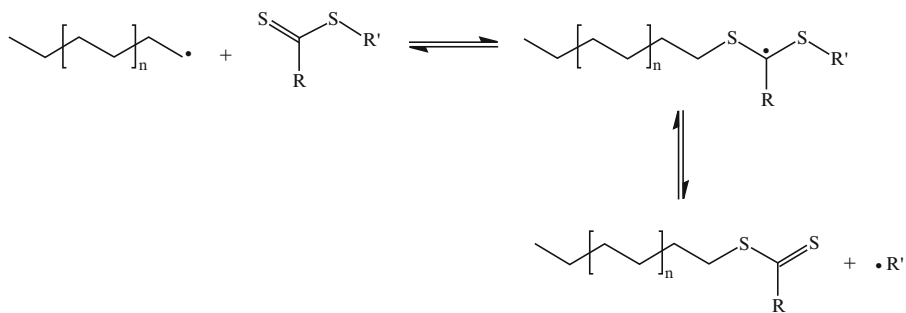


Figure 5.11. Illustration of the general reaction scheme responsible for RAFT polymerization.

the C=S bond forms a stabilized radical intermediate. In an ideal system, these intermediates do not undergo termination reactions, but rather reintroduce a radical capable of re-initiation or propagation with monomer, while they themselves reform their C=S bond (Figure 5.11). The cycle of addition to the C=S bond, followed by fragmentation of a radical, continues until all

monomer is consumed. Termination is limited in this system by the low concentration of active radicals.

A more recent development in living free-radical polymerization is the use of *iniferter* – a single molecule that is capable of *initiating*, *transferring*, and *terminating* the radical polymerization process. Figure 5.12 illustrates the polymerization scheme exhibited by the most common type of iniferter. In these systems, UV absorption generates a carbon radical and sulfur-based dithiocarbamyl radical. Whereas the carbon radicals are extremely reactive toward the monomer, the dithiocarbamyl radical is not sufficiently reactive toward propagation. Termination in iniferter systems may take place through either carbon–carbon or carbon–dithiocarbamyl bimolecular radical termination. The former route results in a dead unreactive polymer, whereas the latter route forms another iniferter species that may reinitiate upon UV light irradiation.

As previously mentioned, addition polymerization may also be *initiated* by cations/anions. In these ionic systems, propagation occurs through the combination of additional monomer with carbocation/carbanion intermediate species. In cationic polymerization, a Lewis acid (*e.g.*, AlCl₃, BF₃, *etc.*) may be used in isolation, or accompanied by a protic Lewis base (*e.g.*, NH₃, H₂O), which renders the **proton** as the actual initiator (Figure 5.13). For cationic polymerization, termination may occur through proton, halide, or hydroxyl abstraction from the counteranion. For instance, AlCl₃ serves as the initiator for the cationic polymerization of isobutylene ((CH₃)₂=CH₂) to yield butyl rubber – used for the inner tube linings of automobile tires. Figure 5.14 illustrates an example of using BCl₃/2-chloroisopropyl benzene as an *inifer* for the *living* cationic polymerization of isobutylene. There are also reports of alkylaluminum chlorides being used for living cationic polymerization,^[16] as well as other base-assisted routes.^[17]

Another example of cationic addition polymerization is the ring-opening polymerization of hexachlorocyclotriphosphazene to yield polydichlorophosphazene (Figure 5.15). The polyphosphazenes represent one of the largest classes of polymers that are used for applications such as fuel cell membranes, flame-retardants, lubricants, and biomedical-related (*e.g.*, microencapsulating agents, biodegradable materials, tissue engineering scaffolds, biocompatible coatings, *etc.*). A living polymerization route toward polyphosphazenes is also possible using N-(trimethylsilyl)-trichlorophosphoranimine in the presence of trace amounts of PCl₅ (Figure 5.16); the PDI and molecular weight may be controlled by varying the ratio of monomer: initiator.

In contrast to cationic routes, anionic addition polymerizations are initiated by using organolithium compounds (*e.g.*, butyllithium) or alkali metal amides (*e.g.*, NaNH₂, Figure 5.17), amines, alkoxides, hydroxides, or phosphines as initiators. Many anionic polymerizations occur via a living process; that is, termination does not occur spontaneously and is controlled through the addition of a Lewis base. However, termination may also occur through unintentional **quenching** due to trace impurities such as oxygen, CO₂, moisture. Polymers that are synthesized via this route include polydiene synthetic rubbers, polymethacrylates, and polystyrene.

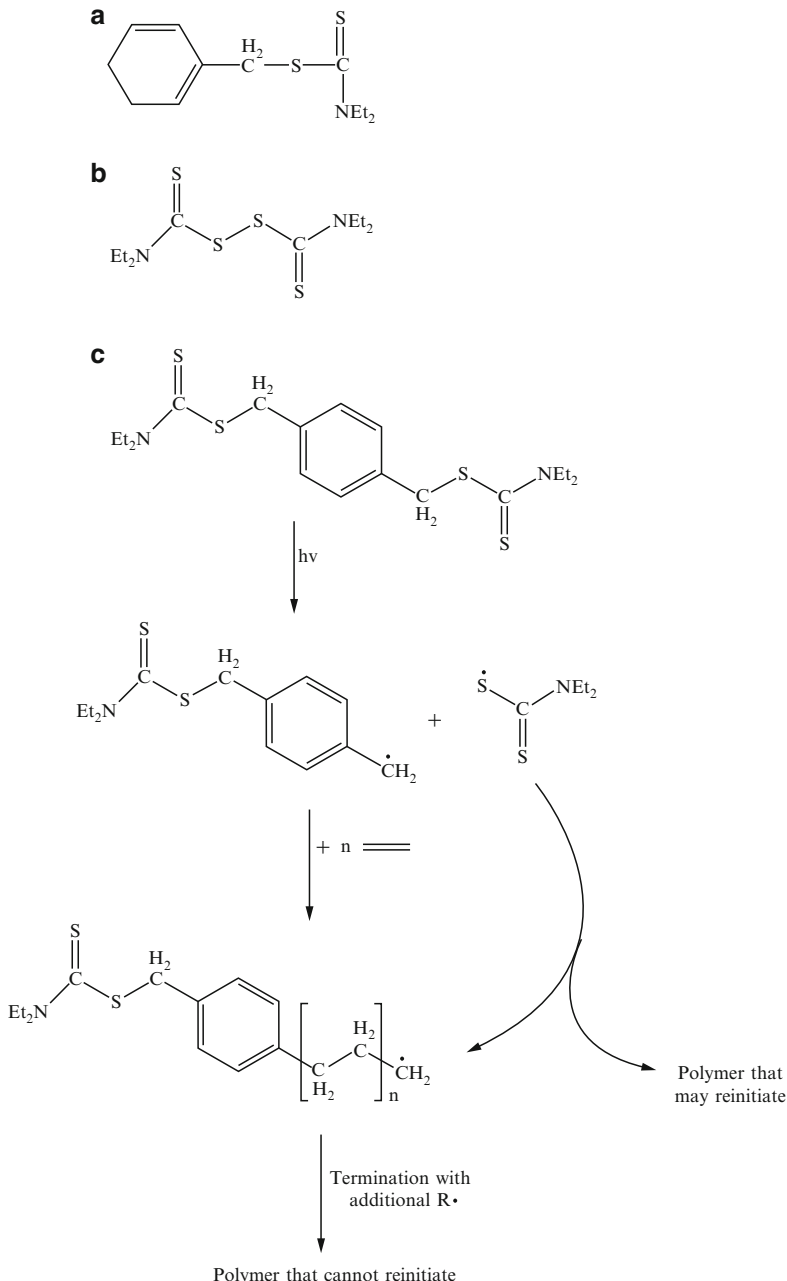


Figure 5.12. Molecular structures of common iniferters (a–c), and illustration of polymerization using an iniferter.

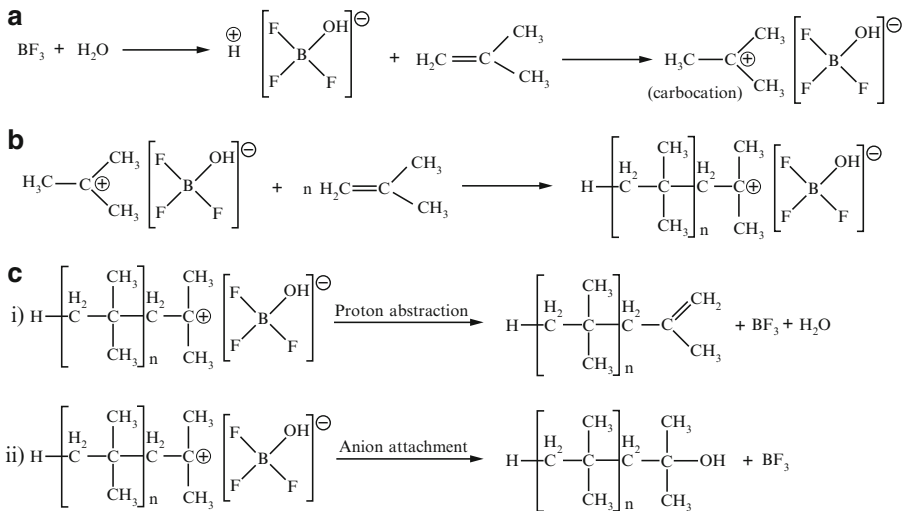


Figure 5.13. Reactions involved in cationic addition polymerization. Shown are (a) generation of a carbocation intermediate from a Lewis acid initiator, (b) propagation of the polymer chain through the combination of the carbocationic polymer chain and additional monomers, and (c) termination of the polymer growth through either proton abstraction (i) or anionic attachment (ii) routes.

5.2.2. Heterogeneous Catalysis

We have considered a variety of precedents for radical/ionic addition polymerization of unsaturated monomers to yield polymeric materials. However, none of the aforementioned techniques offer **stereoselective** control over the growing polymer chain, resulting in purely atactic polymers. In order to introduce such control, it is necessary to spatially confine the reactive site to control the direction of incoming monomer/growing polymer.^[18] The most common method used to control the tacticity of the resulting polymer is *Ziegler–Natta polymerization*.

Ziegler–Natta polymerization is an example of heterogeneous catalysis – a dual-phase system where polymerization occurs on the surface of the catalyst. A crystal of TiCl_3 or TiCl_4 is used in association with an aluminum alkyl co-catalyst (Figure 5.18). Since the Ti sites on the surface are coordinatively unsaturated, monomer may attach along a controlled direction. The aluminum (Lewis acidic) complex acts as an initiator, facilitating monomer coordination through abstraction of a Cl group from the Ti coordination sphere. The Lewis acidic Al site also assists in the intramolecular rearrangements that are essential for chain propagation.

If TiCl_3 is used as the catalyst surface, an isotactic polymer is formed. However, changing the surface to VCl_3 yields a syndiotactic product. This difference may be explained by looking at the relative sizes of Ti^{3+} and V^{3+} . Due to an increase in the effective nuclear charge (Z_{eff}) as one moves from left to right of the Periodic Table, the V^{3+} center is smaller which creates more steric hindrance among the coordinated

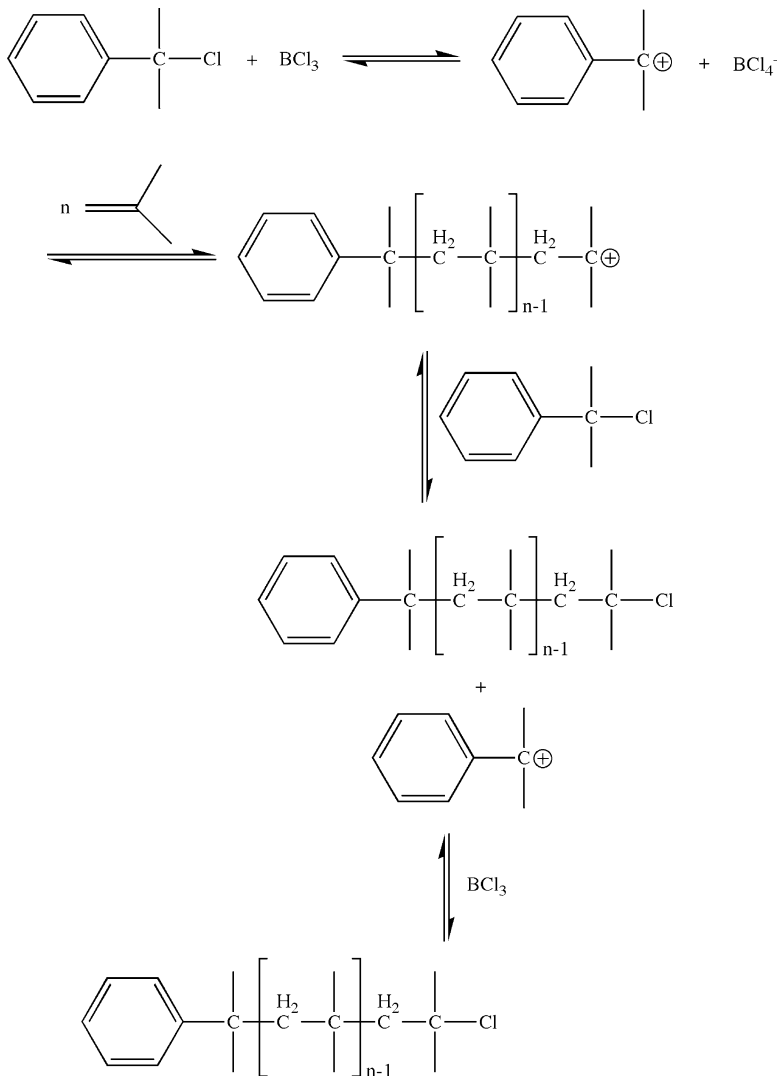


Figure 5.14. Iniferter-based living cationic polymerization of isobutylene.

polymer and incoming monomer. As a result, there is less room for the ligands to undergo an equatorial–axial shift for V^{3+} , and the incoming monomer may approach in two directions. Since this spatial ligand shift readily occurs for the larger Ti^{3+} , the monomer approaches along a single direction, resulting in an isotactic polymer. The decrease in reaction rate and polymerization efficiency upon substitution of Ti with V is likely an artifact of electronic differences. Since V^{3+} has an extra **d-electron** relative to Ti^{3+} (d^2 vs. d^1), there is added Coulombic repulsion with the π -electrons of the incoming olefin.

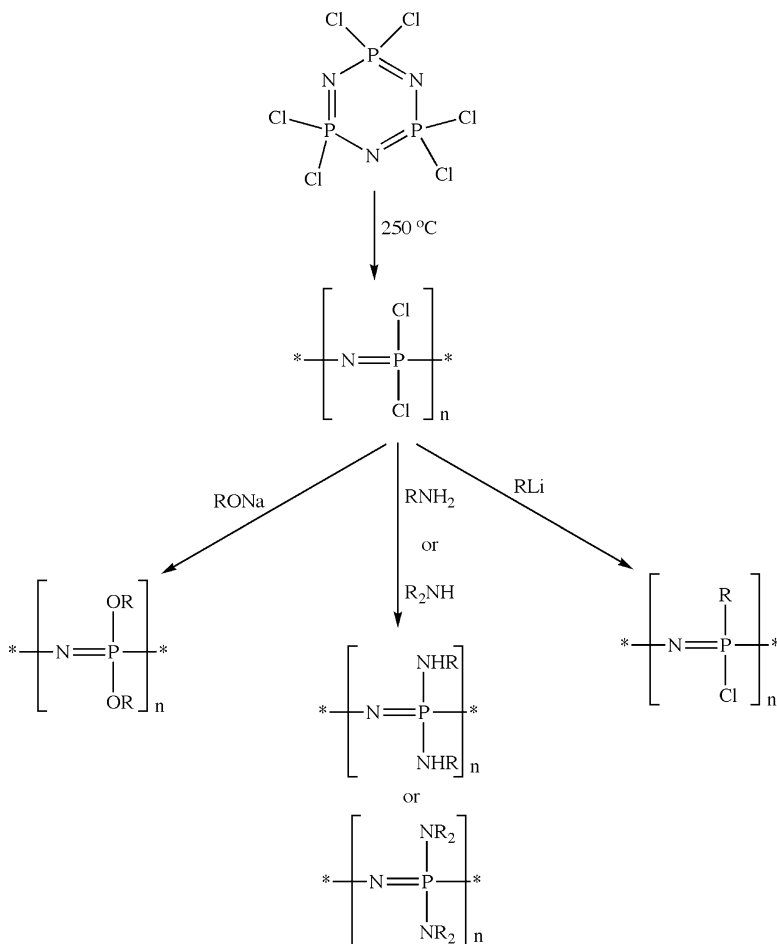


Figure 5.15. Ring-opening polymerization of hexachlorocyclotriphosphazene, and subsequent reactions to yield functionalized polyphosphazenes.

5.2.3. Homogeneous Catalysis

Although separation of products from catalyst is easily accomplished within a heterogeneous system, the **polydispersity** of the product will be relatively high due to multiple reaction sites on the catalyst surface. In order to improve the overall selectivity, a variety of single-phase **homogeneous** catalytic routes have also been developed.^[19] Although the polydispersity of the products are much narrower using homogeneous catalysts, the primary limitation is the difficulty in separating products from reactants/catalyst. However, supercritical fluids (*e.g.*, CO₂ at *ca.* 40°C and 2,000 psi) are now commonly used as the solvent in these systems in order to facilitate product separation.^[20] Supercritical fluids have properties intermediate

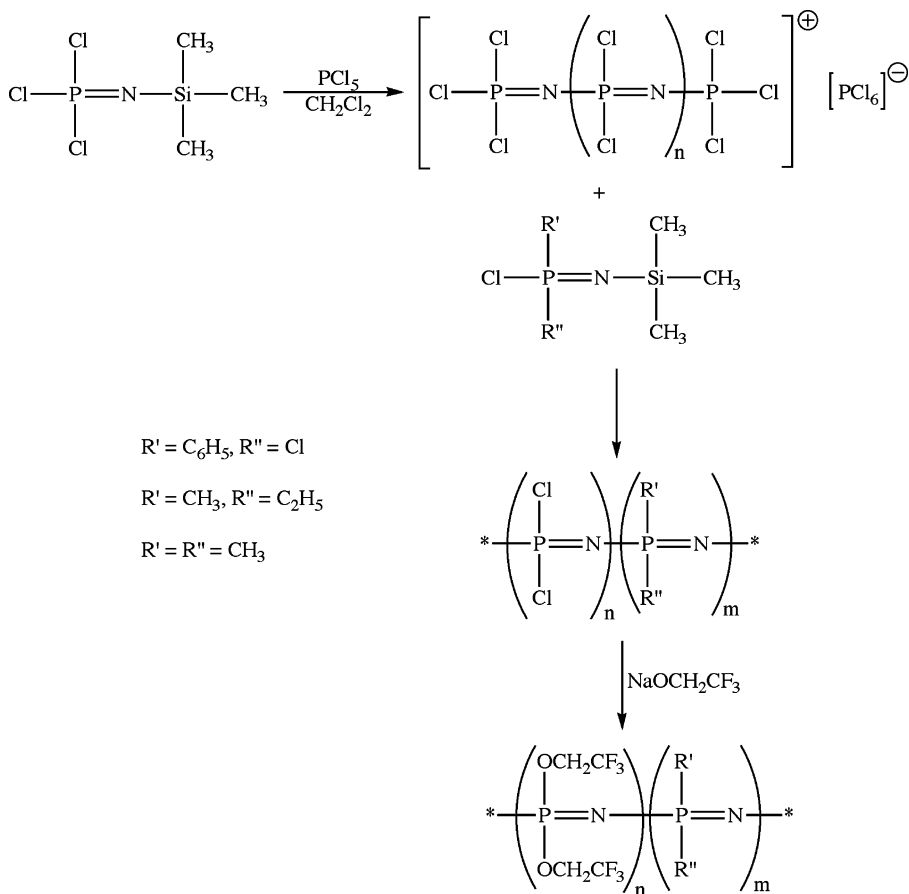


Figure 5.16. An example of a living polymerization route for polyphosphazenes.

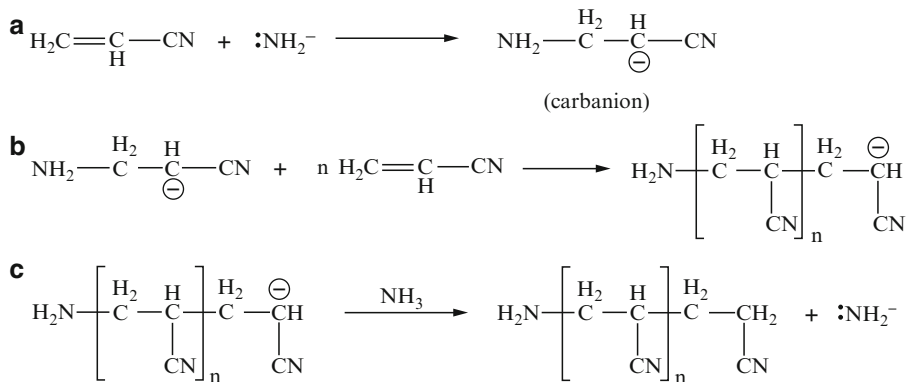


Figure 5.17. Reactions involved in anionic addition polymerization. Shown are (a) generation of a carbanion from a Lewis basic initiator, (b) propagation of the polymer chain through the combination of the carbanionic polymer chain and additional monomers, and (c) termination of the polymer growth through the addition of a Lewis base. Unlike the other addition polymerization schemes, termination does not occur *in situ*, but must be initiated deliberately.

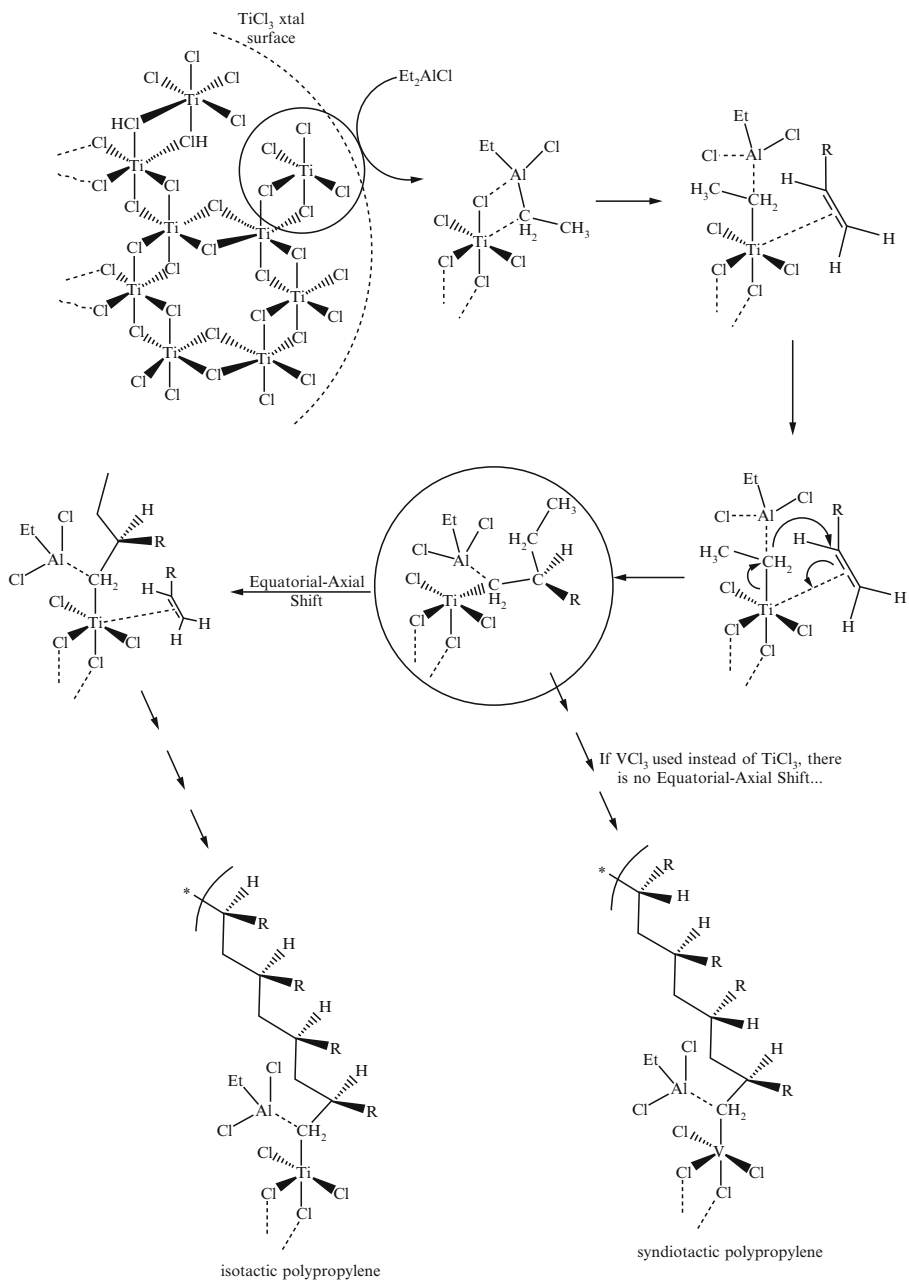
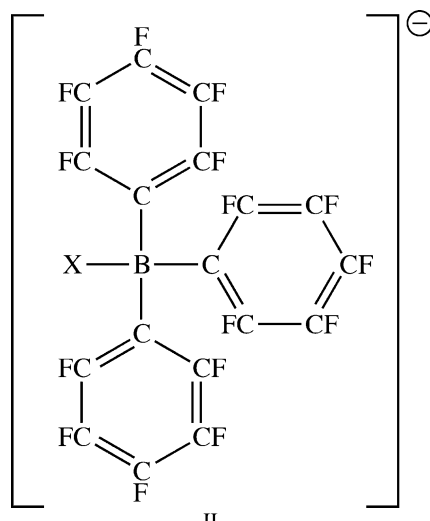


Figure 5.18. Mechanism involved in Ziegler–Natta polymerization for tacticity control over the growing polymer chain.

between gases and liquids; minute changes in pressure/temperature of the fluid near its critical point result in dramatic changes in its density and solubility characteristics.

Homogeneous Ziegler-Natta polymerization catalysts are typically of the *Kaminsky-type*, based on Group 4 metallocene molecules that contain bulky ligands (Figure 5.19).^[21] Based on their sterically-encumbered metal site, it is easy to see how stereocontrol over the polymer is obtained – through limiting the path of approach for the incoming olefin. A more recent technique to offer further stereoselectivity is “heterogenizing” the catalyst by incorporating the metallocene structure into a solid support such as silica or alumina.^[22]

In order to obtain catalytic activity in the system, a co-catalyst featuring an electron-deficient center (*e.g.*, B, Al) must also be present in the solution. The mechanism for activity of aluminum oxide co-catalysts, referred to as *methyl alumoxanes* (MAOs – formed from the controlled hydrolysis of AlMe_3 ^[23]), has been shown to involve the abstraction of an alkyl or chloro group from the metallocene structure.^[24] For aluminum co-catalysts, this yields a $[(\text{Cp})_2\text{MX}]^+ [(\text{'Bu})_2\text{AlX}]^-$ cation/anion pair ($\text{X}=\text{R, Cl}$). This activates the metallocene structure toward polymerization, since the M^+ site more readily accepts electron density from the alkene monomer. In order for the ion pair to be active toward polymerization, the anion must be non-coordinating to ensure a high Lewis acidity toward the incoming olefin. Accordingly, one of the most effective co-catalysts is $\text{B}(\text{C}_6\text{F}_5)_3$, a very strong Lewis acid due to highly electronegative fluorinated substituents that pull electron density away from the central B atom. Upon abstraction of Me or Cl groups, the resulting anion $[\text{BX}(\text{C}_6\text{F}_5)_3]^-$ (**II**) is non-coordinating toward the metallocene structure, which freely allows the catalyst to accept electron density from the incoming monomer.



Since the Lewis acidity of the co-catalyst is most important toward its activity, it was first thought that three-coordinate Al complexes (Figure 5.20) would be most effective for activating the metallocene structure, relative to coordinatively saturated four-coordinate Al compounds. However, it has been shown that the latter

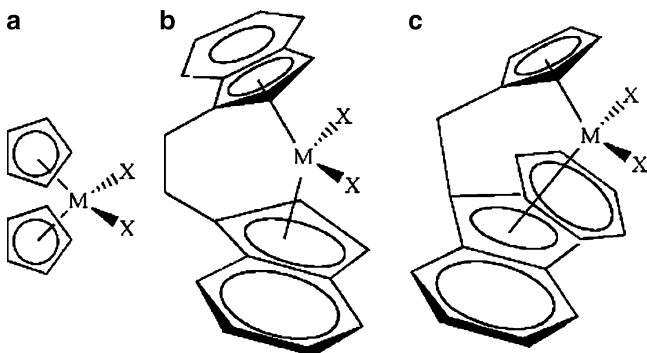


Figure 5.19. Molecular structures of common metallocene homogeneous polymerization catalysts ($M=Zr$, Hf , $X=Me$, Cl). The cyclopentadienyl ligands may be abbreviated as “cp” in the molecular formula (e.g., $(cp)_2HfMe_2$).

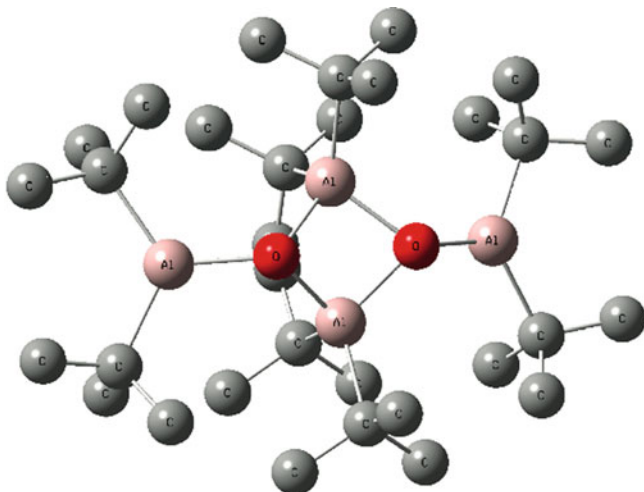


Figure 5.20. Molecular structure of $[(t\text{-Bu})_2\text{Al}(\mu\text{-O})\text{Al}(t\text{-Bu})_2]_2$, featuring three-coordinate, unsaturated Al centers.

structures, $\{(\text{CH}_3)\text{Al}(\mu\text{-O})\}_n$, $n = 6\text{--}12$, which exist as complex caged structures, are most effective for activating the metallocene catalyst. The term “latent Lewis acids” has been coined for these structures by Barron,^[25] indicating that the isolated caged structures do not themselves possess acidity, but become activated due to a cage-opening mechanism upon contact with the metallocene catalyst (Figure 5.21). The magnitude of Lewis acidity is directly related to the cage strain; as one would expect, metallocene activation is more pronounced with increasingly smaller cages.

Three mechanisms have been proposed to explain metallocene-based homogeneous and Ziegler–Natta polymerization schemes. The Cossee–Arlman mechanism

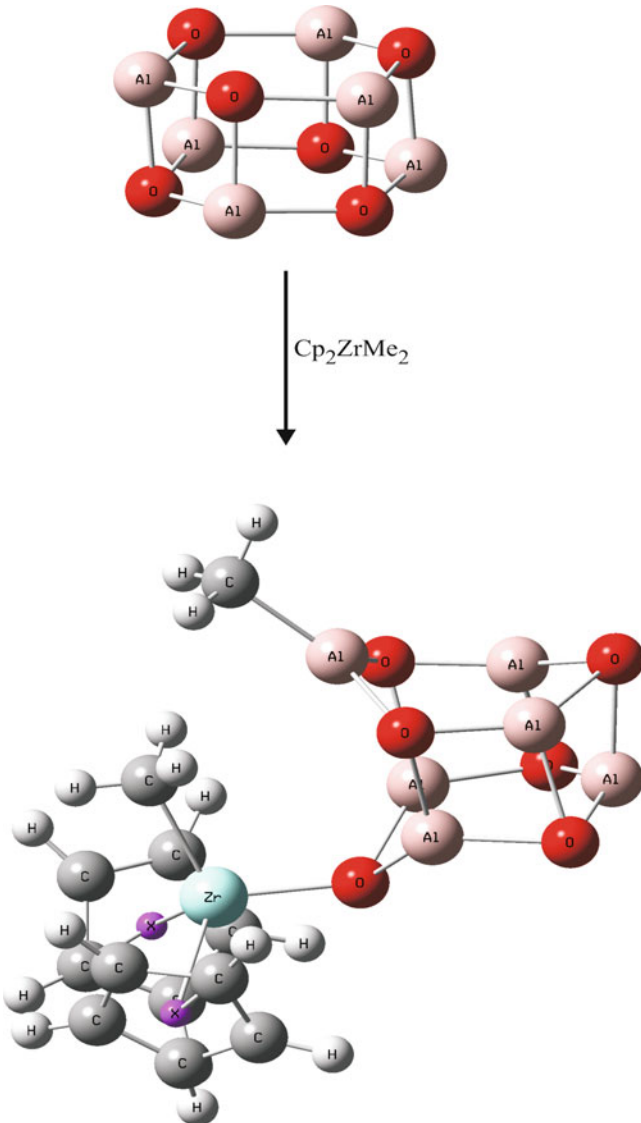


Figure 5.21. Molecular structure of $[\text{MeAlO}]_6$ (methyl groups omitted for clarity), and schematic of the cage-opening mechanism of the alumoxane co-catalyst during metallocene-catalyzed polymerization.

(Figure 5.22a) proposes the coordination of the olefin to the vacant metal site, with its subsequent migratory insertion into the M–P bond (P = growing polymer). The insertion step likely proceeds through a four-membered cyclic transition state. Another mechanism proposes an initial α -hydride elimination, resulting in a metal hydride species that may add an olefin and form a growing polymer chain through

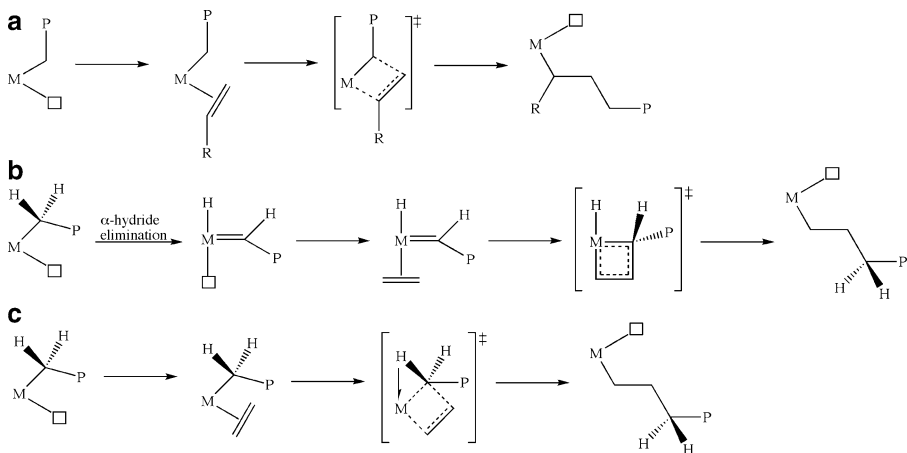


Figure 5.22. Proposed mechanisms for transition metal-catalyzed olefin polymerization.

migratory insertion (Figure 5.22b). The last mechanism that involves α -agostic M–H interactions (Figure 5.22c) is generally accepted as being an important part of the Cossee–Arlman mechanism, serving to slow down the insertion reaction and favor the approach of incoming ligand.

It should be noted that early transition metals (Group 4 or 5) are most favorable for transition metal catalyzed living polymerization. Since these metals have few d-electrons in their valence shell, there is a lesser chance for β -hydride elimination (polymer termination) to occur.^[26] In order to purposely terminate chain growth, either the M–C bond may be broken through reaction with hydrogen gas (Figure 5.23a) or thermally induced β -hydride elimination. Whereas the first termination route results in low polydispersity, the latter method results in terminal olefin (Figure 5.23b) that may insert into a neighboring polymer chain yielding a branched, low-density product.

5.2.4. Step-Growth Polymerization

Thus far, we have considered addition polymerization routes – either catalyzed or uncatalyzed. Although this is sufficient to describe the synthesis of common packaging materials such as polyethylene, polypropylene, polystyrene, etc., other classes of polymers such as nylon, PETE, and polyacrylamide are generated through step-growth mechanisms. Although the synthetic pathway for these polymers is more straightforward than addition polymerization, there are many intricate considerations that affect overall polymer properties.

The general types of step-growth polymerizations are shown in Figure 5.24. Since the resulting polymers contain reactive functional groups on either/both ends, it is referred to as a *telechelic* macromolecule. Although water is typically released as a

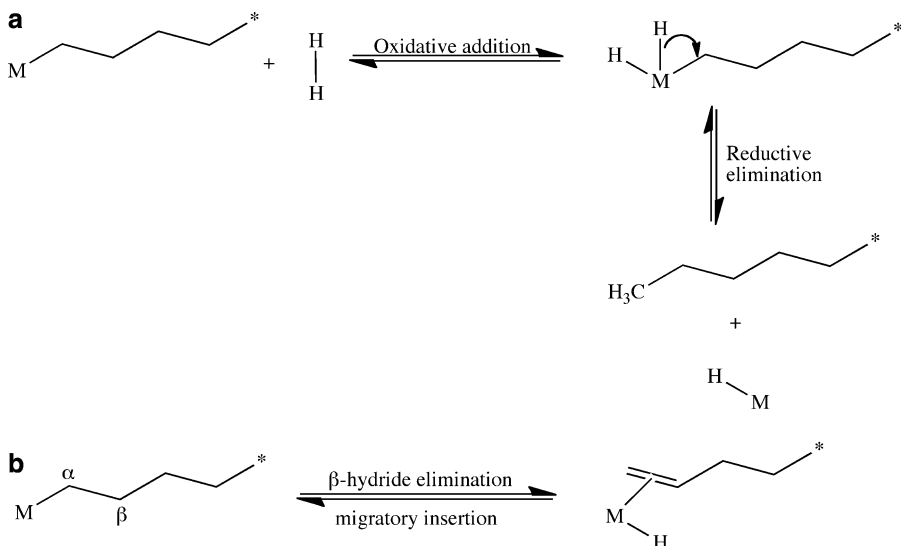


Figure 5.23. Schematic of (a) hydrogenolysis termination of a polymer chain and (b) β -hydride elimination termination, which results in an olefin-terminated polymer chain.

byproduct of these polymerizations, other small molecules such as alcohols and alkyl halides may also be generated based on the monomers that co-condense. In its simplest form, condensation reactions result in linear polymers from the reaction of bifunctional monomers. For example, one of the most common linear step-growth polymers is poly(ethylene terephthalate) (PET; commonly denoted by the trademarks Dacron or Mylar), used for soft drink bottles due to its impermeability toward liquids and gases. This polymer is obtained through a two-step reaction between ethylene glycol ($\text{HO}-\text{C}_2\text{H}_4-\text{OH}$) and the dimethyl ester of terephthalic acid ($\text{CH}_3\text{O}-\text{C}(\text{O})-\text{benz}-\text{C}(\text{O})-\text{OCH}_3$). Both methanol and ethylene glycol byproducts are evolved during the condensation reaction.

In contrast, if the monomers are multifunctional rather than **difunctional**, a branched polymeric structure will result (Figure 5.25). For instance, consider either the “ $\text{AB}_x/\text{AB}_x + \text{B}_y$ ” (Figure 5.25a) or the “ $\text{A}_2 + \text{B}_y$ ” (Figure 5.25b) systems, where A and B refer to the reactive functional groups of the monomers (subscripts indicate the number of reactive functional groups).^[27] In describing branched step-**growth** polymers, it is generally assumed that:

- (i) A and B endgroups react only with each other;
- (ii) All endgroups of a given type are equally reactive;
- (iii) Intramolecular cyclization reactions do not occur;
- (iv) Probability of A–B reactions is independent of molecular size.

It is interesting to note that whereas $\text{A}_x + \text{B}_y$ hyperbranched systems have both A and B endgroups, AB_x -based hyperbranched polymers contain only B endgroups. This leads to the discrepancy between the two systems in forming infinite networks

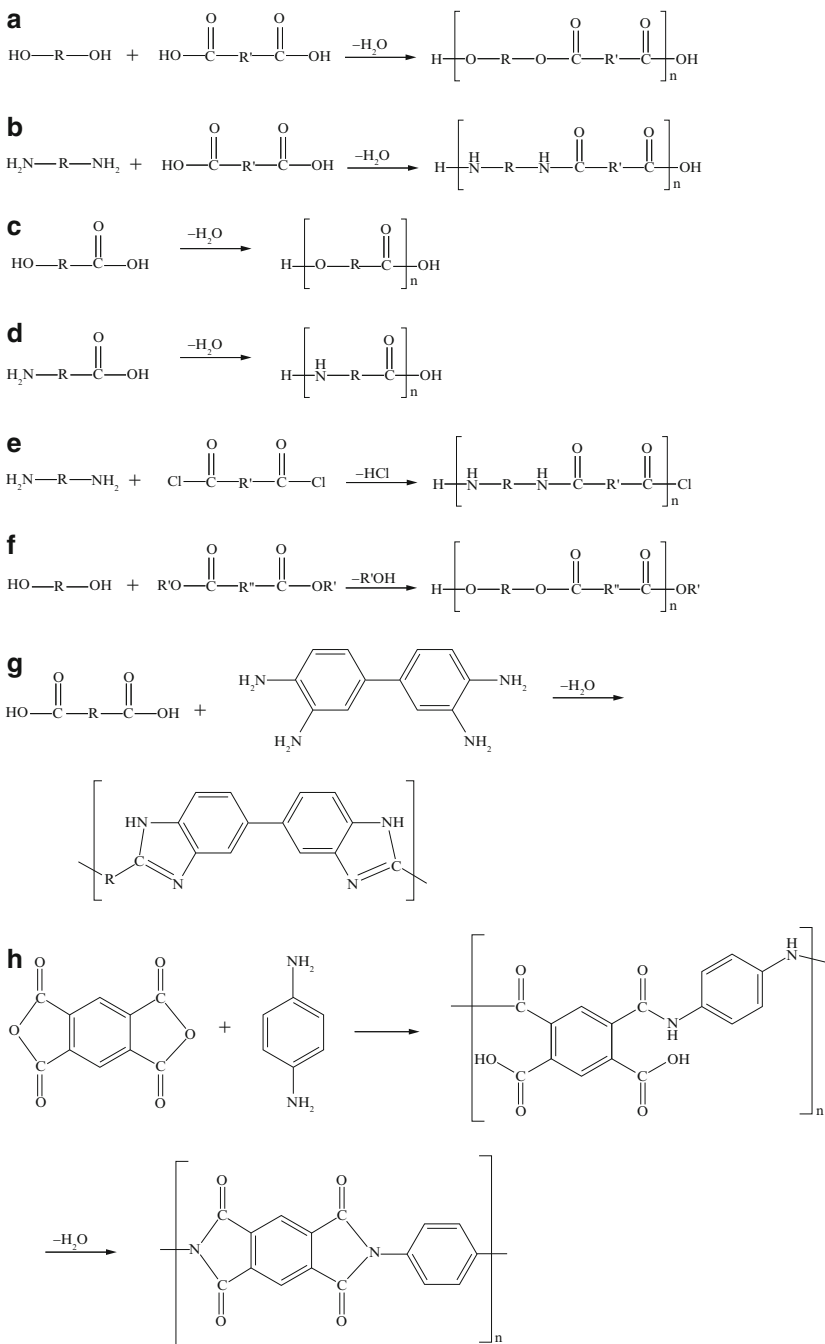


Figure 5.24. Reaction schemes for the most common types of step-growth polymerization. Shown are (a/c) polyester formation, (b/d) polyamide formation, (e) polyamide formation through reaction of an acid chloride with a diamine, (f) transesterification involving a carboxylic acid ester and an alcohol, (g) polybenzimidazole formation through condensation of a dicarboxylic acid and aromatic tetramines, and (h) polyimide formation from the reaction of dianhydrides and diamines.

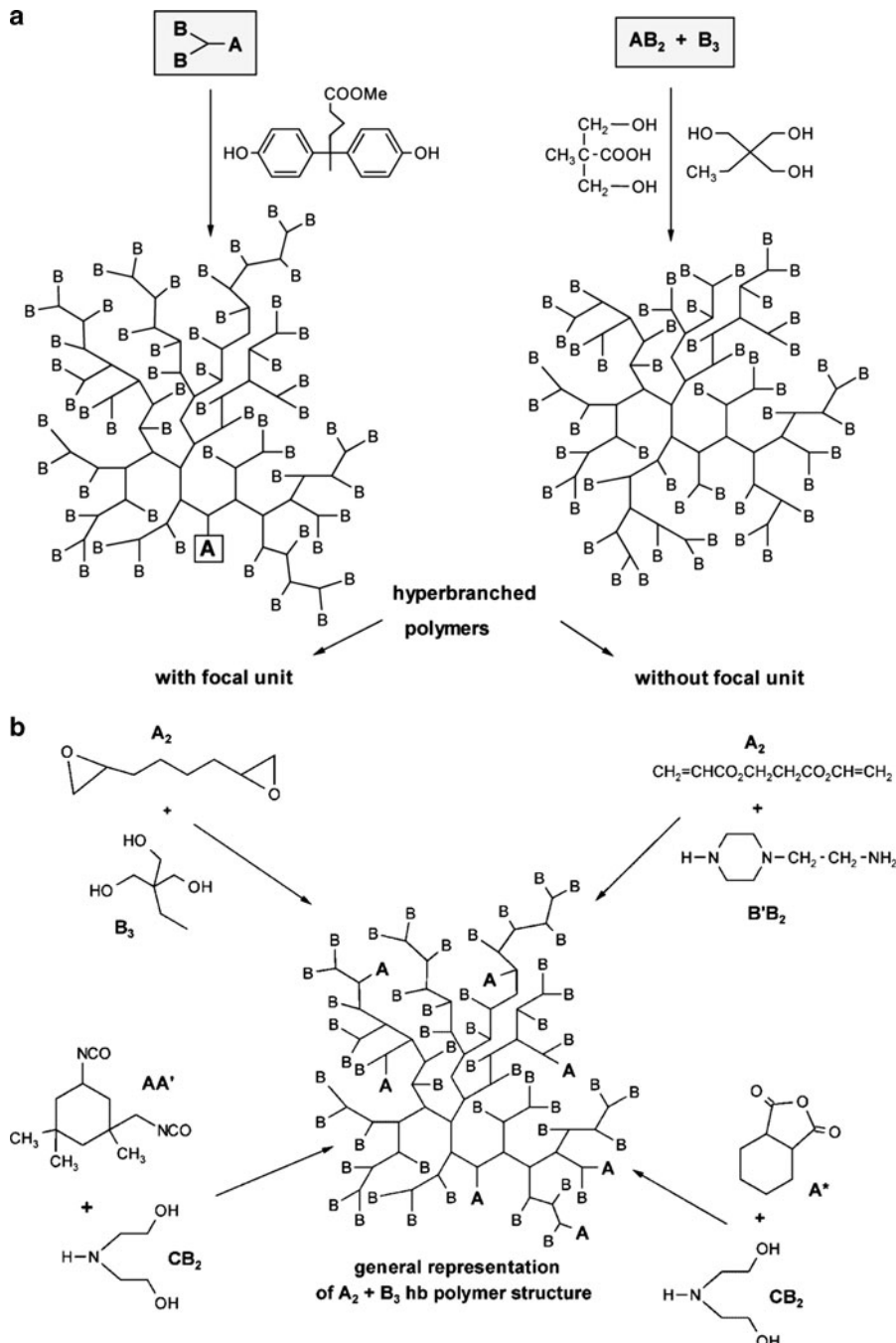


Figure 5.25. (a) Scheme of the formation of hyperbranched polymers via the AB_x and $AB_x + B_y$ approach ($x \geq 2$; here, 2; $y \geq 3$; here, 3). (b) Scheme of the synthesis of hyperbranched polymers by various $A_2 + B_y$ ($y \geq 3$) approaches, with examples of monomer combinations (A^* indicates cyclic monomer; AA' indicates differences in the reactivity). Reproduced with permission from Voit, B. I.; Lederer, A. *Chem. Rev.* 2009, 109, 5924. Copyright 2009 American Chemical Society.

(gels). The $A_x + B_y$ system results in gel formation if $x \geq 2$ and $y \geq 3$, whereas it is not possible to form a gel via the AB_x system. Though the polydispersity of hyperbranched polymers is typically quite large, there is increasing interest for a number of blends/coatings applications due to the high density of peripheral groups, and resultant enhanced solubility/surface adhesion, relative to linear analogues. As a more recent extension, network structures that consist of interwoven hyperbranched polymers may also be synthesized (Figure 5.26), which have been proven useful for lithographic applications.

5.2.5. Dendritic Polymers

Thus far, we have only considered step-growth polymers obtained through random condensation reactions of multifunctional monomers. The pioneering work of Nobel Laureate Flory^[28] in the 1940s helped the polymer community understand the kinetics of branched polymer growth, and suggested that control over sequential step-growth should be possible. However, this was not proven empirically until the work of Vögtle^[29] and Tomalia^[30] in the late 1970s–early 1980s. Vögtle developed a repeatable “cascade” route to produce low molecular weight amines (Figure 5.27). However, due to cyclization side reactions, successful polymer growth via the Vögtle approach was not possible – finally being realized in 1993 for the synthesis of poly(propyleneimine) (PPI). The work of the Tomalia group at Dow Chemical was the first to yield a perfectly defined dendritic polymer structure, with an extremely low polydispersity (*ca.* PDI of 1.00–1.05; Figure 5.28).^[31] These polymers were coined *starburst dendrimers*, referring to the star-branched architecture and the Greek word “dendra” for tree. Not unlike other major scientific discoveries, the first report of the dendritic architecture was riddled with skepticism by the scientific community. Shortly thereafter, Newkome helped silence the critics with his publication of branched dendrimers that he called an *arborol* (Figure 5.29).^[32] To illustrate the novelty of these structures, Table 5.3 lists the comparative properties of dendrimers and linear polymers.

The earliest syntheses of dendritic polymers were divergent in nature; with growth initiating from a core, and outward propagation. The terminal groups of the core are reacted with complementary groups on the monomer, which forms a new branching point for subsequent branching reactions (Figure 5.30a). Most importantly, the terminal functional groups on the monomers are designed to be reactive with only the outwardly growing polymer, which prevents random hyperbranched growth. Such a repetitive procedure results in an exponential increase in reactions that occur on the periphery of the growing polymer, requiring a large excess of reagents. Though this technique is used for the large-scale synthesis of many dendrimers (*e.g.*, poly(amidoamine) – PAMAM), a leading drawback is the relatively high number of defect structures – especially for higher *generations* (a term used to describe the sequential branches emanating from the core of the dendritic structure). With each generation, there is an increased probability for

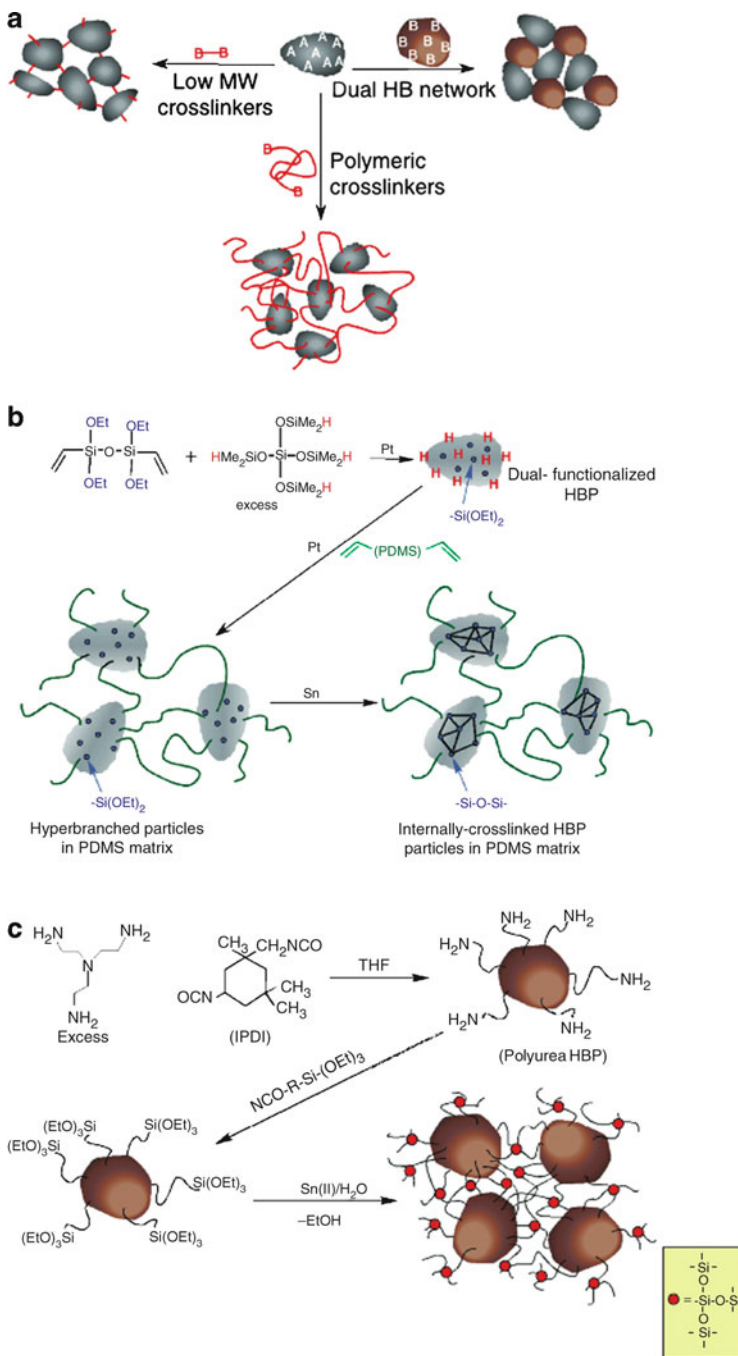


Figure 5.26. The general strategy (a) and examples (b–c) of hyperbranched polymer network structures featuring a siloxane crosslinkage. Reproduced with permission from Meijer, D.; Dvornic, P. R. Fall 2005 ACS meeting, Midland, MI.

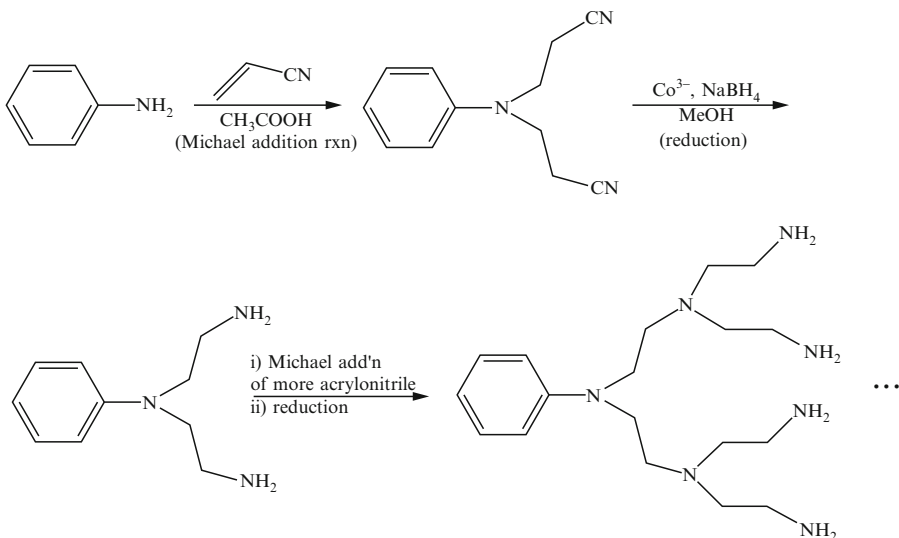


Figure 5.27. The Vögle approach to yield low molecular weight amines via controlled sequential synthesis.

incomplete/side reactions, which are not easily removed from the solution due to their structural similarity to the final product.

In order to circumvent the purity issues associated with divergent syntheses, Frechet and coworkers designed a convergent approach in the late 1980s.^[33] In contrast to the divergent approach, growth initiates from the exterior of the molecule progressing inwardly by coupling endgroups to each branch of the monomer (Figure 5.30b). The functional group at the focal point of the wedge-shaped dendritic fragment (known as a *dendron*) may be reacted with additional monomers to build up higher-generation dendrons. When the desired generation dendron is reached, these units are then attached to a polyfunctional core to form the final dendrimer. This route drastically increases the purity of higher-generation dendrimers relative to divergent syntheses, as there are much fewer reactions per molecule.

In addition, the reactions only require a slight excess of reagent, in contrast to the large excesses that were essential for divergent growth. However, this technique is not useful for commercial large-scale dendrimer synthesis, as the mass of the sample decreases with additional generation growth, and low yields of higher-generation dendrimers due to steric crowding around the focal point of the growing dendron. Nevertheless, this is the only route that offers precise structural control over the growing dendrimer, such as being able to modify the focal point/chain ends to yield well-defined unsymmetrical dendrimers. This strategy is being developed to synthesize “bowtie” dendrimers containing both target and drug-delivery agents (Figure 5.31). As an alternative strategy for drug delivery, surface modification of PAMAM with cancer targets

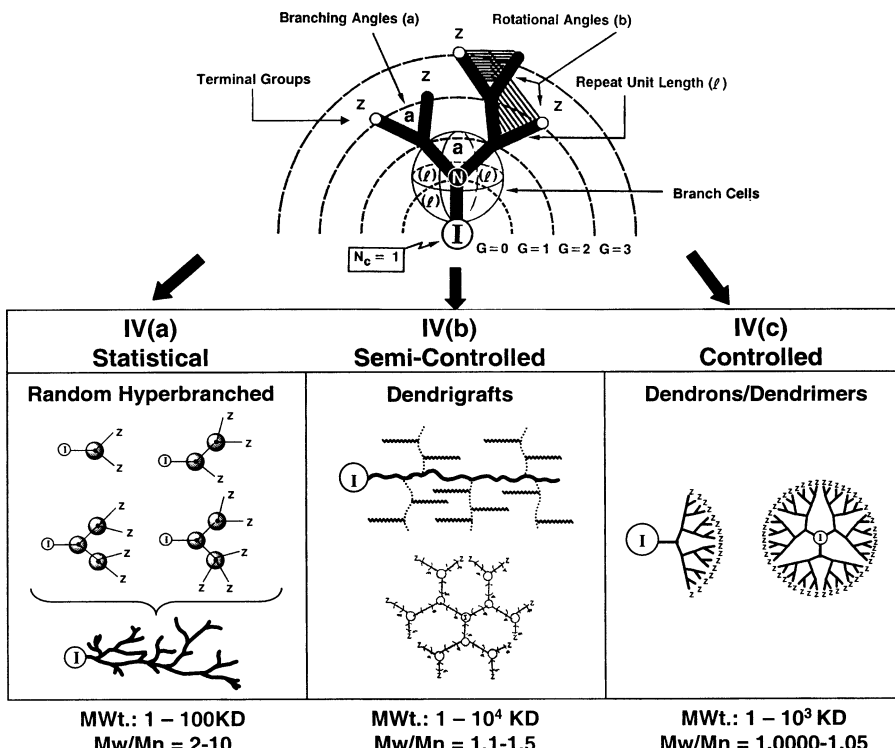


Figure 5.28. Illustration of resultant polymers through varying the degree of control of step-growth polymerization. Each successive growth layer is referred to as a *generation* (G). Reproduced with permission from Frechet, J. M. J.; Tomalia, D. A. *Dendrimers and Dendritic Polymers*, Wiley: New York, 2001.

and anticancer drugs (Figure 5.32) has also been proven successful in preliminary trials. We will further discuss advances in drug-delivery agents later in this chapter.

To date, the PAMAM dendrimer remains the most heavily utilized for applications, due to its facile scale-up and commercial availability. In Chapter 6, we will discuss its use as a nanoreactor/nanocapsule stabilizing agent for nanoparticle growth within both aqueous or organic solvent media.^[34] Not only can one alter its solubility characteristics by changing the peripheral moieties from hydrophilic/hydrophobic character, but also its overall properties. For instance, Starpharma in association with Dendritic Nanotechnologies, Inc. have developed a HIV/AIDS drug that is based on a PAMAM architecture functionalized with sulfonic acid end groups.^[35] However, if the terminal groups are changed to oligo(ethylene glycol), the dendrimer may be used as a pore generating agent in the development of dielectric thin films for microelectronic devices.^[36] Poly(lysine) dendrimers modified with sulfonated napthyl groups have shown activity as antiviral drugs against the herpes simplex virus.^[37] Svenson and Tomalia provide a nice review of the multifaceted

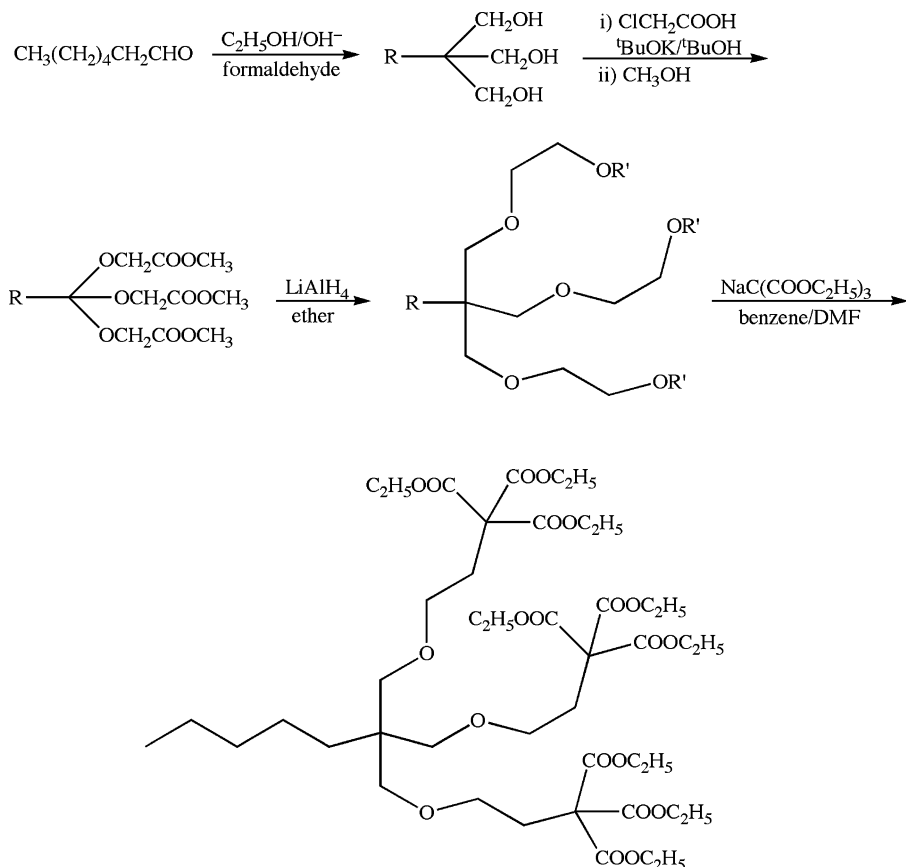


Figure 5.29. The Newkome approach for the sequential step-growth of arborols.

Table 5.3. Comparative Properties of Dendrimers and Linear Polymers^a

Property	Dendrimers	Linear polymers
Structure	Compact, globular	Not compact
Synthesis	Controlled, stepwise growth	Single-step polycondensation
Structural control	Very high	Low
Architecture	Regular	Irregular
Shape	Spherical	Random coil
Crystallinity	Non-crystalline, amorphous	Semi-crystalline/crystalline
T _g	Lower	Higher
Aqueous solubility	High	Low
Nonpolar solubility	High	Low
Viscosity	Non-linear relationship w/ M _w	Linear relationship w/ M _w
Compressibility	Low	High
Polydispersity	Monodisperse	Polydisperse

^a <http://www.pharmainfo.net/reviews/dendrimer-overview>

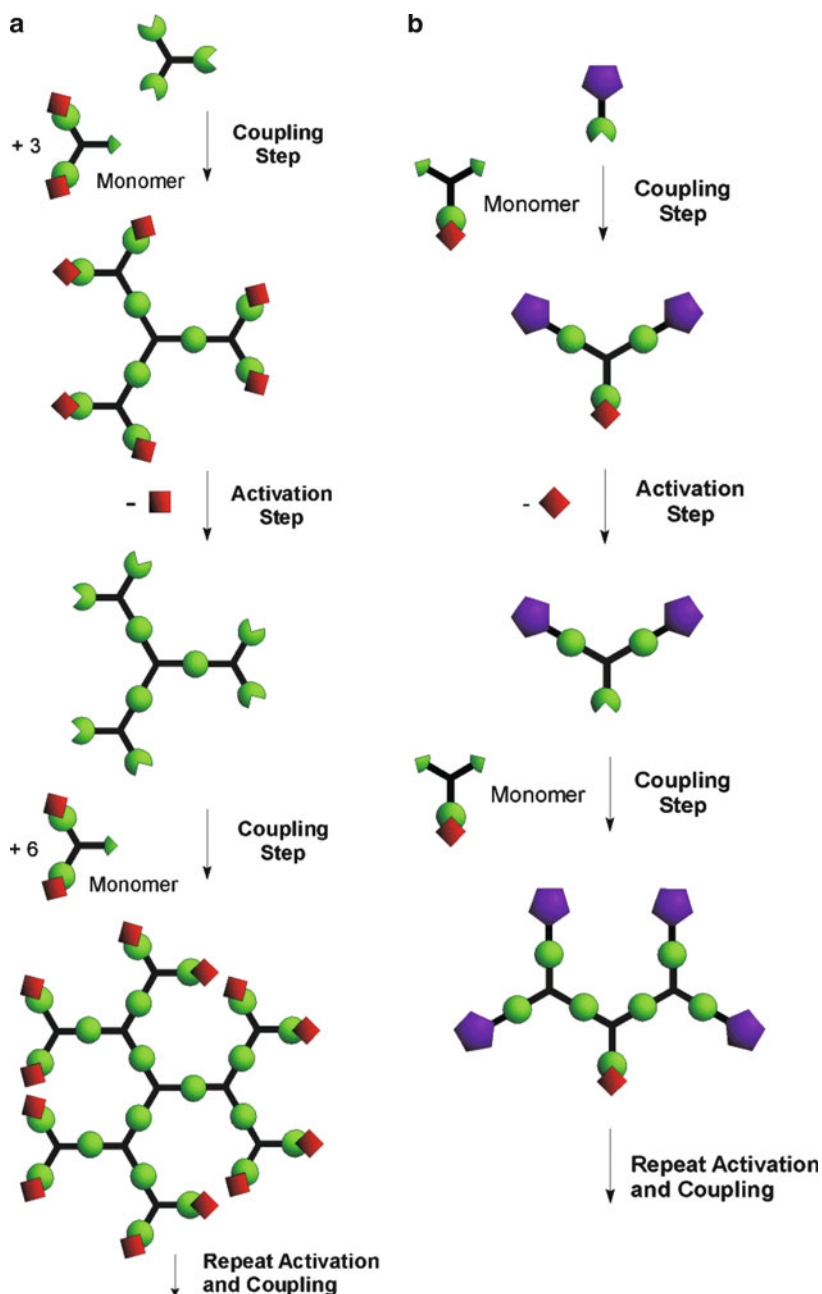


Figure 5.30. Schematic comparison of (a) divergent and (b) convergent dendrimer synthetic routes. Reproduced with permission from Grayson, S. M.; Frechet, J. M. J. *Chem. Rev.*, 2001, 101, 3819. Copyright 2001 American Chemical Society.

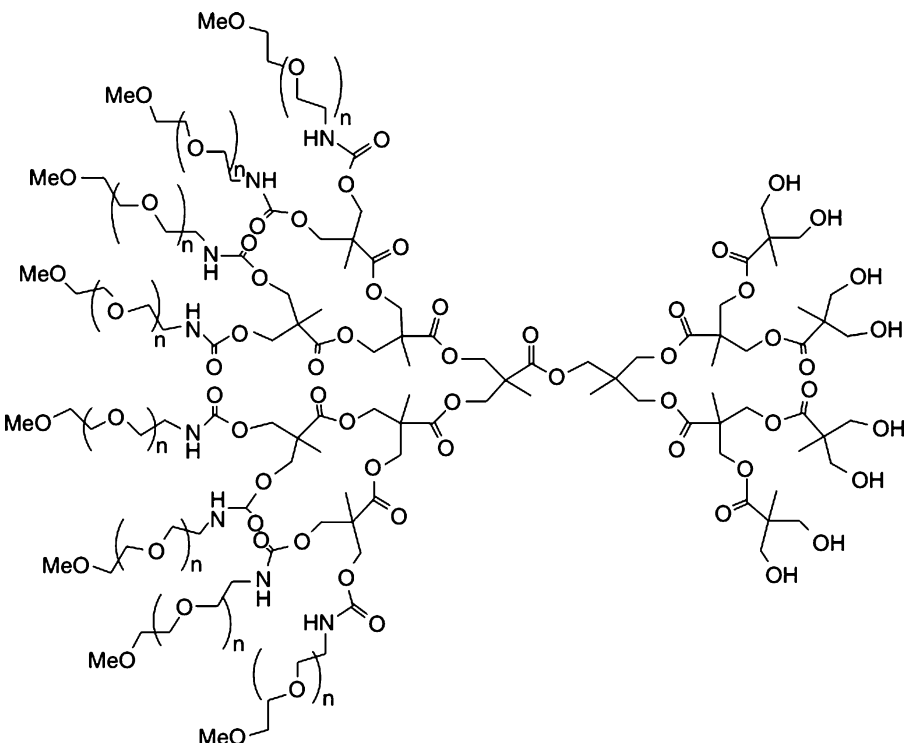


Figure 5.31. Bowtie dendrimer synthesized via the convergent approach, for drug delivery of anticancer drugs to target organs. Reproduced with permission from Gillies, E. R.; Dy, E.; Frechet, J. M. J.; Szoka, F. C. *Mol. Pharm.*, **2005**, 2, 129. Copyright 2005 American Chemical Society.

use of dendrimers for biomedical applications,^[38] Li and Aida provide a review of dendrimer porphyrins and phthalocyanines, which have attracted recent interest as sensitizers for photodynamic therapy (PDT) and biosensing applications.^[39]

The first “co-polymer dendrimer” was developed by Dvornic and coworkers, which feature both a hydrophilic PAMAM core and a hydrophobic organosilicon shell (Figure 5.33).^[40] This structure proves extremely useful for the encapsulation of polar species within organic solvents, for the growth of nanoparticles (Chapter 6). Due to the water-sensitive alkoxy silyl groups (*e.g.*, Si—OCH₃), facile network formation may also take place (Figure 5.34) via the analogous hydrolysis reactions that were previously discussed for sol–gel growth of SiO₂ networks (Chapter 2). The crosslinking of dendritic units to form an extended network is sometimes referred to as a *megamer* – of increasing interest for functional coatings (*e.g.*, sensors, smart fabrics, *etc.*) applications. A further utility of the PAMAMOS structure is its reactivity toward a glass surface, which contains silanol (Si—OH) reactive groups (Figure 5.35). This results in a permanent coating, with a controllable degree of surface adsorption based on the peripheral groups of the dendrimer. These properties

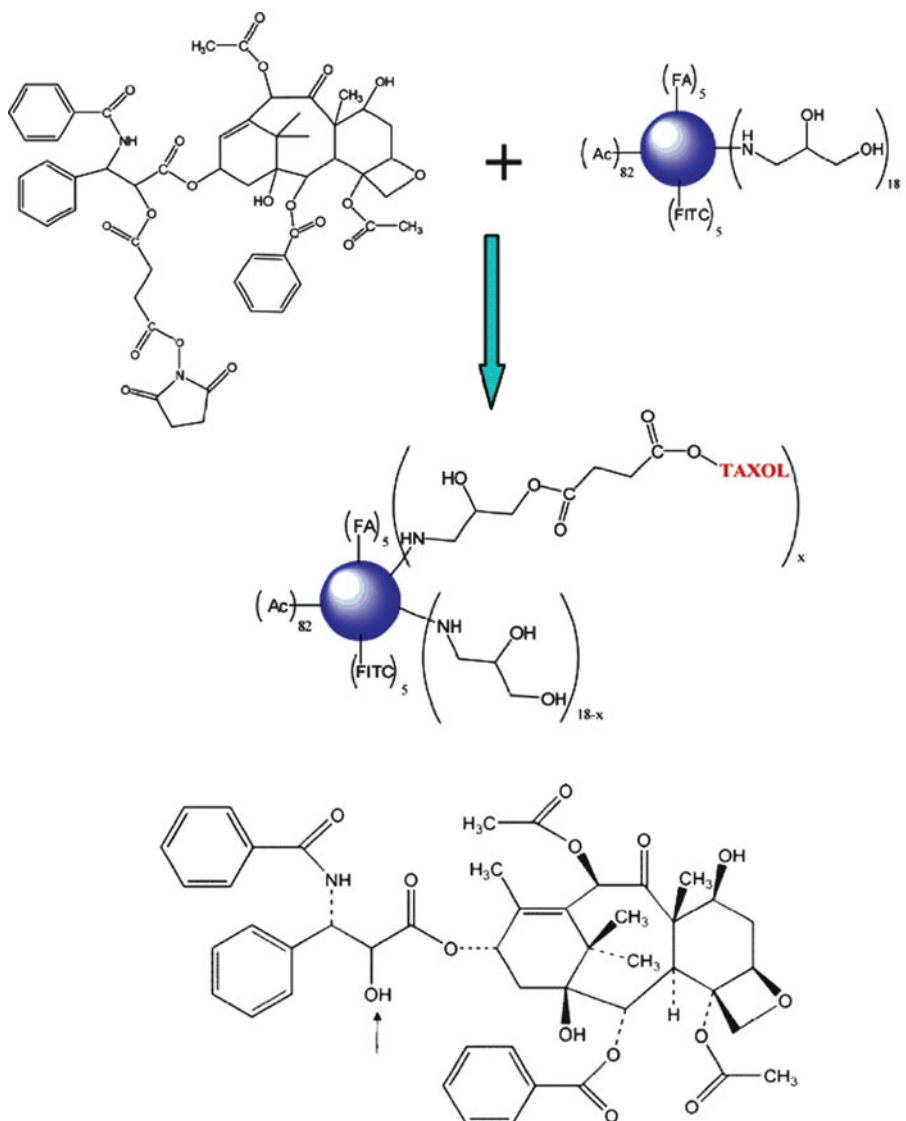


Figure 5.32. PAMAM dendrimer multifunctional conjugates for cancer treatment. The FA group is a folic acid cancer cell target, and FITC is fluorescein isothiocyanate, used as an imaging agent. Also shown (bottom) is the molecular structure for the anticancer drug, taxol, denoting the —OH group that covalently attaches to the dendrimer. Reproduced with permission from Majoros, I. J.; Myc, A.; Thomas, T.; Mehta, C.; Baker, J. R. *Biomacromolecules*, **2006**, *7*, 572. Copyright 2006 American Chemical Society.

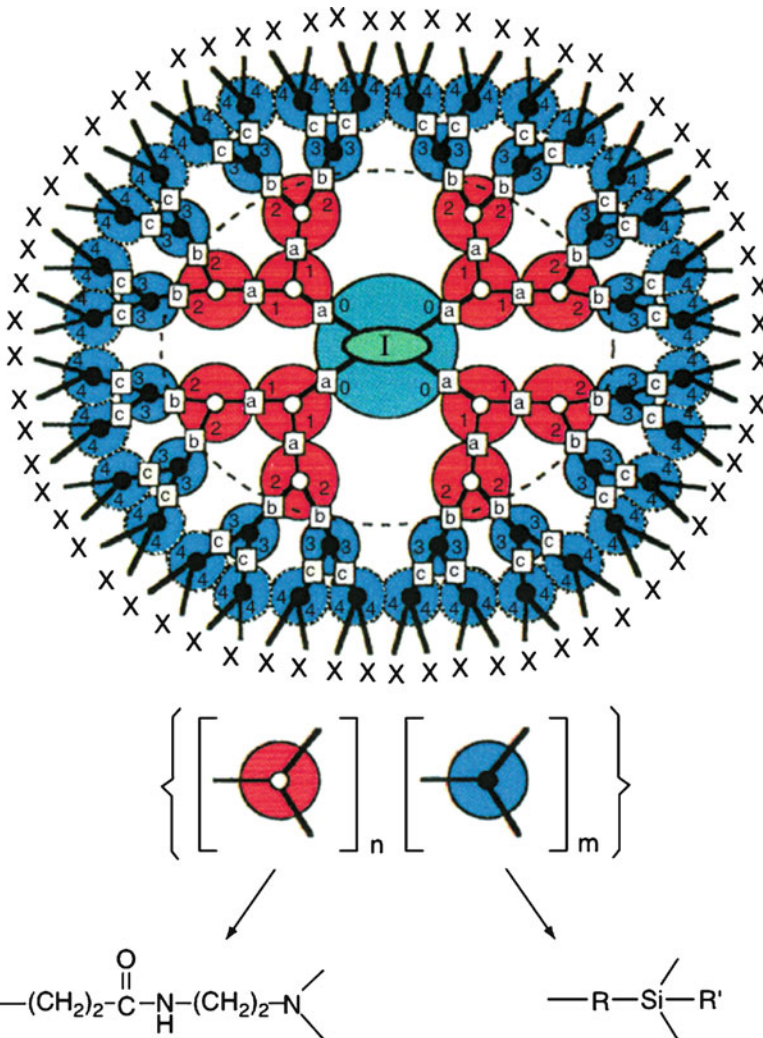


Figure 5.33. Illustration of a poly(amidoamine-organosilicon) (PAMAMOS) dendrimer, with two generations of each PAMAM and organosilicon units. Although the PAMAMOS represents a block copolymer, an unlimited number of other variations that contain a random copolymer array, or varying dendron subunits, may also be synthesized. Reproduced with permission from Dvornic, P. R.; Owen, M. J. *Synthesis and Properties of Silicones and Silicone-Modified Materials*, ACS Symposium Series 838, **2002**, 236.

have recently been exploited by the deposition of copper-encapsulated PAMAMOS anti-fouling coatings on ship hulls, to prevent the adhesion of zebra mussels.^[41]

Although we have described the growth of dendritic polymers as being highly controllable, the resultant size of the polymer is mathematically limited. This is in direct contrast to linear polymers that may increase in size to infinity (as long as they

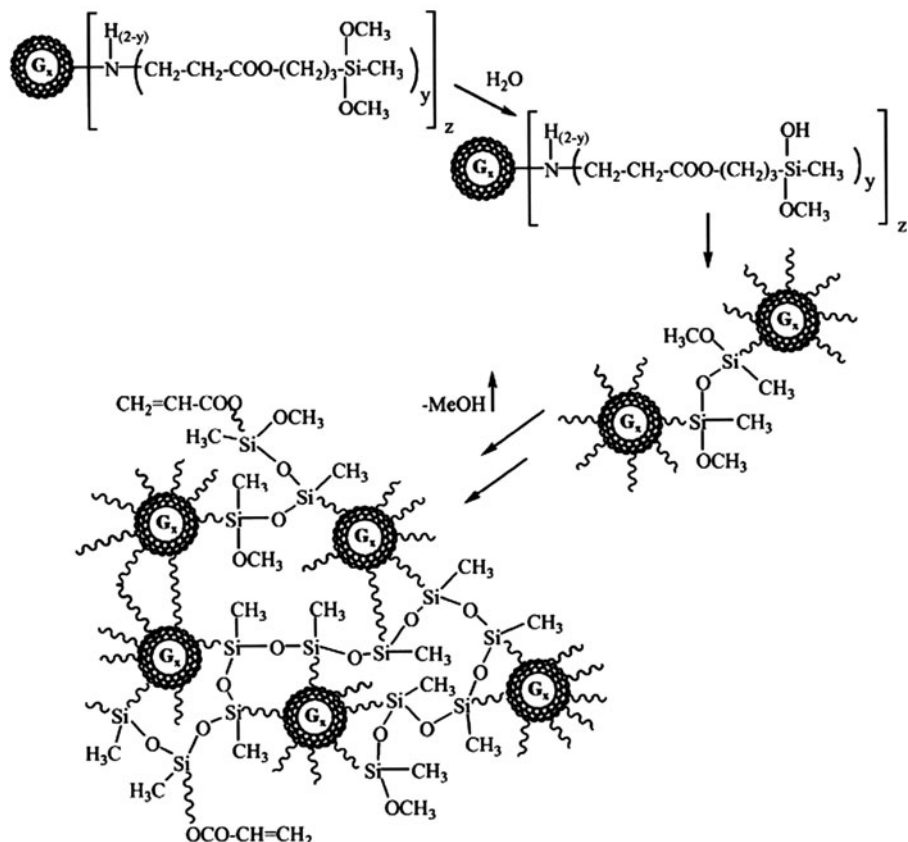


Figure 5.34. Network (megamer) formation through the hydrolysis/crosslinking of neighboring PAMAMOS dendrimer units. Hydrolysis of the C—O—Si bond may also be exploited for the controlled-release of entrained agents (*e.g.*, cancer drugs, *etc.*). It should be noted that subsequent thermal annealing to remove the PAMAM cores results in a nanoporous network that has a dielectric constant (*k*) of *ca.* 1.5 – of extreme interest for next-generation low-*k* IC interconnect applications. Reproduced with permission from Dvornic, P. R.; Li, J.; de Leuze-Jallouli, A. M.; Reeves, S. D.; Owen, M. J. *Macromolecules*, **2002**, *35*, 9323. Copyright 2002 American Chemical Society.

remain soluble within the solvent). As the dendritic structure grows, there become significant steric interactions among the exponentially increasing number of peripheral groups. This phenomenon is known as the *De Gennes dense packing*,^[42] and results in a more structurally flawed, globular structure as the dendrimer generation increases.

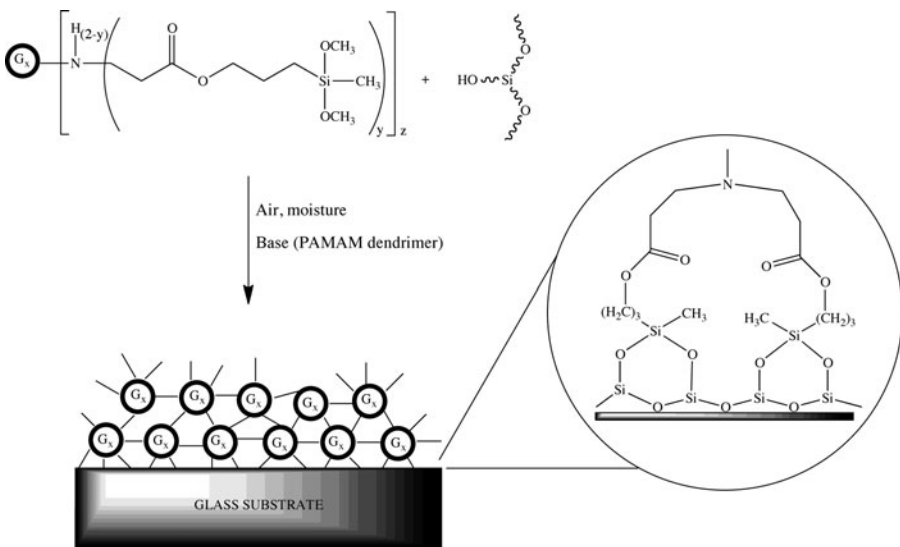


Figure 5.35. The formation of covalently bound coatings of PAMAMOS onto a glass surface. Reproduced with permission from Dvornic, P. R.; Li, J.; de Leuze-Jallouli, A. M.; Reeves, S. D.; Owen, M. J. *Macromolecules*, **2002**, 35, 9323. Copyright 2002 American Chemical Society.

5.2.6. Polymerization via “Click” Chemistry

As we know from experiment, any chemical reaction will result in byproducts and side-reactions that will limit the overall yield to <100%. Quantitative yields are quite rare for synthetic chemistry; that is, until the introduction of *click chemistry* by Sharpless and coworkers in 2001.^[43] By definition, click chemistry involves reactions that occur by high/quantitative yield, generate few/no byproducts, and are stereospecific – setting an important precedent toward mimicking nature’s synthetic efficiency. In particular, nature efficiently links small molecules together via heteroatomic C—X—C bonding to yield primary metabolites (polypeptides, polynucleotides, and polysaccharides – Figure 5.36), which are essential for life.

Click processes occur through simple reaction conditions such as air/moisture insensitivity, solventless or aqueous media, readily available precursors and reagents, and simple product isolation – mostly precluding chromatographic separation (unlike most organic syntheses). The utilization of click chemistry in combination with combinatorial screening will speed up the discovery of new pharmaceuticals that our society will continue to rely upon.^[44]

Beyond small-molecule drug discovery, click chemistry may also be exploited for the synthesis of polymers and supramolecular architectures.^[45] Since the overall properties of the polymer are closely related to its side groups, this technique has

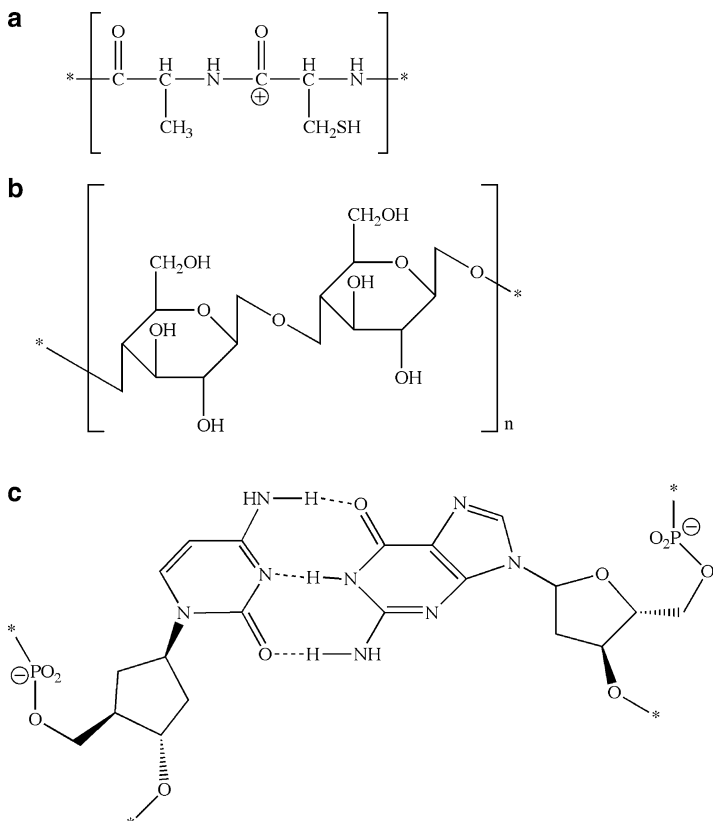
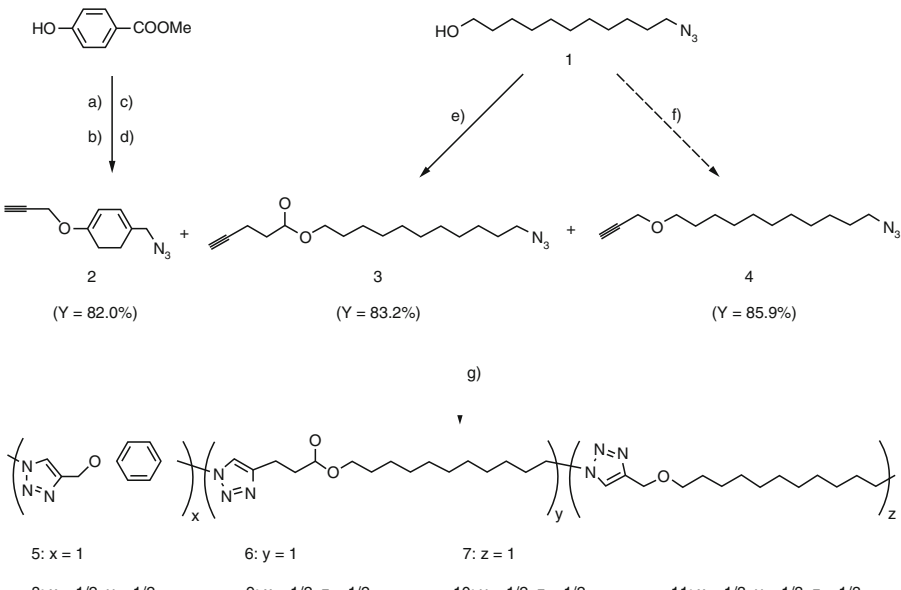


Figure 5.36. Examples of molecular structures for (a) polypeptides, (b) polysaccharides, and (c) polynucleotides.

been used to easily fine-tune polymeric structures by simple high-yield reactions of monomeric units (Figure 5.37). One example is the coupling of two linear-chain polymers to generate a block co-polymer; of significant challenge due to the reduced reactivity of the polymeric chain ends. A strategy to accomplish this difficult chemistry is to functionalize the endgroups with alkynyl or azido groups, which undergo high-yielding Cu(I)-catalyzed dipolar cycloaddition reactions.^[46] Even dendritic polymers may be synthesized or surface-functionalized using click chemistry (Figure 5.38). This may be of extreme interest to the industrial and scientific community, as the current cost of PAMAM dendrimers are still rather high. The latest version of PRIOSTAR™ dendrimers developed by Tomalia and coworkers are generated via click chemistry, and are touted to offer the analogous functionality and applications as PAMAM dendrimers at a fraction of the cost.^[47]



a) propargyl bromide, K_2CO_3 , acetone ; b) LiAlH₄, THF ; c) CBr_4 , $PPPh_3$, THF ; d) NaN_3 , H_2O ;
e) 4-pentynoic acid, DCC, DPTS, DMAP, CH_2Cl_2 ; f) propargyl bromide, NaH, THF ; g) $Cu(PPh_3)_4Br$, DIPEA, $CHCl_3$

Figure 5.37. Click chemistry step growth (co)polymerization of α -azide- ω -alkyne monomers **2–4**. Adapted with permission from Binauld, S.; Damiron, D.; Hammaïde, T.; Pascault, J.-P.; Fleury, E.; Drockenmuller, E. *Chem. Commun.*, **2008**, 4138. Copyright 2008 Royal Society of Chemistry.

5.3. “SOFT MATERIALS” APPLICATIONS: STRUCTURE VS. PROPERTIES

Thus far, we have considered a large number of polymer types, which are used for a diverse range of applications. In this section, we will now consider more specific examples of applications, to show how the molecular structure of the polymer drastically affects its properties. For polymers, only slight changes in the polymer backbone, or interaction with neighboring polymer chains, will lead to very different physical properties (and resultant applications). Whereas the backbone structure affects the polymer's general flexibility, the intermolecular interactions between side groups of neighboring polymer chains affect the overall strength, solubility, crystallinity, and glass-transition temperature (T_g).

As you might expect, the influence of the nature and density of side groups *vs.* the backbone structure will strongly depend on the relative composition of each polymer unit, as well as how open the structure is to its environment. Regarding the relative composition of a polymer, even though a polymer may have a polar backbone structure (*e.g.*, ether and/or ester linkages), the structure may not be soluble within polar solvents. That is, if long nonpolar side chains are also present in the polymeric

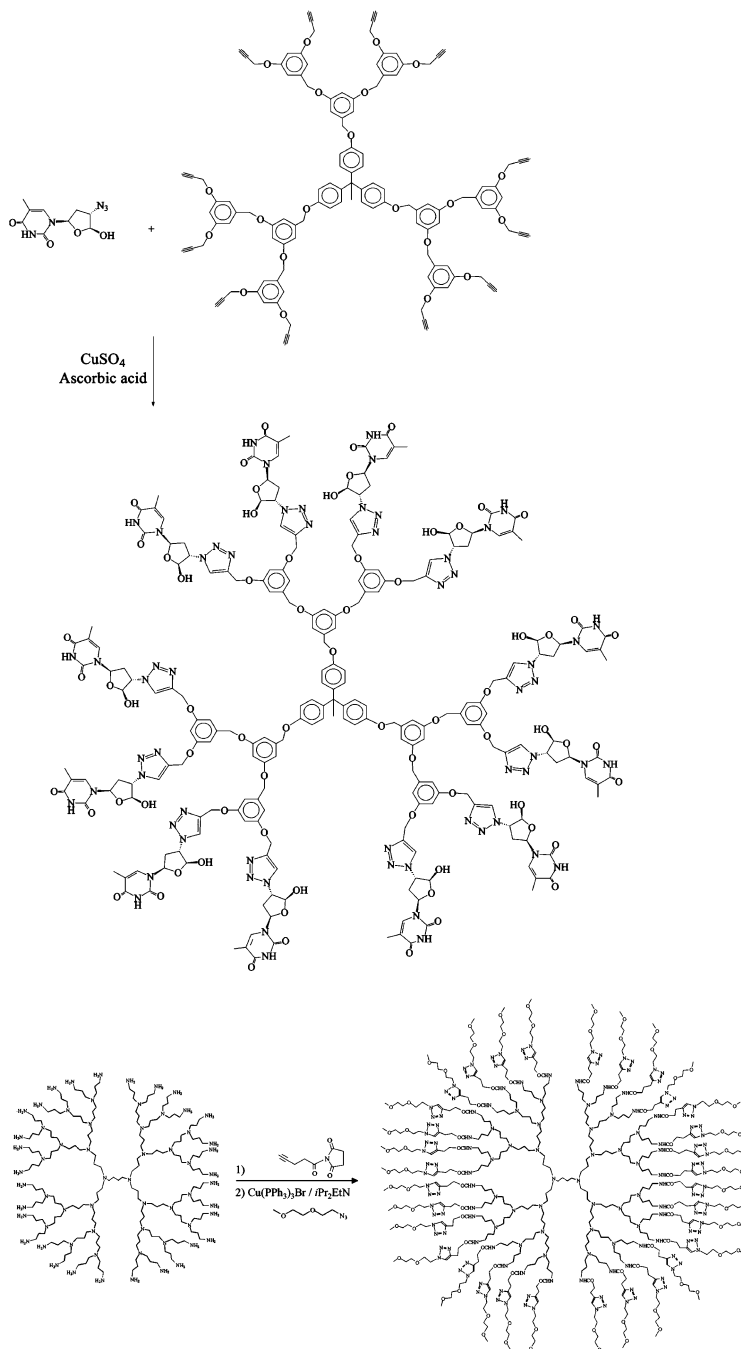


Figure 5.38. Dendrimer synthesis using aqueous click chemistry. Reproduced with permission from Malkoch, M.; Schleicher, K.; Drockenmuller, E.; Hawker, C. J.; Russell, T. P.; Wu, P.; Fokin, V. V. *Macromolecules*, 2005, 38, 3663. Copyright 2005 American Chemical Society.

structure, its solubility and reactivity will be outweighed by the presence of hydrocarbon chains. A useful analogy to keep in mind is the pronounced decrease in water solubility of simple alcohols, from methanol (completely miscible) to hexanol and higher-hydrocarbon chains (complete immiscibility) as the overall ratio of non-polar:polar functionality increases.

Regarding the interaction of a polymer with its environment, consider the PAMAM dendrimers described in the previous section. For higher generations, the pronounced density of the peripheral functional groups prevents the solvent or other environmental molecules from interacting with the core groups. As a result, the solubility/reactivity of these polymers may be fine-tuned by varying the surface functional groups. As we will see in [Chapter 6](#), the inner-core shielding exhibited by dendrimers (*e.g.*, G4–G6 for PAMAM or PPI) allows one to encapsulate a number of species within these “nanocavity reactors” for a number of useful applications for novel nanomaterials synthesis, catalysis, and drug-delivery.

Table 5.4 lists the various functional groups that may be present in the polymer backbone and as side-groups, with their general effect on overall properties. It should be noted that these comparisons are over-simplifications; for example, the presence of crosslinking and/or combinations of different functionalities will yield very different polymer properties. As discussed above, the general trend of chemical inertness and solubility will depend on both the openness of the structure and nature/density of the side groups. For thermal stability, conductivity, and flexibility, the polymer backbone structure is most relevant. Changes from single to multiple bonding, and/or introduction of a delocalized resonance unit in the polymer chain, will have pronounced effects on overall properties. One factor that is not explicitly mentioned in Table 5.4 is the degree of branching. However, it should be intuitive that the greater degree of interaction among adjacent polymer chains will enhance the tensile strength and density of the polymer, as well as increase the T_g . Perhaps the best example of this behavior is for highly branched *low-density polyethylene* (LDPE; used for squeeze bottles, food packaging film, plastic tubing, *etc.*) vs. weakly branched *high-density polyethylene* (HDPE; used for tupperware, milk cartons, plastic bags, *etc.*), as illustrated in Figure 5.39. Whereas the density and tensile strength for HDPE is 0.941–0.965 g/cm³ and 43 MPa, LDPE has values of 0.910–0.925 g/cm³ and 37 MPa, respectively.

The crystallinity of a polymer is related to the packing efficiency of individual polymer chains with respect to one another. Not unlike the formation of small molecule single crystals, processing variables such as temperature and time are paramount for influencing the degree of crystallinity. As previously mentioned, non-amorphous polymers may be considered as semicrystalline at best, with regions of crystallinity within the largely disordered polymer matrix. Typical crystalline polymers are polypropylene and polyethylene (especially isotactic and syndiotactic, Figure 5.40), acetals, nylons, and most thermoplastic polyesters. In general, crystalline polymers have high shrinkage, low transparency, a distinct melting point, and possess good chemical and wear resistance. By contrast, polymers that contain bulkier side-groups on their chains, such as polystyrene, polycarbonate, acrylic,

ABS, and polysulfone, tend to form amorphous polymers. Based on their disordered structure, amorphous polymers have low shrinkage, a transparent appearance, a broad melting point, and poor chemical and wear resistance.

Silicones

Though most of the backbone units appearing in Table 5.4 are carbonaceous, there is one major class of polymers that are comprised of crosslinked $[O-SiR_2]_n$ units. These polymers are known as *silicones* or *polyorganosiloxanes* – infamously popular due to the bad press over a decade ago concerning silicone breast implants. By varying the $-Si-O-$ chain lengths, Si-alkyl groups, and extent of crosslinking, the resultant polymer may exist as a viscous liquid (*e.g.*, vacuum pump oil), a gel (*e.g.*, silicone grease), or rubbery material (*e.g.*, used for remote control key-pads). Figure 5.41 illustrates the diverse use of silicone-based devices within the body. Their extensive use for biomedical applications is due to their biocompatibility, sterilizability, surface adhesion, oxygen permeability, and resistance to attack

Table 5.4. Influence of Polymer Structure on Resultant Properties

^b Backbone unit/ ^a substituent	Induced molecular properties
^b Saturated carbon ($—C—C—$)	Chain flexibility, thermal/oxidative reactivity
^b Unsaturated carbon ($—C=C—$)	Chain rigidity, high T_g , oxidative reactivity
^b Aromatic ($—C=C=C—$)	Chain rigidity, colors, electrical conductivity (if aromatic rings: oxidative resistance, high strength, stacking/self-alignment (liquid crystals ^[48]))
^b Ether ($—C—O—C—$)	Chain flexibility, oxidative/hydrolytic stability (unless in Lewis acidic media), soluble in polar solvents (for small substituents)
^b Anhydride ($—C—C(O)—O—C(O)—C—$)	Chain flexibility, water sensitive (especially for short aliphatic chains)
^b Amide ($—NH—C(O)C—$)	Chain rigidity, crystalline, water sensitive
^b Siloxane ($—R_2Si—O—$)	Chain flexibility and low T_g (especially for small substituents), stable toward oxidation, acid/base reactive
^b Phosphazene ($—R_2P=N—$)	Chain flexibility, high chemical inertness
^b Sulfur ($—S—S—$)	Chain flexibility, thermal/oxidative reactivity
^s Hydrogen ($—H$)	Chain flexibility, low T_g ; if bound to non-C atoms: H-bonding (high T_g , m.p., chemical reactivity)
^s Alkyl ($—CR_3$)	Chain rigidity, hydrophobicity, chemical inertness, noncrystallinity, solubility in nonpolar solvents (properties dependent on size of R groups – most pronounced for aryl groups)
^s Halogens ($—F, —Cl$)	Fluoride: extreme chemical inertness, hydrophobicity, insolubility in virtually any solvent Chloride: chemical inertness, chain stiffness, photolytic sensitivity, ↓ solubility, fire retardancy
^s Hydroxyl ($—OH$)	Hydrophilic, H-bonded rigid framework ($\uparrow T_g$)
^s Cyano ($—CN$)	Hydrophilic, dipole–dipole interactions: $\uparrow T_g$ and crystalline
^s Amide ($—C(O)NH_2$)	Hydrophilic, very high T_g due to strong H-bonding
^s Ester ($—C(O)O—$)	May be hydrophilic or hydrophobic depending on alkyl substituents, T_g also varies with nature of R and tacticity of units
^s Ether ($—O—CR_3$)	Hydrophilic at low temperatures, solubility and properties vary with R groups and tacticity
^s Carboxylic acid ($—C(O)OH$)	Hydrophilic and hygroscopic in solid-state

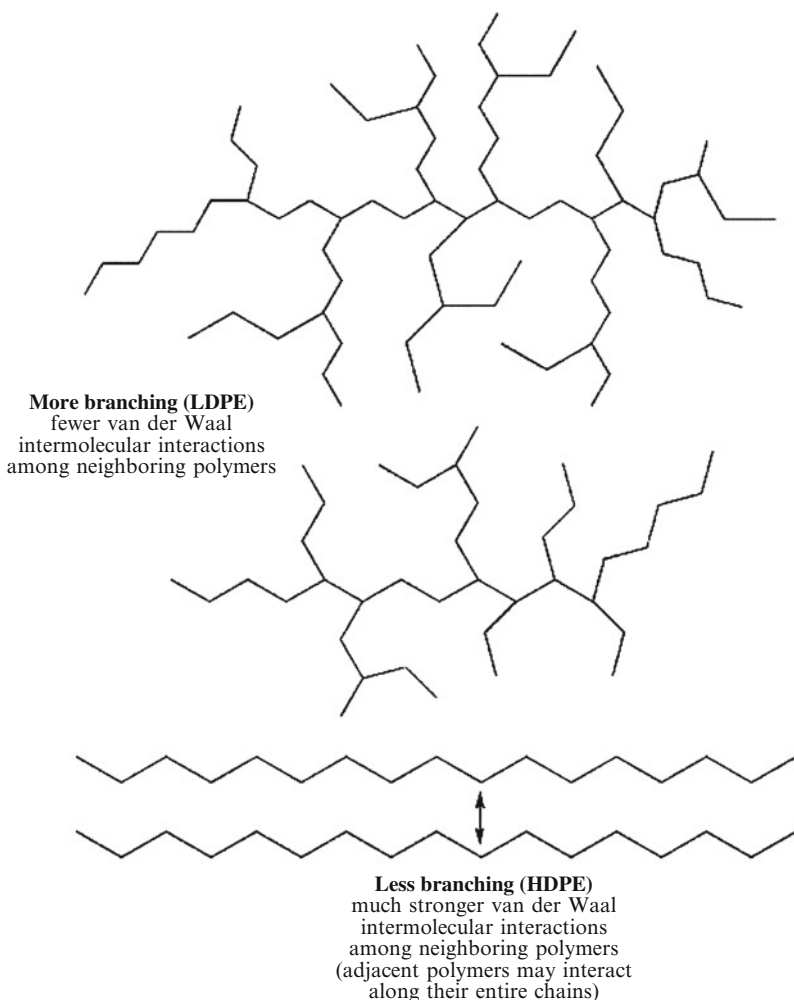
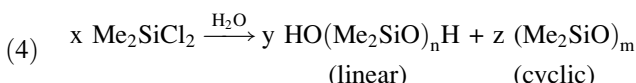


Figure 5.39. Comparison of low-density polyethylene and high-density polyethylene backbone molecular structures. A higher degree of branching (LDPE) results in greater separation of neighboring polymer chains and fewer intermolecular interactions. By comparison, with little/no branching, adjacent chains may closely associate with one another, resulting in strong van der Waal forces along the entire length of the polymer chains.

from body defense systems. The most widely used silicones are known as *poly-dimethylsiloxanes* (PDMS), formed from the hydrolysis of chlorosilanes in the presence of water (Eq. 4). In order to increase the polymer size to that required for most applications, the linear and cyclic oligomeric units are subsequently condensed and polymerized, respectively.^[49]



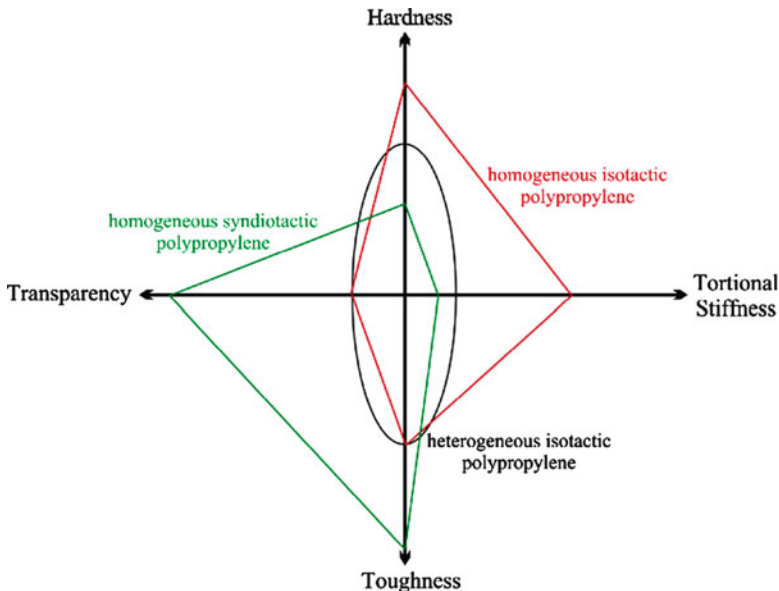


Figure 5.40. Tacticity vs. bulk properties for polypropylene polymers. The “homogeneous” and “heterogeneous” notations refer to whether the entire polymer chains, or only regions, are of a certain tacticity.

5.3.1. Biomaterials Applications

The world of biomaterials is diverse, encompassing ceramics and metals used for orthopedic implants (already discussed in [Chapters 2 and 3](#)), to artificial heart valves, blood vessel stents, and contact lenses. This section will delve into those biomaterials applications that utilize “soft” polymeric-based materials.

Biodegradable polymers

In our ever-increasingly “green” society, it is becoming hard to justify the use of traditional synthetic, non-biodegradable polymers for short-lived applications such as packaging, personal hygiene, surgery, etc. In addition to the persistency of non-biodegradable polymers in the environment, groundwater/soil pollution is also possible via additive leaching. Combustion (and even recycling processes) of these polymers consumes large quantities of energy and may also yield toxic emissions such as dioxins. Anyone who has seen dramatic images of plastic bottle holders wrapped around the necks of wildlife should be moved to evaluate viable alternatives that will break down more readily in the environment.

By definition, *biodegradable* materials exhibit chemical structures that will decompose under aerobic (*e.g.*, composting) and/or anaerobic (*e.g.*, landfill) conditions.^[50] Typical degradation byproducts are CO₂, CH₄, H₂O, inorganic compounds (*e.g.*, PO_x, SiO_x), or biomass. Whereas *degradation* refers to the decomposition of a polymer by chemical means (*e.g.*, hydrolysis), *biodegradation* is carried out by the

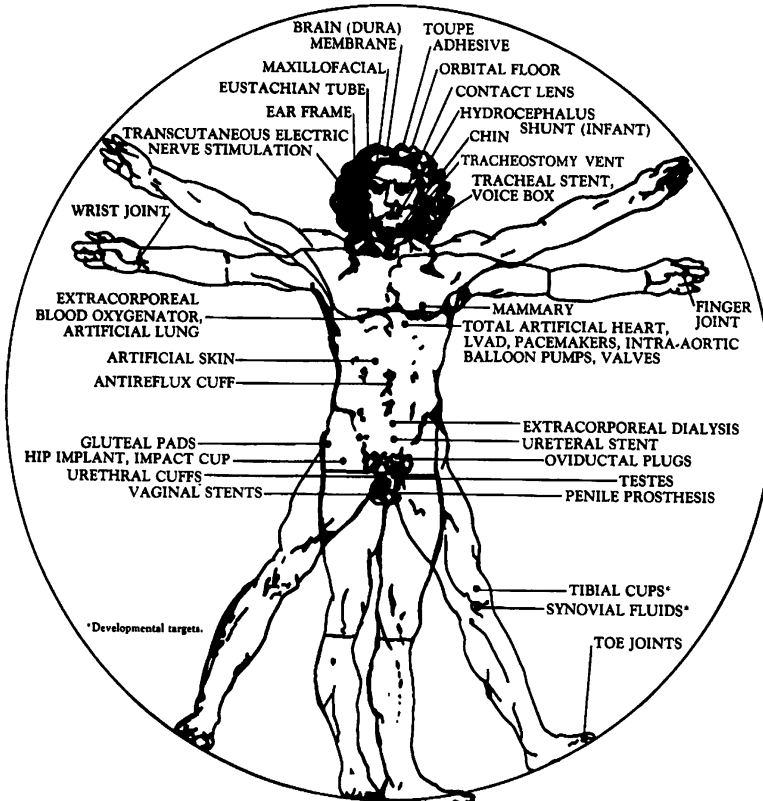


Figure 5.41. Placement of silicone-based medical devices in the body. Reproduced with permission from CHEMTECH 1983, 13, 542.

enzymatic activity of microorganisms. In this latter route, the decomposition of the plastic is afforded by the metabolism by microorganisms that generate an inert humus-like byproduct that is much less environmentally-harmful/pervasive. The terms *bioabsorption* or *biore sorption* refer to the degradation byproducts being used in cellular processes.^[51]

Biodegradable polymers should exhibit the following characteristics:

- (i) Biocompatible (e.g., elicits little/no immune response or is able to integrate with a particular tissue);
- (ii) Tunable and predictable degradation mechanism and rate;
- (iii) Non-toxic degradation products and metabolites;
- (iv) Non-toxic additives (e.g., monomers, initiators, emulsifiers, etc.);
- (v) Easy to synthesize and process into the desired shape;
- (vi) Long shelf-life and facile sterilization

There are two primary classes of biodegradable polymers – either naturally-occurring or generated using synthetic organic procedures (Figure 5.42).^[52] There

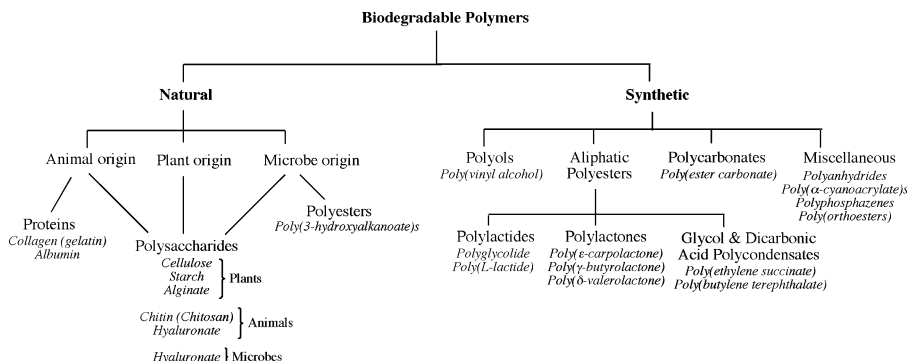


Figure 5.42. Classification scheme for biodegradable polymers.

are three origins of natural polymers, from plants, animals, or microbes. Polymers such as polysaccharides may be formed from all of these sources, whereas natural polyesters (*e.g.*, poly(3-hydroxyalkanoate)s) are generated exclusively from microbial routes. It should be noted that all natural polyesters are biodegradable; however, most synthetic varieties such as those used for fabrics, bottles, tarpaulins, canoes, LCDs, filters, etc., are not.

The majority of biodegradable polymers are synthesized by a *ring-opening polymerization* mechanism (*e.g.*, Figure 5.43).^[53] One example is the ring-opening polymerization of lactide to yield poly(lactic acid) (PLA) – one of the most widely used biodegradable polymers.^[54] This route features an aluminum or tin^[55] alkoxide complex that catalyzes a “coordination insertion” mechanism, which proceeds via rupture of the acyl-oxygen bond of the monomer (Figure 5.44).^[56] Monocarboxylic iron complexes have also been shown to polymerize *l*-lactide by an anionic-based insertion mechanism.^[57] By definition, either cationic or anionic ring-opening polymerization may take place, wherein the reactive center of the propagating chain is a carbocation or carbanion, respectively. Recently, IBM has developed a family of organocatalysts such as N-heterocyclic carbenes, bifunctional thiourea-amines, and “superbases” (*e.g.*, guanidines, amidines) for the controlled polymerization of strained heterocyclics. As Figure 5.45 illustrates, this new synthetic method is amenable for the polymerization of lactones (*e.g.*, PLA; poly(vinylalcohol) – PVA, etc.), cyclic carbonates (*e.g.*, poly(tetramethylene carbonate) – PTMC, etc.), ethers (*e.g.*, poly(ethylene oxide) – PEO), and silyl ethers (*e.g.*, poly(dimethylsiloxane) – PDMS, etc.).^[58] It should be noted that enzymatic routes have also been investigated in recent years – a truly “green” alternative for polymer synthesis.^[59]

Figures 5.46 and 5.47 illustrate the various oxidative and hydrolytic biodegradative reactions, respectively, which are responsible for polymer degradation. As one can see, polymers with C(O)X groups such as esters, amides, urethanes, etc. are particularly hydrolytic degradable. In contrast, groups that are stable toward hydrolysis (non-biodegradable) include hydrocarbon backbones (*e.g.*, polyethylene, polypropylene), halocarbon backbones (polytetrafluoroethylene, poly(vinylidene

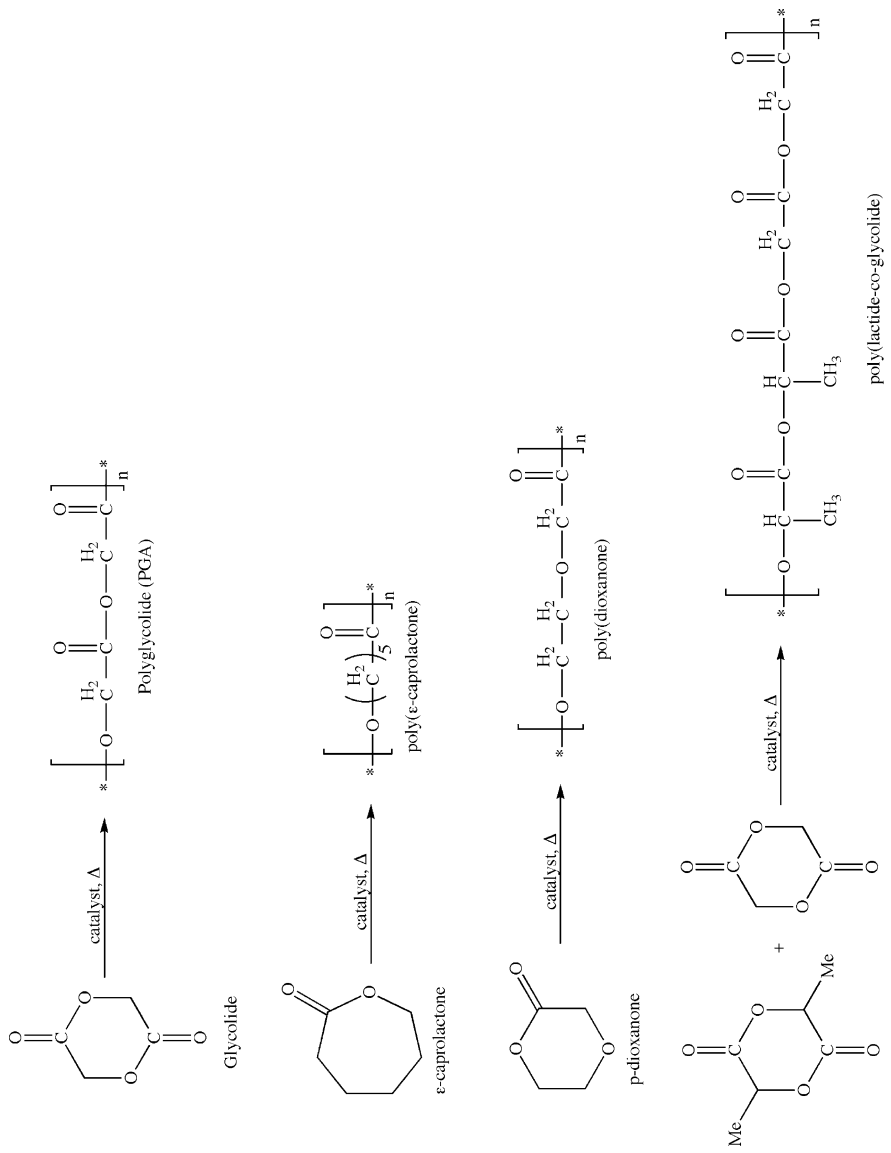


Figure 5.43. Ring-opening polymerization of various biodegradable polymers.

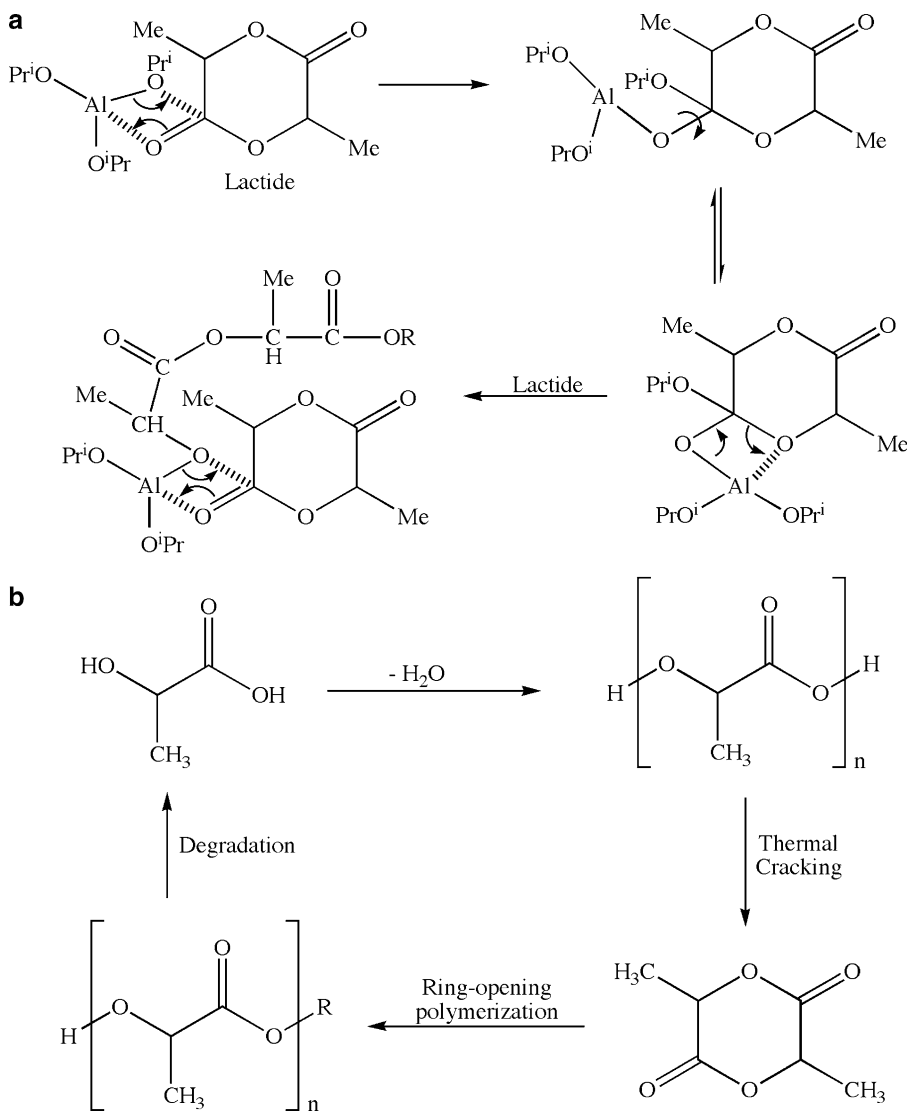


Figure 5.44. Mechanism for the ring-opening polymerization of poly(lactic acid), catalyzed by an aluminum alkoxide complex.

fluoride), polychlorotrifluoroethylene, etc.), alkylsiloxanes (e.g., dimethylsiloxanes, $(\text{R}_2\text{SiO})_x$, etc.), and sulfones ($(\text{OS}(\text{O}))_x$).

The applications for biodegradable polymers span a variety of fields such as:

- Agriculture (e.g., mulch films, temporary planting pots, fertilizer/pesticide delivery)
- Fisheries (e.g., fishing lines, nets, hooks)
- Sporting goods (e.g., golf tees)

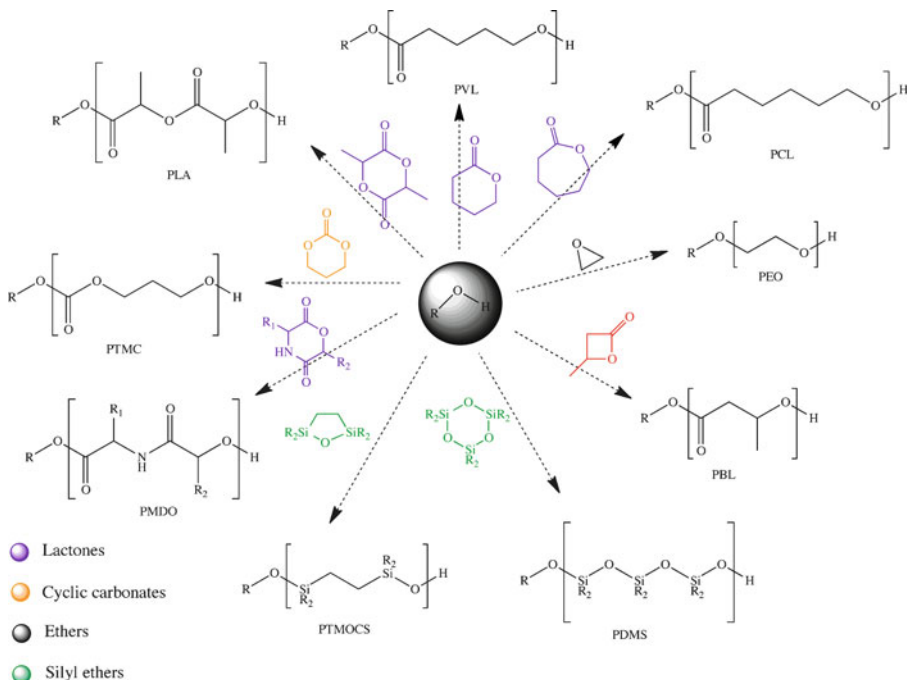


Figure 5.45. Diverse applicability of novel N-heterocyclic carbene, bifunctional thiourea-amine, and “superbase” catalysts for the polymerization of strained heterocyclics. Reprint courtesy of International Business Machines Corporation, copyright 2009 © International Business Machines Corporation.

- Food packaging (e.g., disposable plates, cups, bags, cutlery, bottles, retail bags, six-pack rings)
- Hygiene (e.g., feminine hygiene products, refuse bags, cups)
- Medical (e.g., suturing, fractured bone fixation, wound covering, skin/blood vessel/nerve reconstruction, controlled drug delivery).

For biomedical applications, an implanted polymer may be designed to degrade at an appropriate rate to transfer stress to surrounding tissues as they heal. This is afforded by designing the bulk geometry of the implant, the chemical stability of the polymer backbone, and the presence/concentration of additives such as plasticizers.^[60] The degree of polymer crystallinity also plays a crucial role in its overall degradation kinetics. For instance, whereas amorphous poly(*dl*-lactide), is 100% degraded in 3–6 months, it may take 1–2 years for crystalline PLA to degrade under analogous conditions. Accordingly, one may design a polymer with varying degrees of crystallinity for time-delayed drug delivery applications.^[61] The preferred use of PLA for implantable biomedical applications is due to its high degree of bioresorption via degradation to lactic acid, which is metabolized through the Krebs cycle. Accordingly, since its development in the 1960s, there are now more than 200 biomedical products made from PLA or PLA-based co-polymers.

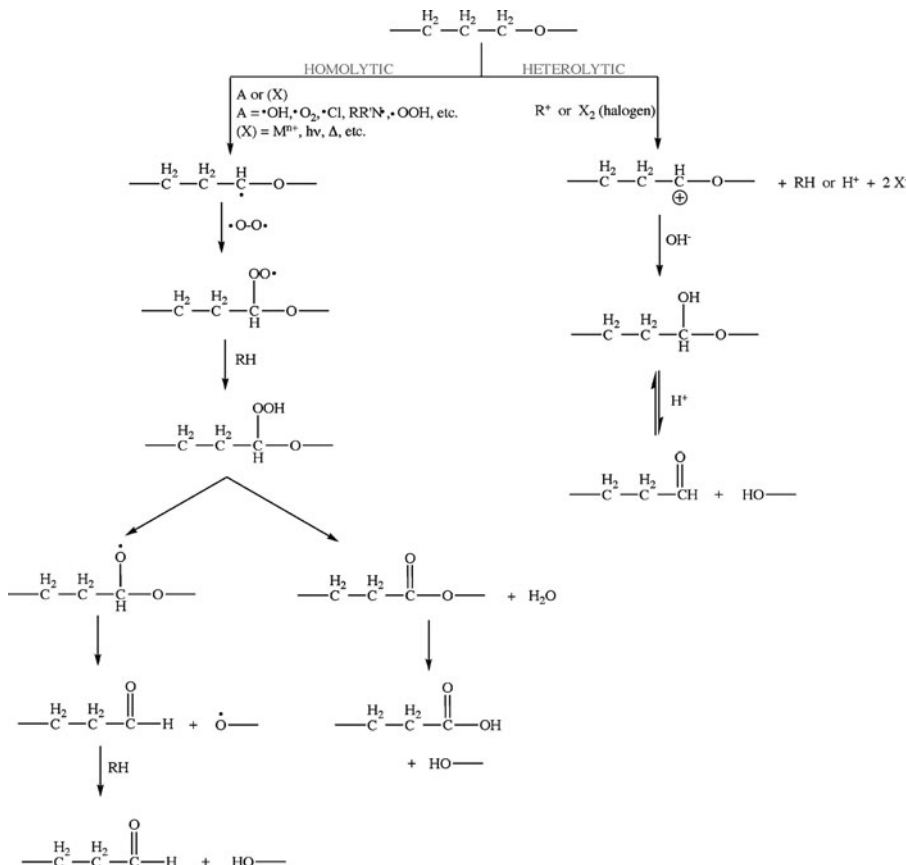


Figure 5.46. Stepwise degradation routes for a biodegradable polymer via oxidative chemical reactions.

To further illustrate the effect of polymer structure on its degradation (of importance for its viability for implant applications), let's consider silicone breast implants – developed by Dow Corning in 1961 and first implanted in 1962. Due to reports of numerous health complications resulting from breast implants, countless class-action suits were brought against Dow Corning in the mid-1980s – late-1990s.^[62] The ensuing multi-billion dollar settlement in 1998 nearly caused the financial ruin of Dow Corning Corporation.^[63] One of the early generations of implants featured a poly(ester urethane) (**III**) coating on the silicone shell, in order to prevent *capsular contracture* – an abnormal response of the immune system to foreign materials. However, due to the large numbers of ester linkages, this polymer was shown to degrade resulting in carcinogenic aromatic amines such as 2,4-toluenediamine.^[64] Limiting the number of ester groups (e.g., **IV**, poly(ether urethane) or **V**, poly(ester urethane urea)) results in a significant improvement in the hydrolytic stability of the polymer. As shown by structures **III–V**, the polymeric coating must exhibit a tunable

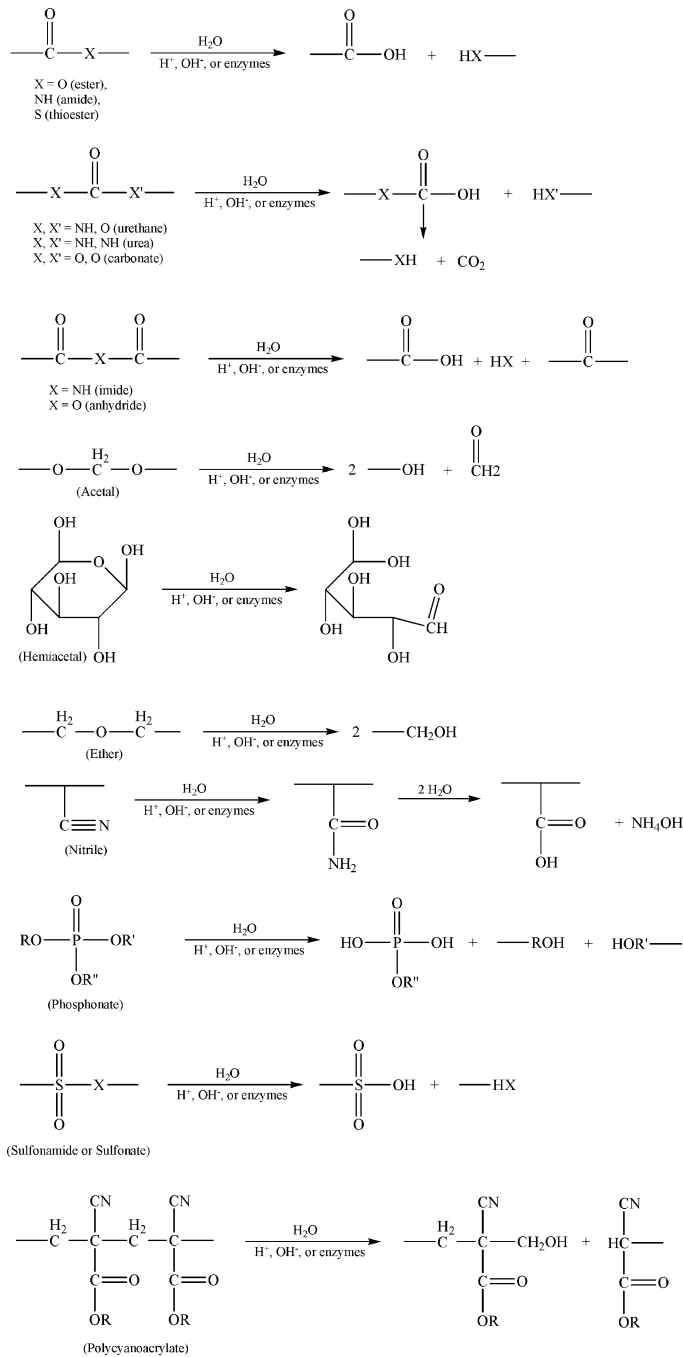
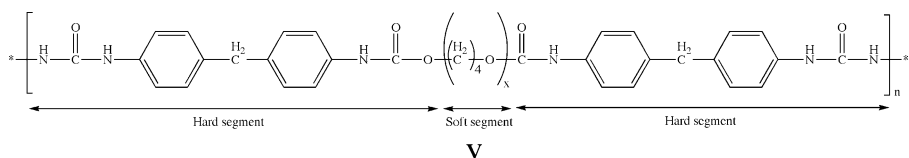
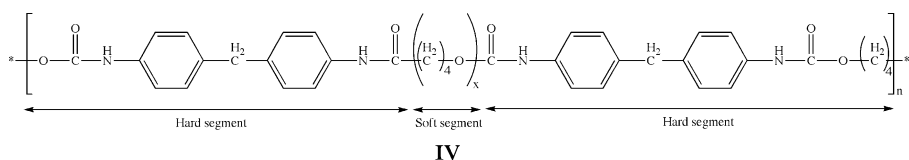
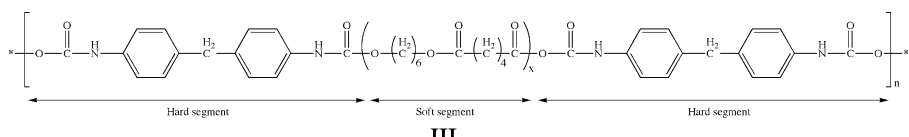


Figure 5.47. Degradation of various functional groups via hydrolytic chemical reactions.

stiffness (“hard” and “soft” regions) that will hold the silicone gel in place while suitably interacting with the surrounding soft tissue.



For applications that require sealing or adhesion to tissues, liquids such as 2-cyanoacrylates are commonly used that rapidly cure to form an adhesive gel. We are all familiar with the fast-setting ethyl-2-cyanoacrylate adhesive that is sold under the trade name of Super Glue or Krazy Glue (ethyl-2-cyanoacrylate). Veterinary glues employ n-butyl-cyanoacrylate (Vetbond and LiquiVet), whereas medical grade adhesives such as LiquiBand, SurgiSeal, and Dermabond employ 2-octyl-cyanoacrylate. Polymerization is catalyzed by the presence of moisture; chain initiation occurs via the nucleophilic attack of the ethylenic carbon by hydroxide ions (Figure 5.48). The fast-setting properties of the monomer to form a strong water-proof polymer (often in <1 min) is due to the presence of additives such as toluidine (o-methylaniline, or 2-aminotoluene; $C_6H_4(NH_2)(CH_3)$).

Another important application for biodegradable polymers is the design of *arterial stents*, used to prevent or counteract restricted blood flow that may lead to heart attacks or strokes if left unaddressed. Every year, over 800,000 angioplasty procedures are performed in the U.S., consisting of expanding the lumen of the coronary artery with a balloon.^[65] Though this is a more desirable option to coronary

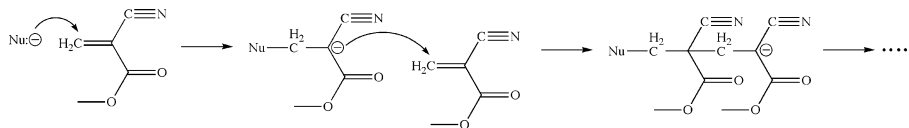


Figure 5.48. Mechanism for the polymerization of methyl-2-cyanoacrylate, catalyzed by the nucleophilic attack of OH^- .

bypass surgery, *ca.* 30–50% of angioplasty patients soon develop significant narrowing of the artery through migration and nucleation of smooth muscle cells, known as restenosis.

In order to offset the high restenosis rate following angioplasty, scaffolding devices known as *endoprostheses* or *stents* have been used in recent years to facilitate fluid flow through a diseased coronary artery.^[66] However, *ca.* 10–50% of patients receiving stents still develop restenosis; consequently, patients must receive close monitoring (and possible additional treatment) long after the surgery is performed.^[67] Magnetic resonance imaging (MRI) is emerging as a preferred method to detect, diagnose, and monitor the formation of dangerous plaques within arteries. However, most stents are comprised of metal alloys, which produce distortion in MR images. In order to circumvent these problems, DeSimone and coworkers at the University of North Carolina at Chapel Hill have developed stents that are comprised of biodegradable/erodable polymers.^[68] Most importantly, these stents may contain a variety of agents (*e.g.*, sensitizers, dissolution inhibitors, photo-acid generators, thermally-, pH-, irradiation-, or light-activated catalysts, etc.) that allows one to achieve a controllable rate of degradation. In addition, the stent has also been shown to effectively elute a drug such as everolimus – an immunosuppressant used to prevent restenosis.^[69] Studies showed that the stent was completely bioabsorbed in patients after 2 years after implantation, with full restoration of vasomotion (ability of the blood vessel to contract/expand). Due to the drug-eluting properties of the stent, patients had a 0% rate of stent thrombosis (blood clot formation). This work sets an amazing precedent for “smart” implantable devices, which perform their designed function(s) and then completely disappear without any side-effects!

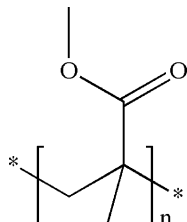
Contact lenses

The concept of contact lenses was first reported by Leonardo DaVinci (1508) and Rene Descartes (1632). However, it wasn’t until the late 1800s that the first contact lenses were developed by Muller, Fick, and Kalt.^[70] The lenses were comprised of blown glass, being molded from rabbit and cadaver eyes.^[71] While these early designs proved to be successful for eye protection and vision correction, you might imagine that a piece of glass covering the entire eye would be quite uncomfortable. In fact, there are reports that the pain resulting from wearing these lenses was so intense that a cocaine-based anesthetic was required!^[72]

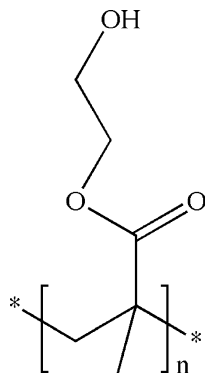
It is easy to get overwhelmed when one considers the requisite properties of contact lenses. In addition to being fabricated inexpensively and reproducibly, the lenses must also be biocompatible. That is, the polymers used in modern lenses must be capable of being in direct contact with the eye for an extended duration, as well as produced in such a way that any residual monomer/additive/catalyst does not pose a health risk. Further, since the lens floats on a layer of water known as the tear film, the polymer must be hydrophilic (especially for extended-wear varieties), while resisting the deposition of other components contained in tear drops such as protein, lipids, ions (*e.g.*, Na^+ , Ca^{2+} , HCO_3^-), and enzymes.^[73] In addition, the lens must be lightweight with sufficient mechanical strength to avoid being torn or scratched; of course, this must be balanced with a relatively high modulus of elasticity to facilitate

overall comfort when in use and ease of handling. The thickness of the lens must be optimized to afford the desired optical correction and gas permeability (sufficient O₂ supply and CO₂ removal), while not interfering with eyelid functions. Lastly, the specific weight of the lens must be of the same order of magnitude as tear drops, so it will not migrate around the corneal surface. With so many property constraints, contact lens design represents a remarkable challenge for zealous materials chemists and scientists!

The first plastic ('hard') corneal contact lens was developed in 1936, fabricated from poly(methyl methacrylate), PMMA (**VI**).^[74] However, these lenses were not commercially available until the mid 1960s. In comparison, 'soft' contact lenses were first comprised of poly(hydroxyethyl methacrylate), PHEMA (**VII**), and became commercially available shortly thereafter. Both types of lenses are comprised of a 3-D amorphous network of cross-linked polymer chains. However, the 'soft' vs. 'hard' character of a lens material is directly related to the ambient operating temperature relative to its glass-transition temperature (T_g). Whereas PMMA has a T_g of 100–120°C, the T_g of PHEMA (*ca.* 10–15°C) lies below room temperature.^[75]



VI

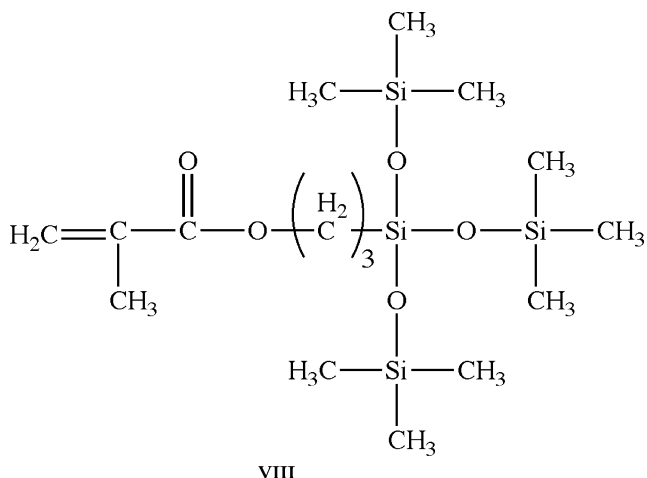


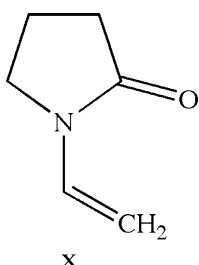
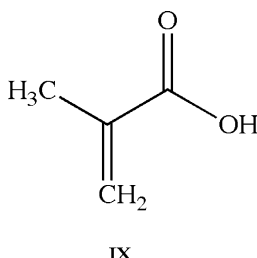
VII

The first type of hard contact lens was fabricated exclusively from PMMA. These lenses are hydrophobic, which effectively repels protein build-up; however, these

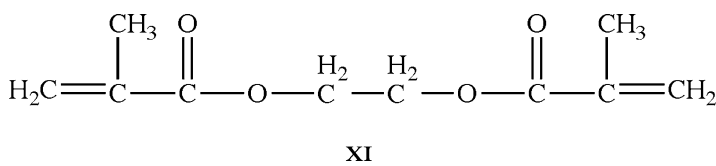
materials are impermeable toward gases such as O₂ and CO₂. Due to the lack of blood vessels within the cornea, the cornea must obtain oxygen directly from the atmosphere. Hence, it is essential to afford the highest level of oxygen diffusion through the lens in order to prevent hypoxia and promote corneal health by avoiding chronic limbal inflammation and facilitating turnover of epithelial/limbal cells during wear.^[76]

Though tears generated from normal blinking may facilitate sufficient oxygen transport, the impermeability of PMMA lenses may be overcome by co-polymerization of MMA (to maintain its structural rigidity) with silicone monomers. Accordingly, the first rigid gas-permeable (RGP) lens was comprised of methacryloxypropyl tris(trimethylsiloxy) silane (TRIS, **VIII**) copolymerized with MMA. Since silicones are hydrophobic, a hydrophilic monomer such as methacrylic acid (MAA, **IX**) or N-vinylpyrrolidone (NVP, **X**) must be added to improve the wettability and overall comfort.^[77] Even with these improvements, PMMA-TRIS lenses exhibit a relatively low gas permeability, which limits their use to no more than *ca.* 8 h at a time. In order to design extended-wear RGP contacts, MMA-TRIS lenses may be doped with fluoromethacrylates, which allows greater gas permeability via increasing its free volume, while more effectively repelling proteins and lipids. However, since fluorinated chains are hydrophobic, it is also necessary to cap the chains with hydrophilic methacrylate groups.^[78] With these modifications, one is able to wear such RGP lenses for up to 7 days.





The earliest soft lenses were fabricated from polymers such as PHEMA, later crosslinked with monomers such as ethylene glycol dimethacrylate (EGDMA, XI). These polymeric materials are classified as *hydrogels* since they are extremely hydrophilic, being able to absorb 10–1,000 times their dry weight of water. The polymer chains of hydrogels are normally decorated with hydrophilic groups such as —OH or —COOH to facilitate H-bonding with surrounding water molecules. The copolymerization of hydrogels with MAA and NVP will yield a polymer with much greater moisture content – up to 70% for modern lens designs. Network formation may be afforded by entanglement of (co)polymer chains, covalent crosslinking, or association of polymeric units via ionic or intermolecular forces (Figure 5.49). The water within hydrogels is either strongly bound or freely exchangeable, which is also paramount regarding their use as drug-delivery agents (*e.g.*, Figure 5.50) and mineralization media.^[79]



The latest varieties of contact lenses are based on silicones, first brought to the commercial market by Bausch & Lomb (PureVisionTM)^[80] and Ciba Vision (Focus

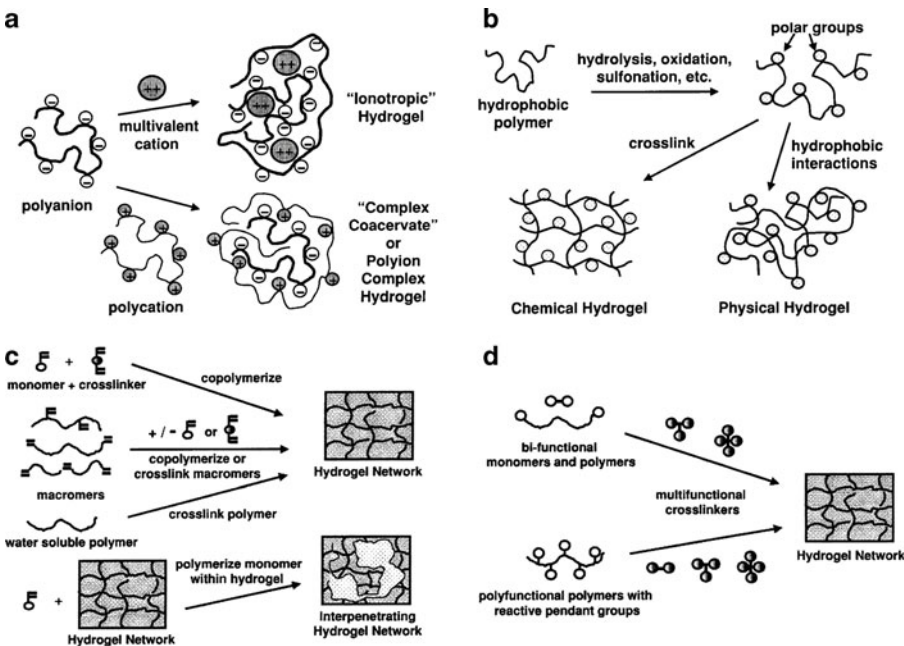


Figure 5.49. Four techniques used to synthesize hydrogels. (a) ionic hydrogel formation by gelling a polyelectrolyte solution with a multivalent ion of opposite charge (e.g., sodium alginate + CaCl_2), or by mixing polyanion and polycation solutions to form a complex gel (e.g., sodium alginate + polylysine); (b) chemical conversion of a hydrophobic polymer (e.g., partial hydrolysis of acetate groups in PVAc to $-\text{OH}$ groups in PVA); (c) copolymerization of a monomer and crosslinker in solution via free radical reactions (e.g., crosslinked PHEMA and PEG gels); (d) crosslinking of polymers in solution (or solid state) with multi-functional reactive compounds (e.g., PEG + diisocyanate to yield a PU hydrogel). Reproduced with permission from *Adv. Drug Deliv. Rev.* 2002, 43, 3.

Night & DayTM). The primary benefit of silicone hydrogels is their significantly greater water capacity, while retaining the comfort, wetability, and biofilm resistance of non-silicon based hydrogels. However, due to their pronounced hydrophobicity, the oxygen permeability of silicone hydrogels decreases exponentially as water content increases (Figure 5.51). Consequently, there has been much research devoted to improving their wetability via surface functionalization to replace siloxane groups. Thus far, this has been successfully accomplished by grafting polyoxyethylene to the surface, as well as using surfactants containing copolymers of lauryl-, hexyl-, and methyl-methacrylate and polyethylene glycol methacrylate.^[81]

The flux of oxygen through a polymeric contact lens is governed by *Fick's Law* (Eq. 5). In fact, Fick's law is used to predict the shelf life for food/beverages that are encased within polymeric packaging (e.g., polyethylene terephthalate (PET), etc.). The units of transmissibility are $10^{-9} \text{ cm s}^{-1} \text{ m LO}_2 \text{ mL}^{-1} \text{ mmHg}^{-1}$, which is equivalent to units of Barrer cm^{-1} . The first RGP lenses exhibited Dk/t values of $< 12 \text{ Barrers cm}^{-1}$, corresponding to a lower oxygen flux than a cornea of a non-

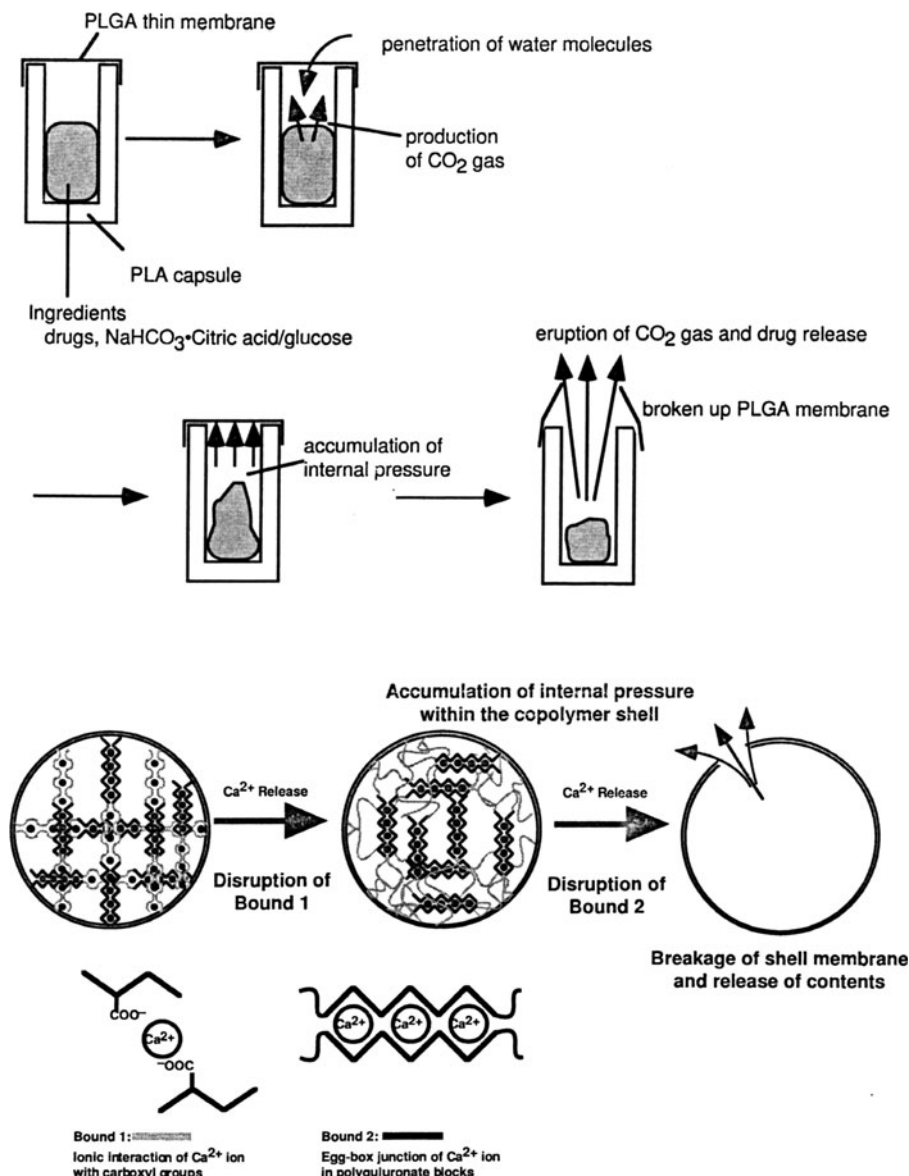


Figure 5.50. Examples of drug delivery using hydrogel membranes. Top: carbon dioxide gas pressure causes rupture of membrane, controlled by the membrane thickness and amount of CO₂ being produced. Bottom: drug release from a polysaccharide alginate capsule, facilitated by multivalent/monovalent ion-exchange, controlled by the molecular weight of the alginate and size of the capsule. Reproduced with permission from *Adv. Drug Deliv. Rev.* **2002**, 54, 53.

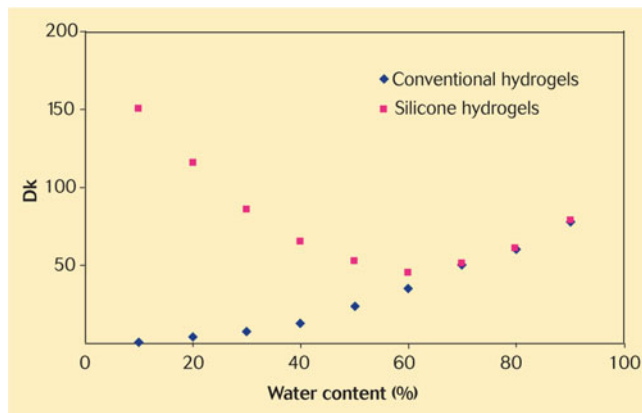


Figure 5.51. Variation of oxygen permeability with equilibrium water content for conventional and silicone-based hydrogels. Reproduced with permission from *Optician*, 2005, 230, 16.

Table 5.5. Oxygen Transmissibility for Various Soft Contact Lenses^a

Lens	Dk/t ^b	J _{open-eye} ^c	% of maximum	J _{closed-eye} ^c	% of maximum
100 µm HEMA	7.5	3.95	52%	1.50	25%
Acuvue 2	26	6.65	88%	4.09	68%
Acuvue advance	86	7.31	97%	5.55	92%
Purevision	110	7.37	98%	5.68	94%
O ₂ optix	138	7.4	98%	5.8	96%
Acuvue oasys	147	7.4	98%	5.8	96%
Focus night and day	175	7.44	99%	5.84	97%
No lens	∞	7.54	100%	6.04	100%

^a Data taken with permission from (a) French, K. *Optician* 2005, 6030, 16 and (b) Morgan, P.; Brennan, N. *Optician* 2004, 5937, 27.

^b Manufacturer values quoted for -3.00DS lenses.

^c Units: µL cm⁻² h⁻¹.

wearer (both open-eye and closed-eye).^[82] Most typical modern RGP lenses have Dk/t values of 15–25 Barrers cm⁻¹, whereas soft lenses have much higher values (Table 5.5). For a lens to be approved for extended-wear applications, the Dk value must be ≥ 100 Barrers.

$$(5) \quad J = \left(\frac{Dk}{t} \right) \Delta P,$$

where:

J = oxygen flux (units: m s^{-1})

Dk/t = transmissibility (*i.e.*, permeability per unit thickness, t); D = diffusion-coefficient, and k = solubility coefficient

ΔP = difference in oxygen partial pressure between the front and back of the lens (P_{front} : 159 mmHg (open eye) and 59 mmHg (closed eye); $P_{\text{back}} \propto$ lens transmissibility)

As one would expect, there is a difficulty in determining the pressure at the posterior surface of the lens; consequently, a value known as the equivalent oxygen percentage (EOP, Eq. 6) may be used. The EOP provides an indirect measure of this pressure, determined empirically by placing a membrane-covered sensor against the corneal surface and determining its oxygen consumption rate.^[83] Whereas lenses with low Dk/t values such as PMMA result in very rapid O_2 -uptake rates, a lens-free cornea would deplete oxygen at a much slower rate. As Figure 5.52 illustrates, there is a large increase in the oxygen flux with increasing Dk/t until a threshold value is reached, corresponding to meeting the corneal oxygen demand.

$$(6) \quad \text{EOP} = 0.252(\text{WC}) - 2.912\log(L) - 20.611,$$

where:

WC = water content of the lens (relevant for 'soft' hydrogel lenses)

L = thickness of the lens, in μm (typical center thicknesses: 30–50 μm for soft; *ca.* 100 μm for hard)

As one can see from Eq. 6, the permeability of a soft contact lens is directly proportional to its water content (Figure 5.53). Whereas the moisture content of early PHEMA lenses was only *ca.* 35%, more recent silicone-based hydrogels contain up to 70% water. Though hydrophilic lenses are able to absorb water and permit extended wear without corneal irritation, an increase in water content also corresponds to lower mechanical strength that may result in tearing/scratching.

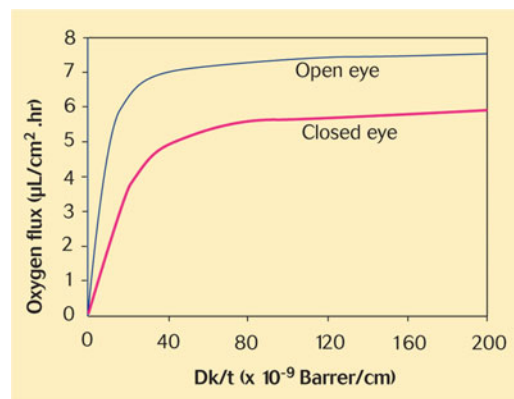


Figure 5.52. The relationship of oxygen flux and oxygen transmissibility for open- and closed-eye wearing conditions. Reproduced with permission from *Optician*, 2005, 230, 16.

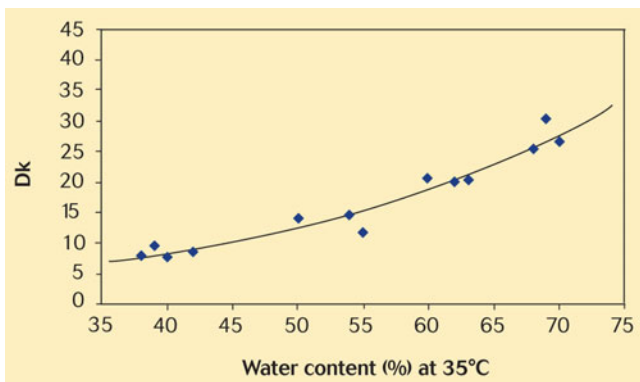


Figure 5.53. Relationship between oxygen permeability and water content for conventional hydrogel lenses at 35°C. Reproduced with permission from *Optician*, 2005, 230, 16.

Drug delivery

Anyone who has taken time-release medications (*e.g.*, nasal decongestants, allergy medications, etc.), or witnessed a loved one undergo chemotherapy has experienced a tangible application for biodegradable polymers: as *drug-delivery systems* (DDS).^[84] In the last few years, these materials have evolved from pills that generate systemic negative side-effects, to miniaturized devices that are able to target the region of interest and control the kinetics of drug release. Current DDS feature both spatial control (allowing for lower dosage and decreased side effects) and temporal control (to minimize fluctuations from the *therapeutic window*).^[85] Typical means of control over drug release include: diffusion (membrane-controlled – osmosis, swelling), chemical (biodegradable polymer backbones), particulate (polymer-drug conjugates, liposome systems, polymeric micelle systems, etc.), and responsive (T, solvents, pH, mechanical/magnetic/ultrasound, etc.). Future “smart” DDS are currently in development, which will contain a variety of sensors for the ‘on-demand’ release of a drug in the proper dosage based on the patient’s varying conditions. For instance, the delivery of insulin based on varying glucose levels, and growth hormones at key developmental stages to promote tissue growth.^[86]

An ideal “smart” drug-delivery agent will have the following characteristics:^[87]

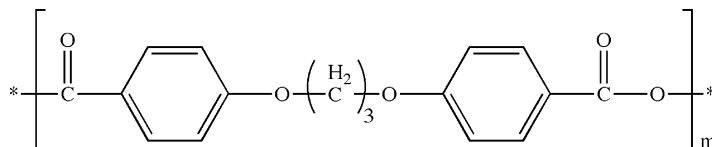
- (i) Inexpensive fabrication;
- (ii) Ease of drug loading;
- (iii) Biocompatible – minimal trauma during both ingestion/implantation and drug delivery;
- (iv) Facile tracking within the body, with external control via pre-/post-programming;
- (v) Small size for ease of ingestion/injection and to allow for precise spatial positioning of drug release (<1 μm is ideal for passage through all capillaries with minimal risk of damage or embolism).^[88]

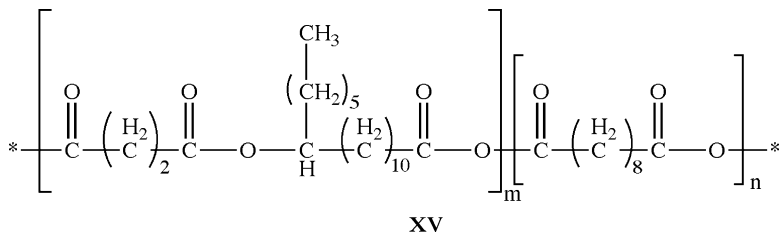
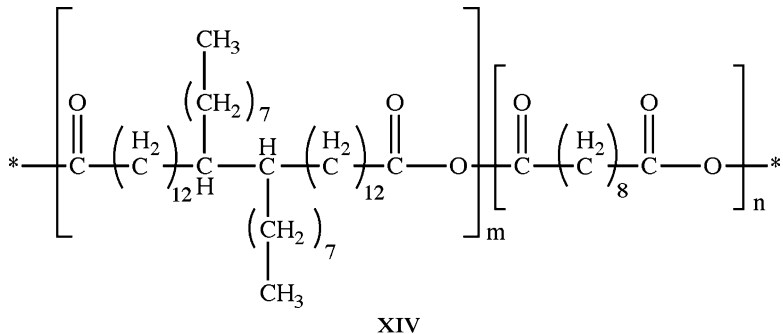
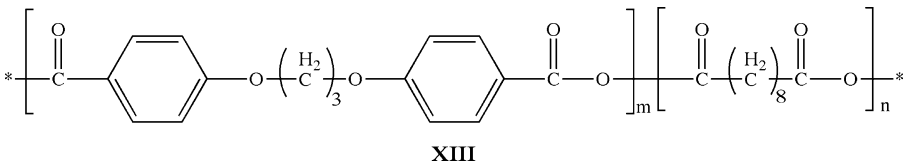
No current device meets all of these parameters. Diffusion-controlled release is demonstrated by transdermal patches (*e.g.*, birth-control, nicotine, etc.), whereas particulates such as metallic micro-/nanoparticles have been used to ablate cancer cells by localized heating with near-IR light.^[89] Whereas normal blood vessels have pore sizes <100 nm, the vessels adjacent to cancer cells have pore sizes between 100 and 200 nm. Hence, if DDS particulates (*e.g.*, liposomes, polymeric micelles, metallic nanoparticles) are of this size regime, they will automatically situate nearby cancer cells. However, it usually takes at least 1 day of blood circulation to accumulate sufficient amounts. In order to "hide" the particles from the immune system, the particulates must be covered with a 'stealth liposome' such as poly(ethyleneglycol), PEG; otherwise, the particulates will be filtered out of the body via the liver as urine.

Though the above strategies are currently in use for a variety of treatment options, most efforts in the design of DDS have been focused on biodegradable reservoir systems; for example, the treatment of prostate cancer and protein hormone delivery. In these materials, degradation occurs in four steps:

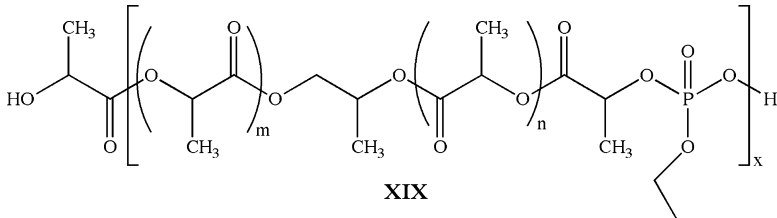
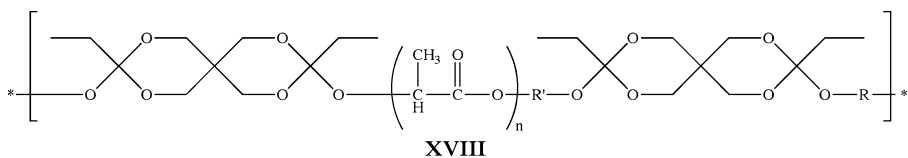
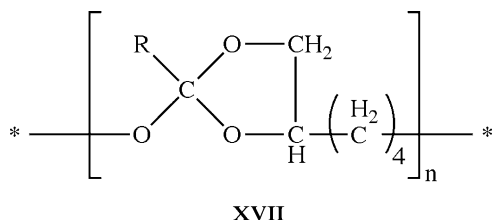
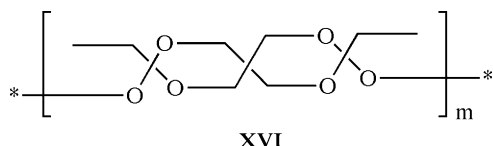
- (i) Water flows into the device, swelling the matrix and ester bond cleavage;
- (ii) The interior degrades faster due to a high concentration of acid (product, catalyst);
- (iii) Oligomers become solubilized and diffuse out of the device;
- (iv) Slow erosion of the shell.

The most common biodegradable polymers used for DDS include PGA, PLA and their copolymers. The rate of degradation may be controlled by its composition as well as crystallinity. However, due to the faster degradation of the interior, the localized acid concentration may become high enough to harm the therapeutic agent. A base such as Mg(OH)₂ may be incorporated to offset this acidity. For the treatment of malignant brain cancer, the use of polyanhydrides (*e.g.*, bis(p-carboxyphenoxy propane) – PCPP, **XII**) has proven successful; control over degradation rates may be afforded by decorating the backbone with aromatic groups, as well as copolymerization (*e.g.*, with sebacic acid – SA, **XIII**). The use of nonlinear polyanhydrides offers the benefit of enhanced mechanical properties, with the degradation rate being controlled by copolymerization (*e.g.*, an erucic acid dimer/sebacic acid copolymer, **XIV**, and a ricinoleic acid/sebacic acid copolymer, **XV**).

**XII**

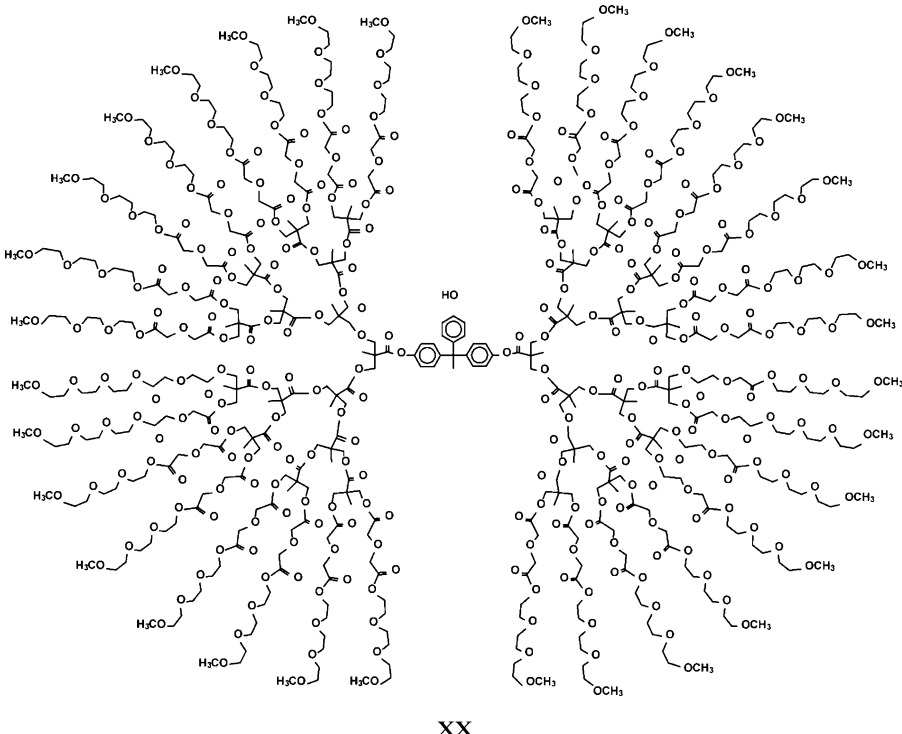


Another class of biodegradable polymers used for DDS includes poly(orthoesters), POEs. The benefits of these polymers include facile synthesis and control over degradation rates and mechanical properties (*e.g.*, POE **XVI** – rigid vs. POE **XVII** – flexible liquid/gel). Due to the highly hydrophobic nature of their backbones, POEs normally exhibit slow degradation; however, copolymerization with PLA (**XVIII**, used for periodontal disease and anesthetics) offers control over these kinetics. Though originally developed as flame retardants, poly(phosphoesters) may also be used as biodegradable DDS (*e.g.*, polylactophate (**XIX**), used for the controlled release of insulin and paclitaxel (cancer treatment)). These structures feature an extensive range of mechanical properties, while generating non-toxic degradation byproducts of phosphate ions, alcohols and diols.

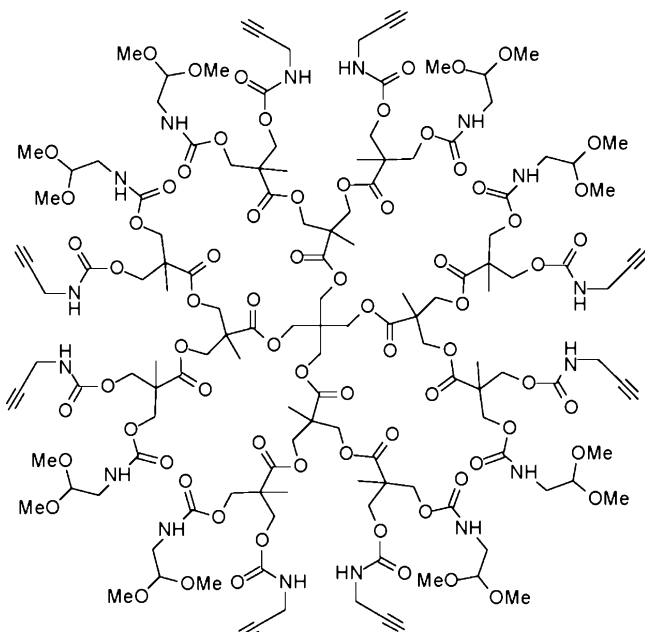


As mentioned earlier (Figure 5.32), dendritic polymers may also be used for drug-delivery applications. Due to their unique 3-D structures and the high availability and tunability of surface functional groups, drugs may be loaded within the interior, as well as attached to the periphery via electrostatic or covalent interactions. The use of PAMAM dendrimers is in development for the delivery of doxorubicin, an anti-cancer drug, as well as VivaGel®, a vaginal anti-HIV microbicide that is currently in Phase II clinical trials.^[90] However, PAMAM dendrimers resist degradation within the body, which has spurred recent interest in the development of

alternative dendritic polymers that are biodegradable. For example, Frechet and coworkers have developed polyester dendrimers based on the monomeric unit 2,2-bis (hydroxymethyl)propanoic acid, **XX**, for the controlled delivery of doxorubicin.^[91] Biodegradable bifunctional dendrimers, **XXI**, may also be synthesized, which will offer a greater opportunity for the binding of varied functionalities (*e.g.*, drugs, targeting/imaging agents, etc.) to the periphery relative to symmetric analogues.^[92]

**XX**

In recent years, advanced DDS have been fabricated using advanced lithographic techniques. As briefly discussed in Chapter 4, ‘soft’ imprint lithographic techniques such as solvent-assisted micro-molding (SAMIM), micro-molding in capillaries (MIMIC) and microcontact printing (μ -CP or MCP) most frequently employ PDMS as the material of choice for the mold. Though PDMS is used due to its UV transparency, biocompatibility, gas permeability, and low Young’s modulus (allowing for conformal contact and facile release from the (nonplanar) master without cracking), its use for small-feature patterning has recently been usurped by fluorinated analogues.



Desimone and coworkers have developed fluorinated elastomers for a technique coined as *pattern replication in nonwetting templates* (PRINT), which allows one to fabricate surface-bound or free polymeric structures of virtually any size and shape, with feature sizes reaching well below 100 nm.^[93] Figure 5.54 illustrates the PRINT technique, which is analogous to the MIMIC technique, with the use of

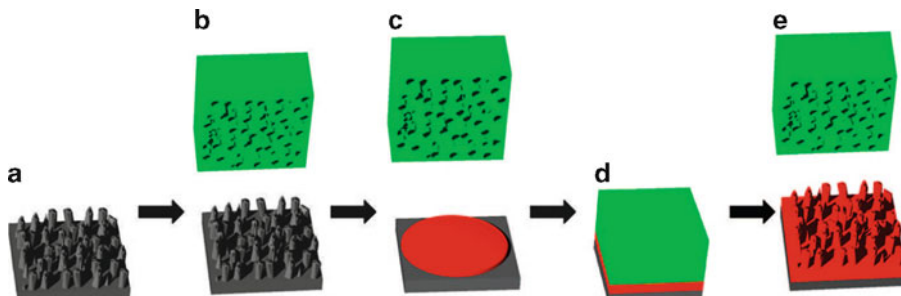
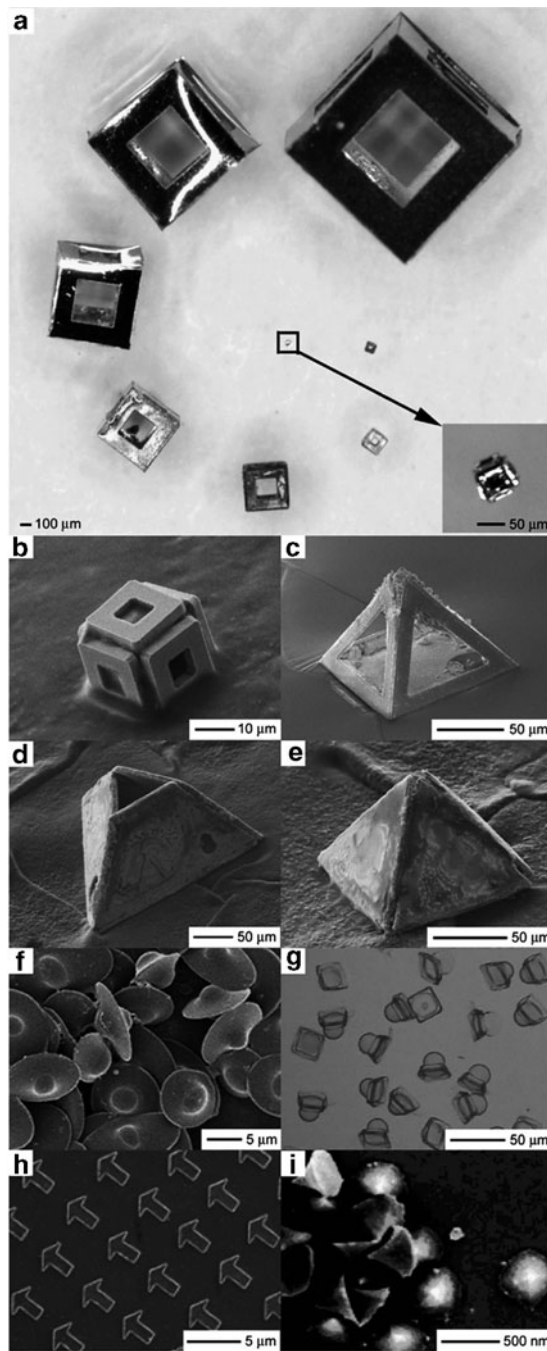
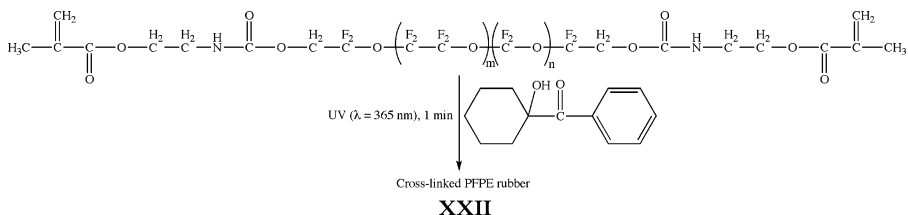


Figure 5.54. Illustration of the PRINT process. Shown are (a) Si master template, (b) mold release from master template, (c) molding a liquid precursor, (d) pattern transfer to a substrate at elevated temperature and pressure, and (e) mold release from replica film. Reproduced with permission from *Chem. Mater.* **2008**, *20*, 5230. Copyright 2008 American Chemical Society.



perfluoropolyether (PFPE, **XXII**) elastomers to realize the following benefits, relative to standard PDMS molds:



- (i) Lower surface energy, which allows selective filling of nanosized cavities in the mold with any organic liquid;
- (ii) Significantly greater swelling resistance in organic solvents;
- (iii) Greater chemical inertness, which allows the array of surface features to be easily separated from the mold to yield free-standing micro- or nanostructures;
- (iv) Greater tunability of the modulus by varying the precursor molecular weight, which allows one to pattern a variety of sol-gels into $<100 \text{ nm}$ features.

In addition to using PRINT to fabricate a variety of complex shapes (see Chapter 4 – Figure 4.73 and Figure 5.55f–i), a clever approach employs photolithography and self-assembly to generate cubic and pyramidal structures via “micro-/nano-origami” (Figure 5.55a–g and Figure 5.56). In this approach, a 2-D structure is formed with temperature-sensitive hinges that fold into the desired 3-D shape upon heating.^[94] As shown in Figure 5.56 (bottom), the drug-release characteristics may be fine-tuned in these structures, from isotropic to anisotropic, based on the relative porosity/permeability of its sidewalls.

5.3.2. Conductive Polymers

Though one generally considers polymeric materials as being non-conductive, there are specific structures that feature either metallic or semiconductive electrical properties. Unlike their inorganic analogues, conductive polymers generally feature high elasticity, toughness, solvent solubility, and low-temperature synthetic routes with facile structural (and property) tunability. Accordingly, these polymers are used for an

Figure 5.55. (a) An optical image showing free-standing, self-assembled fabricated cubic containers over 2 orders of magnitude in size from 2 mm to 50 μm and (b) 15 μm along with (c–e) different shapes. (f) Scanning electron micrograph of polystyrene particles, “UFOs”, created by film stretching techniques. Reproduced with permission from *Proc. Nat. Acad. Sci.* **2006**, *103*, 4930. (g) Optical micrographs of microcapsules in water, reproduced with permission from *Small* **2007**, *3*, 412. (h) SEM image of 300 nm conical-shaped poly(lactic acid) particles generated by using the Particle Replication In Nonwetting Templates (PRINT) method. (i) Manipulation of shape using PRINT: 3 μm arrow poly(ethylene glycol) particles. Images (a–c) reproduced with permission from *Langmuir* **2007**, *23*, 8747, (d–e) reproduced with permission from *J. Am. Chem. Soc.* **2006**, *128*, 11336, and images (h–i) reproduced with permission from *J. Am. Chem. Soc.* **2005**, *127*, 10096. Copyright American Chemical Society.

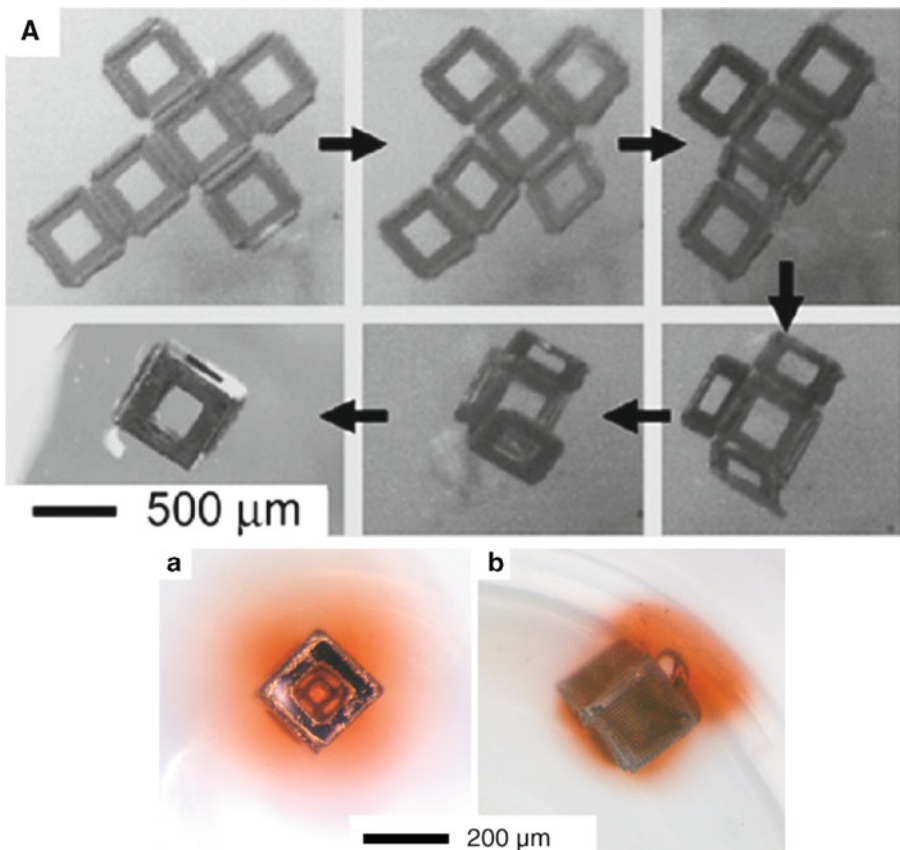


Figure 5.56. Top: video snapshots showing the self-assembly of a lithographically fabricated template into a 3D hollow container. Reproduced with permission from *Adv. Drug Deliv. Rev.* **2007**, *59*, 1547. Copyright 2007 Elsevier Science. Bottom: optical images of chemical release from containers: (a) isotropic release of a dye from a container with identical porosity on all faces; (b) anisotropic release of a dye from a container with varied porosity (five faces with an array of 5 μm pores; the sixth face has a 160 μm window). Reproduced with permission from *J. Am. Chem. Soc.* **2006**, *128*, 11336. Copyright 2006 American Chemical Society.

increasing number of applications such as: antistatic electromagnetic shielding, conducting fibers, electrochemical batteries, electrochromic “smart” windows, light-emitting electrochemical cells, organic field-effect transistors, organic light-emitting diodes (OLEDs), photovoltaic devices,^[95] nonlinear optics, and many more.^[96]

Whereas traditional polymers feature a saturated sp^3 -carbon framework, conductive polymers feature an unsaturated carbon backbone with 1 e⁻/C atom placed in sp^2p_z (π) orbitals. As we know from resonance structures, the overlap of π -orbitals on successive C atoms leads to electron delocalization along the length of the polymeric framework. Though one may surmise that such an inter-connected 1-D

array with delocalized electrons would result in metallic conductivity, this is not the case. In the 1930s, Peierls^[97] asserted that a 1-D chain of equally-spaced ions is energetically unstable, and will distort via an electron–phonon coupling mechanism to lower its overall energy.^[98] One may consider the Peierls distortion for chain structures as analogous to the Jahn-Teller effect for transition metal complexes.

A prototypical example of Peierls distortion is the bond alteration exhibited by polyacetylene (PA) first synthesized by Natta and coworkers in 1958 (Figure 5.57). Rather than considering polyacetylene as having equivalent C–C bond distances, adjacent bond lengths differ by *ca.* 6 pm (Figure 5.58). This conformational distortion is enough to increase its bandgap, making PA a semiconductor in its pristine (undoped) state; other pristine conductive polymers such as polyaniline are insulators (Figure 5.59).

In order to increase the conductivity, a dopant may be added to the polymer that will either remove or add electrons (Table 5.6). The influence of doping on resultant conductivity is striking; whereas the conductivity of pristine PA is *ca.* 1×10^{-7} S cm⁻¹, doping may yield values as high as 1×10^5 S cm⁻¹ – an improvement of 12

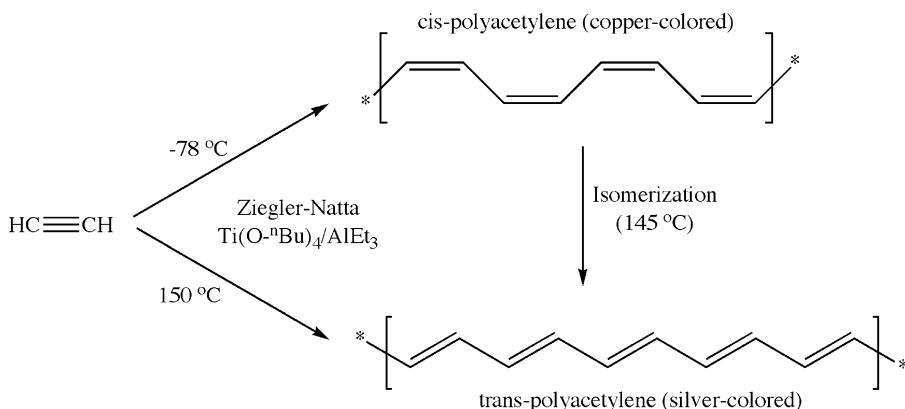


Figure 5.57. Synthetic routes for cis- and trans-polyacetylene. It should be noted that the trans-isomer of PA is more stable than the cis-isomer since the former has two degenerate ground states (two energetically-equivalent arrangements of alternating double bonds).

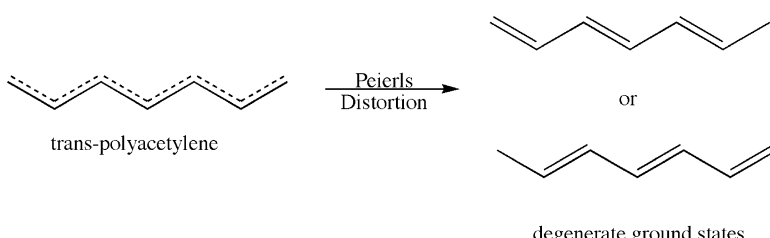


Figure 5.58. Illustration of differing C–C bond lengths for polyacetylene.

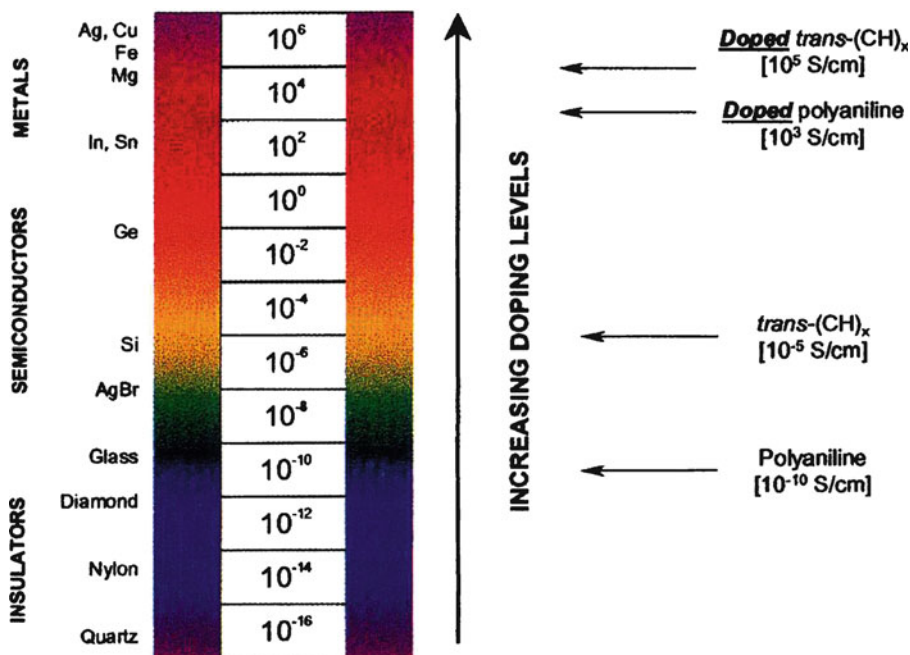
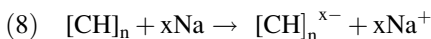
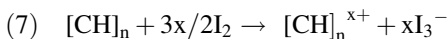


Figure 5.59. Conductivity values for pristine (undoped) and doped conductive polymers, relative to common metals, semiconductors and insulators. Reproduced from MacDiarmid, A. G. *Synthetic Metals: A Novel Role for Organic Polymers*, Nobel Lecture, Dec. 8, 2000.

orders of magnitude! However, before discussing polymer doping in more detail, we should first point out the difference in nomenclature used by solid-state physicists and chemists. Whereas physicists refer to the generated carriers as polarons, bipolarons, and solitons, chemists are more familiar with the terms radical cations/anions, carbocations/carbodianions, and radicals/carbocations/carbanions, respectively (Figure 5.60).

Redox doping is the first method used to enhance the conductivity of a conjugated polymer. *Oxidative doping* (p-doping) occurs when an oxidizing agent such as I_2 , Br_2 , ClO_4^- , AsF_5 , $FeCl_3$, $NOPF_6$, etc. is added to the polymer, resulting in an abstraction of an electron and formation of a *radical cation*, also known as a *positive polaron* (Eq. 7). In contrast, *reductive doping* (n-doping) occurs when a reducing agent such as alkali metals, $LiBu$, or $Li(C_{10}H_8)$ is added to yield a *radical anion*, also known as a *negative polaron* (Eq. 8).



It should be noted that in contrast to classical band theory, the doped electrons/holes generated in conductive polymers are not fully delocalized. The reason for

Table 5.6. Common Conductive Polymers

Polymer	Structure	Dopants	$\Omega^{-1} \text{ cm}^{-1}\text{a}$
Polyacetylene	* *	I ₂ , Br ₂ , Li, Na, AsF ₅	20,000–150,000 ^b
Polyphenylene	* *	AsF ₅ , Li, Na	10,000
Polyparaphhenylene vinylene	* *	AsF ₅	10,000
Polypyrrole	* *	BF ₄ ⁻ , ClO ₄ ⁻	7,500
Polythienylvinylene	* *	AsF ₅	2,700
Polyethylenedioxy thiophene (PEDOT)	* *	BF ₄ ⁻ , ClO ₄ ⁻	550 ^c
Polythiophene	* *	BF ₄ ⁻ , ClO ₄ ⁻	500
Polyphenylene sulfide	* *	AsF ₅	500
Polyaniline (PANI)	* *	HCl	200
Polyfuran	* *	BF ₄ ⁻ , ClO ₄ ⁻	100

(Continued)

Table 5.6 (Continued)

Polymer	Structure	Dopants	$\Omega^{-1} \text{ cm}^{-1}$ ^a
Polyisothianaphthene		BF_4^- , ClO_4^-	100
Poly(3-alkylthiophene)		BF_4^- , ClO_4^-	100
Polyazulene		BF_4^- , ClO_4^-	2.5

^aMaximum conductivity of doped polymers; the conductivity of pristine (undoped) polymers is *ca.* 0.001–0.1 $\Omega^{-1} \text{ cm}^{-1}$. The unit $\Omega^{-1} \text{ cm}^{-1}$ is equivalent to S cm^{-1} .

^bThe maximum anisotropic (stretch oriented) conductivity for polyacetylene: Naarmann, H.; Theophilou, N. *Synth. Met.* **1987**, 22, 1.

^cMaximum conductivity of PEDOT is obtained by doping with poly(styrene sulfonate) – PSS. Accordingly, PEDOT:PSS is the industry leader in transparent conductive polymer films, with *ca.* 80% light transmission.

the localization of polarons is due to Coulombic attractions to their counter ions (*e.g.*, I_3^-), which normally have very low mobilities. However, in order to achieve high electrical conductivities, the polarons must be able to migrate along the polymer chain. Figure 5.61 illustrates the migration mechanism of a polaron; in order to migrate, a high concentration of the counter ions must be present to induce the movement of the polaron into the Coulombic field of nearby ions. Accordingly, high doping levels are required to achieve sufficient conductivity in conductive polymers. This may be compared with inorganic-based semiconductors such as Si, which require minute concentrations of dopants due to the pronounced mobility of electrons/holes through the extended solid-state lattice.

If a second electron is abstracted from a section of the polymer that is already oxidized, either a second independent polaron may be generated, or two polarons may condense to form a *bipolaron*.^[99] The two positive/negative charges of the bipolaron are not independent, but rather move as a pair similar to the Cooper pair of

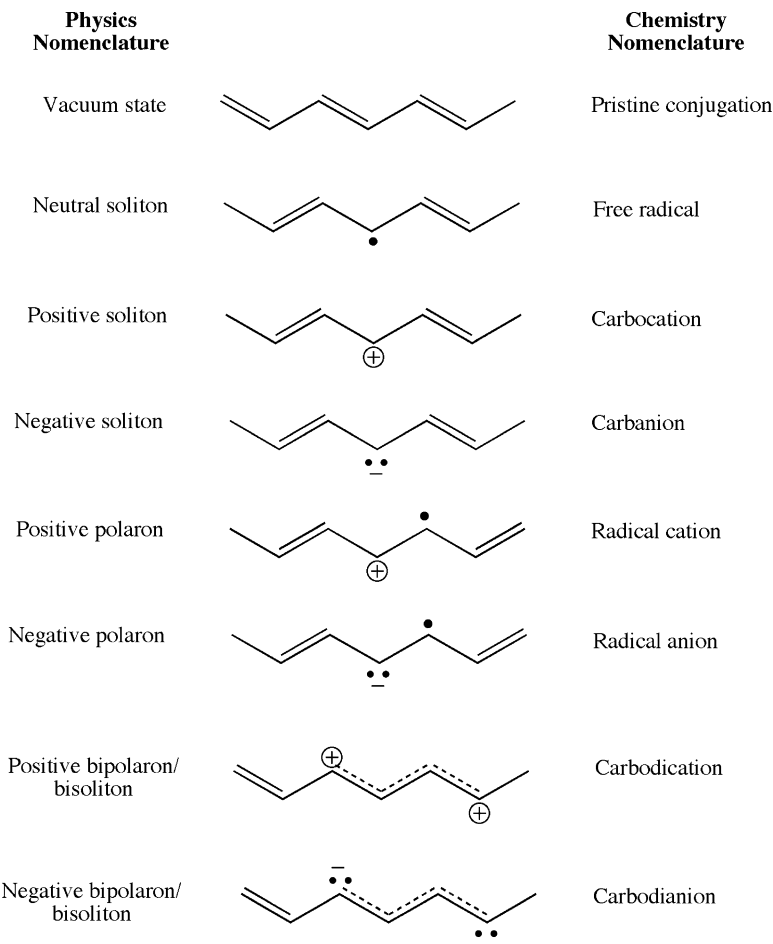


Figure 5.60. Nomenclature of the generated carriers within conductive polymers.

superconductors. In order to broaden the discussion beyond polyacetylene, Figure 5.62 shows both polaron and bipolaron formation for polypyrrole.

Another type of carrier is known as a *soliton*, formed by two primary modes: doping or bond-alternation defect formation (*e.g.*, thermal isomerization of *cis*-polyacetylene, Figure 5.63a). Not surprisingly, solitons generated via doping are more prevalent than those formed by thermal isomerization. As illustrated in Figure 5.63a, solitons may migrate along individual polymer chains by pairing with an adjacent electron; however, they may also contribute to charge transfer between different chains via *intersoliton hopping* (Figure 5.63b). This latter mechanism is important for bulk conductivity, since carriers must move readily among various chains in order to facilitate macroscopic electrical conductivity of the polymer. As the number

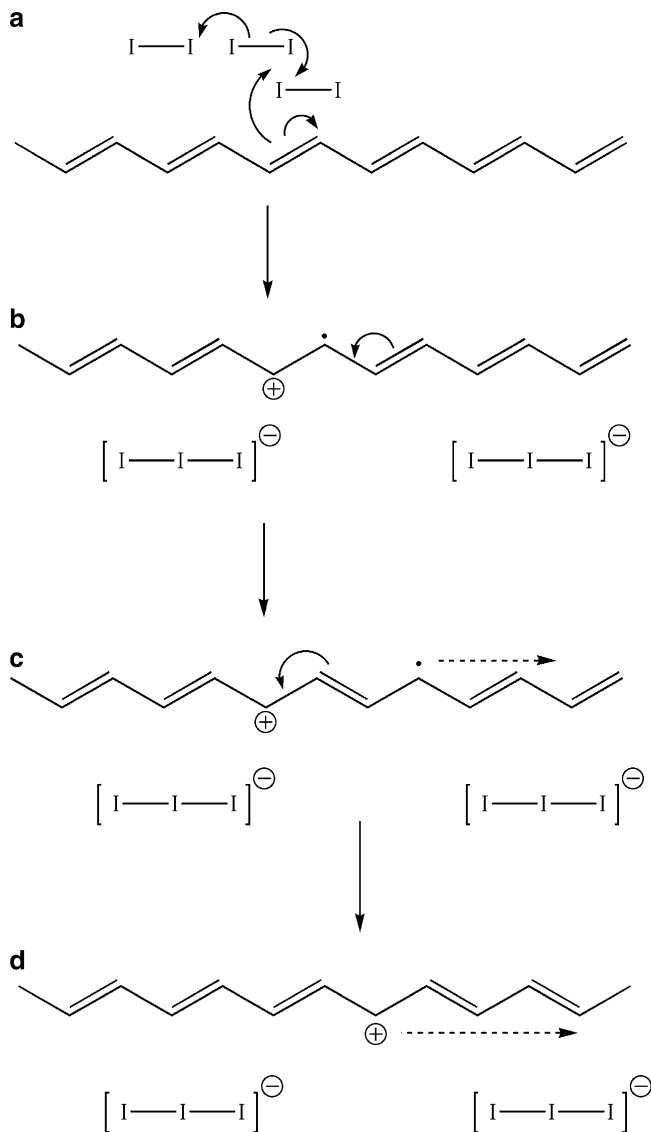


Figure 5.61. The formation and migration mechanisms of a polaron.

of solitons increases, their spheres of influence overlap leading to metallic-like conductivity.

Before closing this topic, let's consider the band structure and optical properties of doped conductive polymers, once again considering the most widely studied structure, polyacetylene. If all C—C bond distances were equivalent, one would expect a partially-filled π -band and metallic conductivity (Figure 5.64a). However,

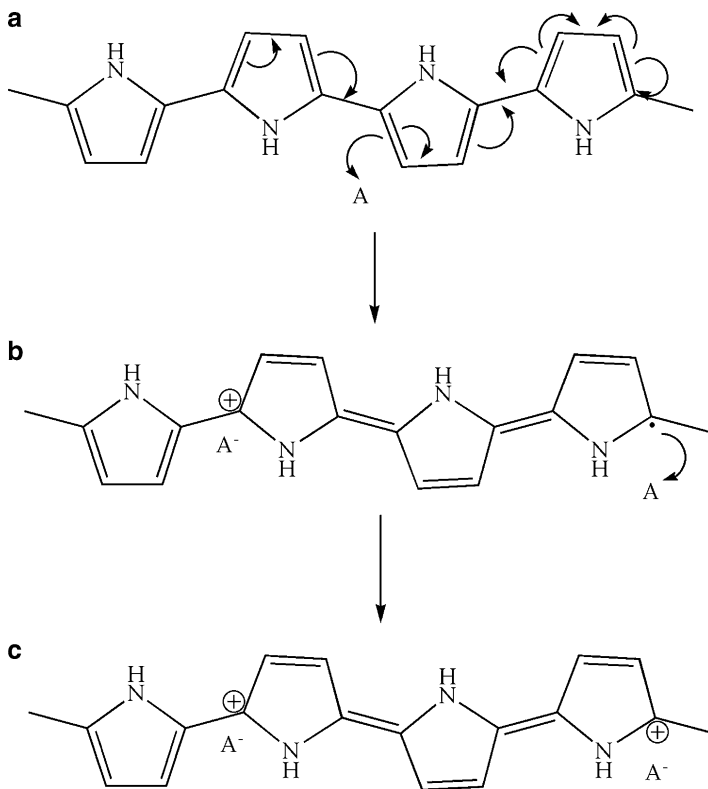


Figure 5.62. Polaron and bipolaron formation for polypyrrole.

due to Peierls distortion, the π -band splits in half, and a bandgap is now introduced at the Fermi level (Figure 5.64b). The introduction of polarons and solitons via doping (or thermal isomerization for soliton formation) generates mid-gap states (Figure 5.64c, d) whose optical absorption intensity grows at the expense of the E_g transition (Figure 5.65).

The tremendous benefit of conjugated polymers is the ability to fine-tune the bandgap via modification of the polymer structure. This may be achieved via sterics or electronic effects, by varying either the main chain or its pendant functional groups. Figure 5.66 lists some of the major applications for conjugated polymers, from battery to LED applications. Not unlike inorganic-based LEDs, conjugated polymers may also be designed to exhibit a full range of colors, from PPV ($E_g = 2.5$ eV, yellow) to MeH-PPV ($E_g = 2.1$ eV, red) to polyphenylene ($E_g = 2.7$ eV, blue). A polyacetylene battery has also been reported, which employs a silver anode and I_2 -doped PA as the cathode.^[100] Conjugated polymers may also be exploited for the design of wearable electronic systems that incorporate sensing, monitoring, and information processing capabilities (Figure 5.67).^[101]

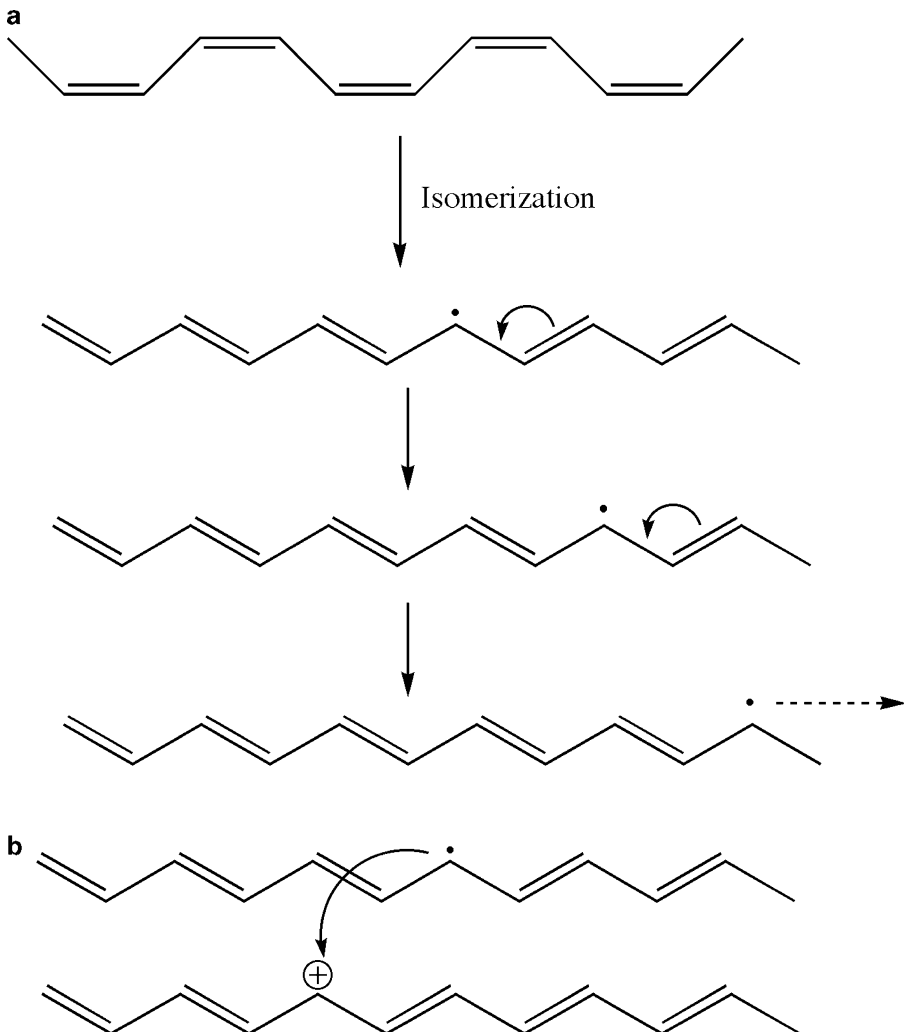


Figure 5.63. (a) Soliton formation via isomerization of cis-polyacetylene, and migration along the polymer chain by pairing to an adjacent electron. (b) Illustration of intersoliton hopping. Charged solitons (bottom chain) are trapped by dopant counter ions, while neutral solitons (top chain) are free to move. A neutral soliton on a chain close to one with a charged soliton may interact, with the hopping of an electron from one defect site to another.

5.3.3. Molecular Magnets

Magnetic materials may date back as far as 2,000 B.C., with the first magnetic mineral, magnetite, discovered in *ca.* 500 B.C.^[102] Present-day magnetic materials are typically alloys containing iron, cobalt, or other lanthanide metals. In Chapter 3,

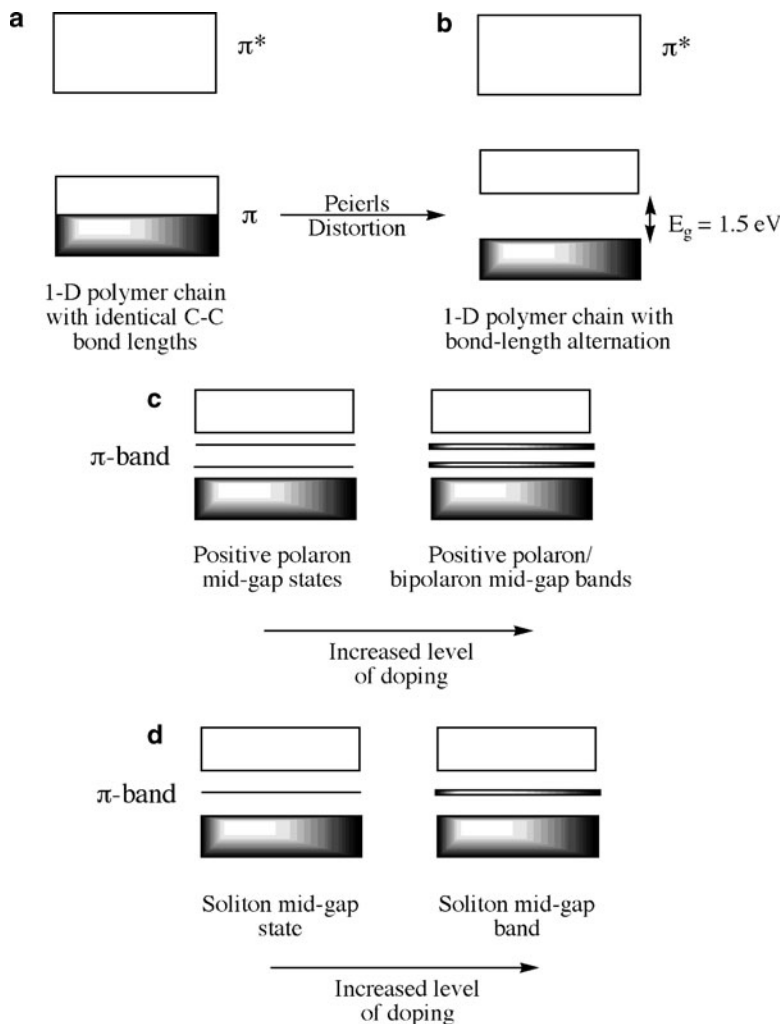


Figure 5.64. Simplified band diagrams for a conductive polymer. Shown are: (a) polyacetylene if all C—C bond distances were equivalent (metallic), (b) actual band diagram for PA, resulting from Peierls distortion, (c) polaron mid-gap states and bands formed upon doping, and (d) soliton mid-gap state and band formed upon doping. For (c) and (d), note that at higher levels of doping, the midgap bands grow at the expense of the valence and conduction bands, as midgap states are taken from band edges.

we discussed a variety of magnetic materials and phenomena, which were focused on inorganic alloys and clusters. Since organic compounds are generally diamagnetic (all electrons paired), organic-containing molecules have long been overlooked as candidates for magnetic materials. However, the world of magnetic materials was forever changed in 1967 when the first organic-based molecular

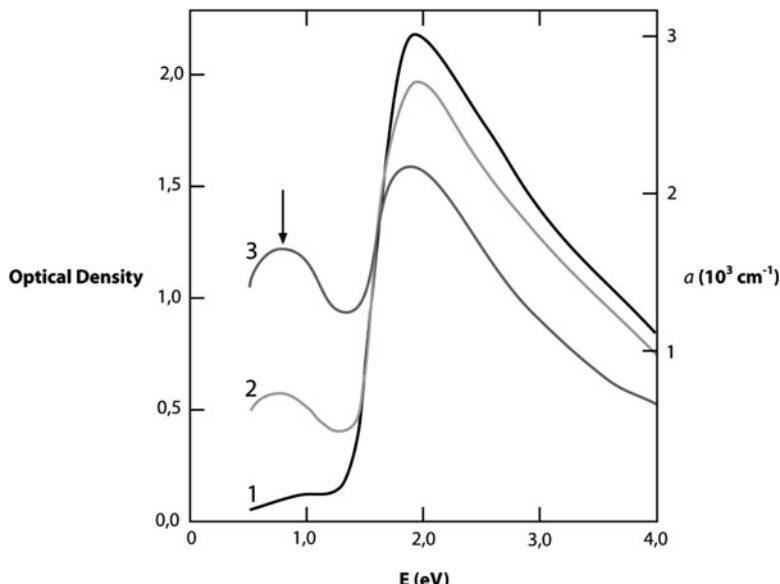


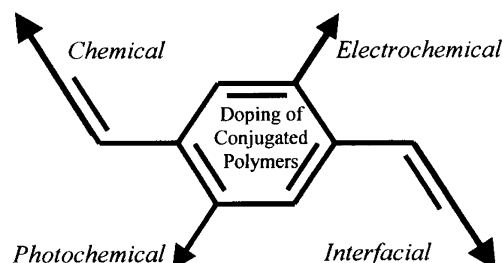
Figure 5.65. Optical absorption of undoped polyacetylene (curve 1). Curves 2 and 3 show the absorption of polyacetylene with increasing dopant concentrations. A midgap state (arrow at 0.7 eV) emerges upon doping, becoming more intense with further doping levels, at the expense of other peaks. Results adapted from Roth, S. *One-Dimensional Metals*, Weinheim VCH, 1995.

Electrical conductivity

Conductivity approaching that of copper
Chemical doping induces solubility
Transparent electrodes, antistatics
EMI shielding, conducting fibers

Control of electrochemical potential

Electrochemical batteries
Electrochromism and “Smart Windows”
Light-emitting electrochemical cells



High-performance optical materials

1-d Nonlinear optical phenomena
Photoinduced electron transfer
Photovoltaic devices
Tunable NLO properties

Charge injection without counterions

Organic FET circuits
Tunneling injection in LEDs

Figure 5.66. Doping mechanisms and related applications. Reproduced from Heeger, A. J. *Semiconducting and Metallic Polymers: The Fourth Generation of Polymeric Materials*, Nobel Lecture, Dec. 8, 2000.

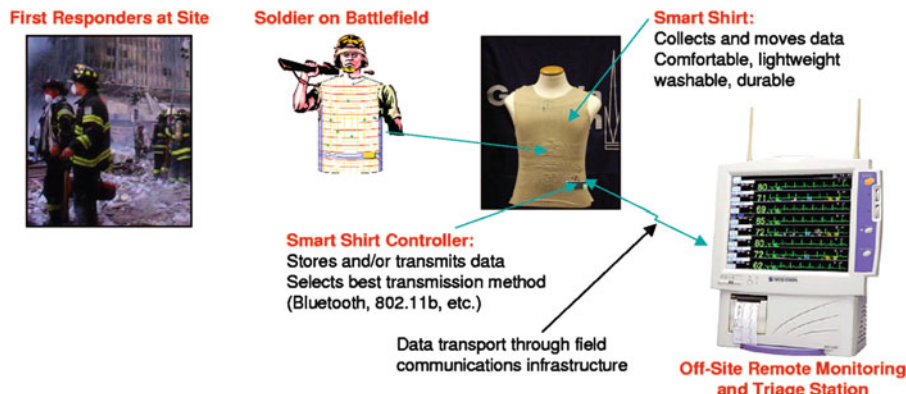


Figure 5.67. Illustration of a 'smart-shirt' application that could be designed to incorporate conductive polymeric materials for remote sensing and monitoring applications. Reproduce with permission from Parks, S.; Jayaraman, S. *MRS Bull.* **2003**, 28, 585. Copyright 2003 Materials Research Society.

magnet was discovered at Bell Laboratories.^[103] Miller and coworkers greatly progressed the field of molecular magnetism in the mid-1980s.^[104]

In contrast to inorganic compounds that require high temperature sintering processes, organic magnets are synthesized at low temperatures using traditional synthetic techniques. The benefits of organic-based magnets relative to inorganic analogues are their lightweight architecture, tunable conductivity (insulating – semiconductive), tunable solubility, and biocompatibility. With virtually every electronic device employing magnets (*e.g.*, automobiles, computers, audio speakers, televisions, telephones, radios, *etc.*), there will be an increasing market for applications that employ these materials. In particular, the small size of individual molecules relative to inorganic lattices creates the possibility of much greater storage densities for magnetic storage applications (*e.g.*, computer hard drives) – perhaps as high as 200,000 Gb in⁻², which is *ca.* three times greater than current alloy thin film materials.^[105]

In comparison to inorganic magnets in which electrons reside in d- and/or f-orbitals, organic magnets contain unpaired electrons in p-orbitals. One example of an organic magnet is 4-nitrophenylnitronyl nitroxide (**XXIII**), with a T_c of 0.6 K. In general, the critical temperatures of purely organic magnets ($T_c \leq 1.48$ K) are significantly lower than those that contain metal ions. Hence, for an observable magnetic response at a higher T_c , the p-electron spins are most often coupled with unpaired d-electrons on metal ion(s). The first organometallic (containing both a metal and ligand, with M–C bonds) magnets exploited ligands with conjugated π -systems, capable of metal-like electrical conductivity. To date, the most commonly used ligand systems are reduced forms of TCNQ (7,7,8-tetracyano-*p*-quinodimethane) and TCNE (tetracyanoethylene) (Figure 5.68). Interestingly, if $[\text{TCNQ}]^-$ is replaced

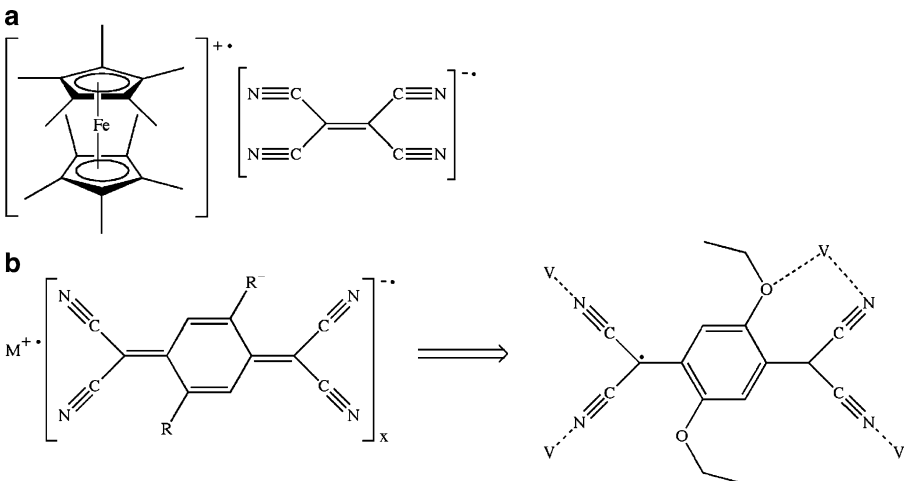
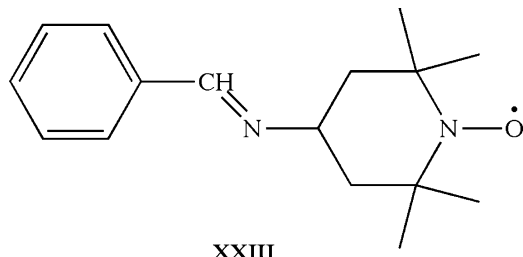


Figure 5.68. Molecular structures of organometallic/transition metal molecular magnets. Shown are (a) $[\text{Fe}(\text{Cp}^*)_2]^{++}[\text{TCNE}]^{-\bullet}$ and (b) $[\text{M}^+]_x[\text{TCNQR}_2]_{2-x}$, where M=Mn, Fe, Co, Ni, and V; R=H, Br, Me, Et, ¹Pr, OMe, OEt, and OPh. For M[TCNQ]_x complexes (b), it was shown that the metal may bind through the terminal N moiety of the cyano group, as well as with the oxygen from a nearby alkoxy group if the steric bulk is not sufficiently high (*i.e.*, the seven-membered ring will not form with $-\text{OPh}$ groups). This chelate formation results in greater stability, which enhances the magnetic coupling and increases the T_c .^[106]

with $[\text{TCNE}]^{-\bullet}$, one unpaired electron is delocalized over a smaller molecular structure that results in a greater spin density and magnetic response. Consequently, the coercivity (1,000 Oe at 2 K) of $[\text{Cp}_2\text{Fe}]^{++}[\text{TCNE}]^{-\bullet}$ is of the same magnitude as CoPtCr (*ca.* 1,700 Oe), used for magnetic storage. In fact, on a mole-basis, metal TCNE complexes are stronger ferromagnets than iron. However, the low T_c (4.8 K) makes this material impractical for many potential applications.



The solid-state structure of $[\text{Cp}_2^*\text{Fe}]^{++}[\text{TCNE}]^{-\bullet}$ consists of alternating layers of the cationic and anionic species (Figure 5.69). Upon charge transfer between the donor (cation) and acceptor (anion) within a layer, a triplet $S = 1$ state ($\uparrow\uparrow$ vs. singlet $\uparrow\downarrow$) is formed through the transfer of a d-electron to the π^* -orbital on TCNE

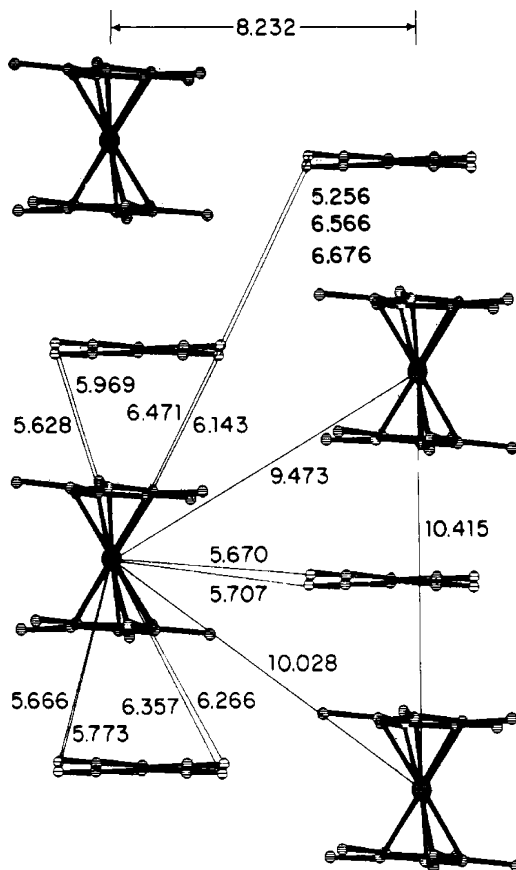


Figure 5.69. Solid-state structure of $[\text{Cp}_2^*\text{Fe}][\text{TCNE}]$, showing relevant intra- and interchain distances. Reproduced with permission from Miller, J. S.; Calabrese, J. C.; Rommelmann, H.; Chittipeddi, S. R.; Zhang, J. H.; Reiff, W. M.; Epstein, A. J. *J. Am. Chem. Soc.*, **1987**, *109*, 769. Copyright 1987 American Chemical Society.

(Figure 5.70). Such intrachain spin alignment serves to stabilize the $[\text{Cp}_2^*\text{Fe}]^{*+} [\text{TCNE}]^{-}$ repeat units; however, for bulk macroscopic ferromagnetism, there also has to be interchain spin alignment. This does occur at $T < T_c$, since the distances between $[\text{TCNE}]^-$ species and both inter- and intrachain Fe^{3+} ions are roughly equivalent.

The mixture of TCNE and hexacarbonyl vanadium(0) in an organic solvent yields an organic-based magnet with the highest critical temperature to date – *ca.* 400 K (Eq. 9). However, the detailed solid-state structure of this compound has not been determined due to its air/water reactivity, amorphous morphology, and solvent insolubility. The entrapped solvent is at least partially responsible for its air sensitivity and magnetic susceptibility. That is, CVD of $\text{V}[\text{TCNE}]$ in the absence of

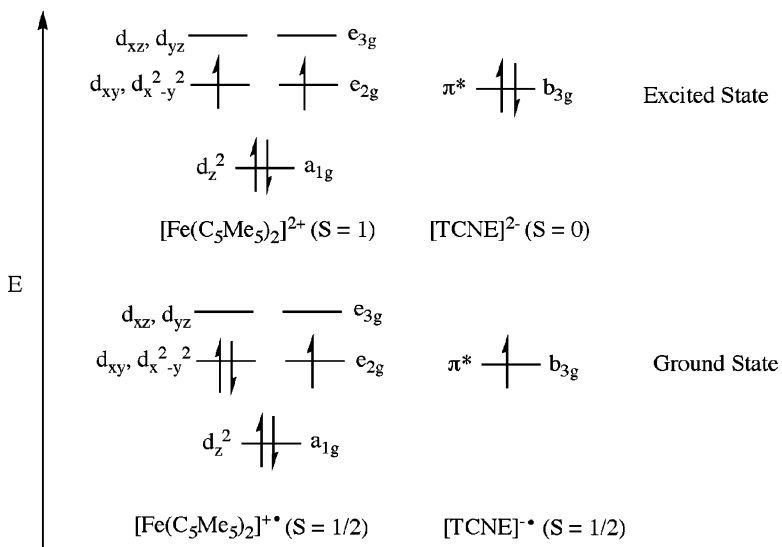
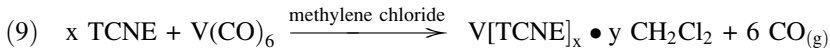


Figure 5.70. Ground- and excited-state electronic configurations of $[\text{Fe}(\text{C}_5\text{Me}_5)_2]^{2+}$ and TCNE species. Adapted from Miller, J. S.; Calabrese, J. C.; Rommelmann, H.; Chittipeddi, S. R.; Zhang, J. H.; Reiff, W. M.; Epstein, A. J. *J. Am. Chem. Soc.*, **1987**, *109*, 769. Copyright 1987 American Chemical Society.

methylene chloride yields air stable films, and acetonitrile-processed V[TCNE] has a significantly lower T_c due to V—NC—CH₃ interactions (less effective ferromagnetic coupling).



The observed magnitude of bulk ferromagnetic ordering depends on both the number and 3-D arrangement of unpaired electrons throughout the entire lattice. Since bulk spin coupling is a consequence of the overall solid-state structure, the determination of crystal structures of molecular magnetic materials by X-ray and neutron diffraction remains an active research area. Even at the single-molecule level, the magnetic properties of the material may be complex, and (hopefully) tunable. For example, the antiferromagnetism of a sterically encumbered nickel azide complex may be switched on or off by thermally manipulating the geometry about one of the nickel ions (Figure 5.71). Other examples of light-induced structural transformations represent another emerging area of molecular magnetic research.^[107]

Although this chapter is focused on “soft” organic-based materials, we would be remiss if other more recent and active molecular magnetic materials were not mentioned. A number of materials known as *single-molecule* magnets have been identified, with the majority being transition metal oxo clusters that exhibit a 2-D honeycomb-layered structure (Figure 5.72a). However, the oxo ligand exhibits multiple bridging possibilities with a wide variability of the M—O—M angles, which greatly

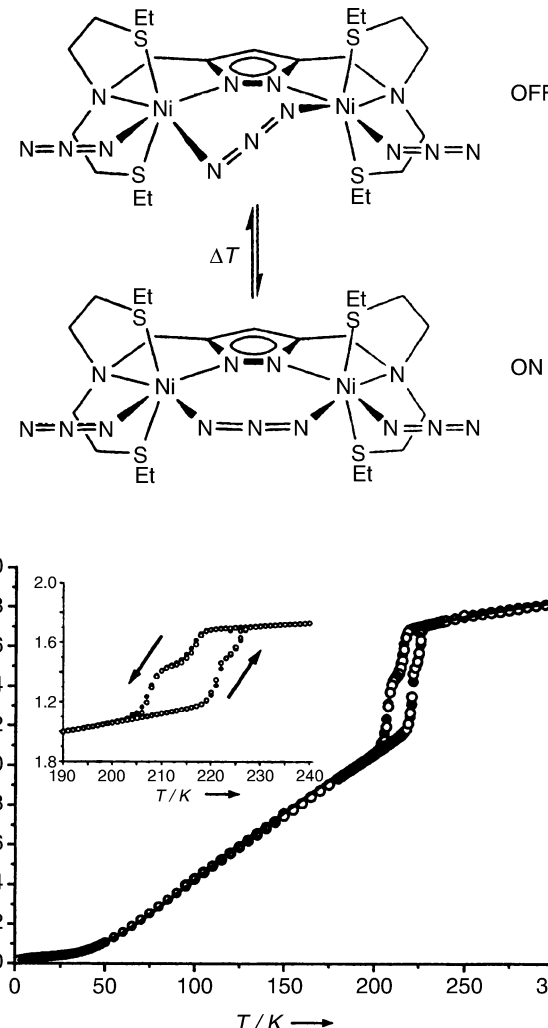


Figure 5.71. Molecular structure (top, showing off/on states for antiferromagnetic coupling of Ni^{2+} ions) and hysteresis curve (bottom) for $[LNi_2(N_3)_3]$ – inset is a magnified view of the 200–225 K region. Reproduced with permission from Leibeling, G.; Demeshko, S.; Dechert, S.; Meyer, F. *Angew. Chem. Int. Ed. Eng.*, **2005**, 44, 7111. Copyright 2005 Wiley-VCH.

affects the M–M magnetic coupling in the solid. Consequently, more recent work has been focused on transition metal cyano ($-\text{CN}$) complexes, which result in a much greater structural control since the ligand may linearly bridge only two metal centers (M—CN—M'). The most widely studied cyano complexes that exhibit either ferri- or ferromagnetic behavior are analogues of Prussian Blue, $\text{Fe}_4^{\text{III}}[\text{Fe}^{\text{II}}(\text{CN})_6]_3 \cdot \text{H}_2\text{O}$ (Figure 5.72b).

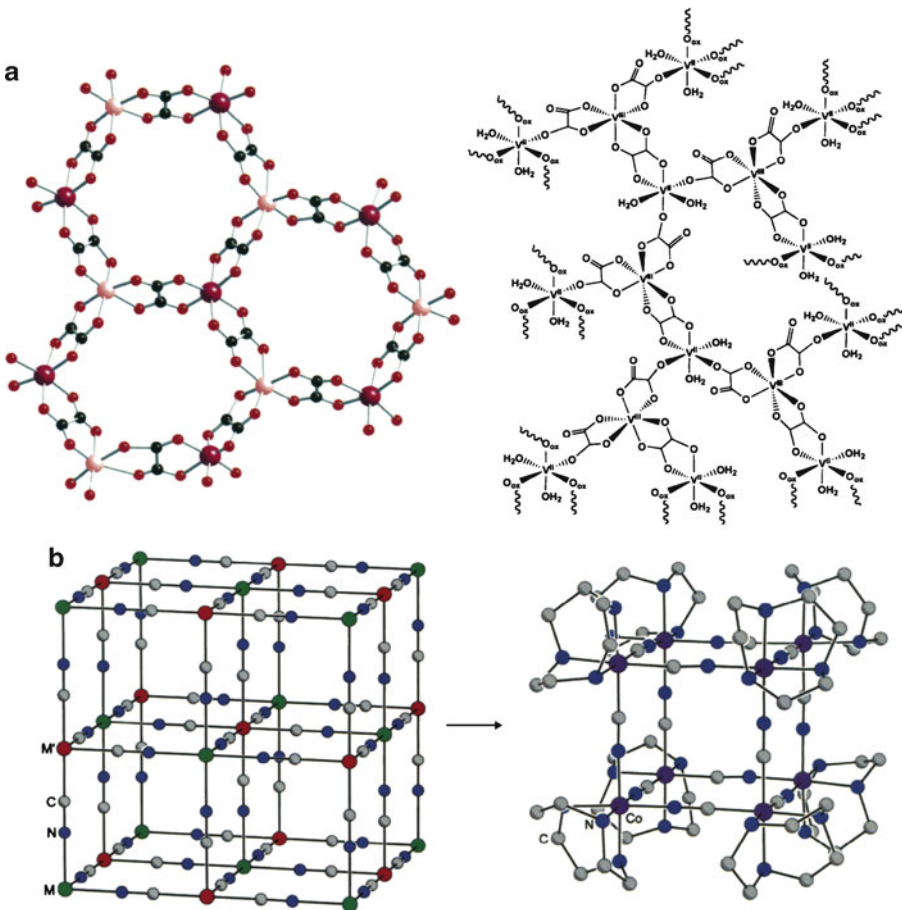


Figure 5.72. Molecular structures of other molecular magnetic materials. Illustrated are (a) tris(oxalato) metalates $[M^{II}M^{III}(ox)_3]$, where $M^{II}=\text{Mn, Fe, Ni, Co, Cu, Zn}$; $M^{III}=\text{Cr, Fe, Ru}$, and (b) the simplified crystal structure of Prussian Blue, with an example of the analogue structure $[(\text{tacn})_8\text{Co}_8(\text{CN})_{12}]^{12+}$, where the tacn ligand is 1,4,7-triazacyclononane. Reproduced with permission from (a) Min, K. S.; Rhinegold, A. L.; Miller, J. S. *Inorg. Chem.*, **2005**, *44*, 8433, and (b) Beltran, L. M. C.; Long, J. R. *Acc. Chem. Res.*, **2005**, *38*, 325. Copyright 2005 American Chemical Society.

Before we delve further into these cyano-based structures, let us review a bit of inorganic chemistry, to understand the ligand effect on the electronic configuration of the metal ions in a complex. As you are aware, all ligands behave as a Lewis base toward a metal center, donating an electron pair(s) through filled σ - or π -orbitals. The cyano ligand (and others such as $-\text{CO}$ and $-\text{C}_2\text{H}_4$, etc.) represents a special case since it contains an unsaturated (triple) bond. Accordingly, the metal is able to donate electron density back to the ligand into its empty π^* -orbitals, a process known as $\text{M} \rightarrow \text{L}$ “back-bonding.” As you would expect, this phenomenon is most

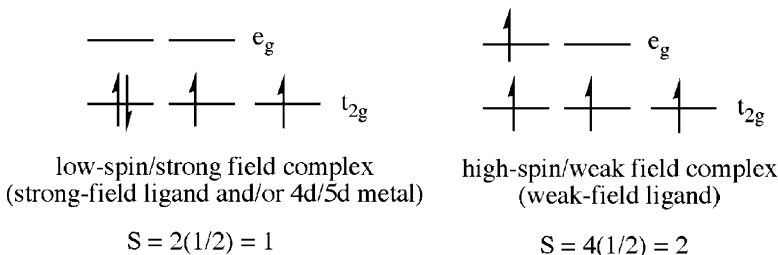


Figure 5.73. Comparative electronic configurations of low-spin (strong-field) and high-spin (weak-field) d^4 metal ions (e.g., Mn^{3+} , Cr^{2+} , V^+).

pronounced for metals in low oxidation states, where the metal ion is most apt to reduce its buildup of negative charge. This synergistic electron donation and back-donation delocalizes the electron density between the ligand and metal, which greatly strengthens the M–L bond. Consequently, a comparative scale known as the *spectrochemical series* has been developed to indicate whether a ligand is active toward back-bonding with the metal. Whereas unsaturated ligands are all considered “strong-field”, halides and other σ -donors are all weak-field ligands since they do not have available empty orbitals to accept electron density from the metal.

A number of factors such as identity/oxidation state of the metal and structure/charge of the ligand(s) will determine the electronic configuration of the metal center in a transition metal complex. For an octahedral complex, the d-orbitals of the transition metal are not degenerate, but are split based on their relative interactions with the ligands. For a metal with ≤ 3 d-electrons, there is no ambiguity with regard to its electronic configuration. However, for d^4 and higher, the fourth electron may be placed either in the lower or higher orbital groups (Figure 5.73). In particular, complexes containing 4d/5d metals, low oxidation-state metals (preferring $M \rightarrow L$ back-bonding), and strong-field ligands will dictate a strong-field (low-spin) configuration. Depending on whether the complex adopts a low-spin or high-spin configuration, the number of unpaired electrons will vary significantly. For example, consider a d^4 complex: low-spin has two unpaired electrons ($S = 1$), whereas high-spin has four unpaired electrons ($S = 2$).^[108]

As a terminal ligand, the $-\text{CN}$ group always results in a low-spin complex. However, when bridging two metals each end will exhibit different ligand field strengths. That is, the C-end ($M \leftarrow \text{CN} \rightarrow M'$) will yield a low-spin configuration for M , but the N-end ($M \leftarrow \text{CN} \rightarrow M'$) will yield a high-spin configuration for M' . Hence, for Prussian Blue, which has the $\rightarrow \text{Fe}^{II} \leftarrow \text{CN} \rightarrow \text{Fe}^{III} \leftarrow \text{NC} \rightarrow \text{Fe}^{II} \leftarrow$ bonding motif, the $d^6 \text{Fe}^{II}$ sites will be low-spin ($S = 0$), whereas the $d^5 \text{Fe}^{III}$ sites will be high-spin ($S = 5/2$). This means that ferromagnetic ordering may only occur through distant Fe^{III} – Fe^{III} sites, which occurs at a relatively low T_c (5.6 K). In order to improve the ordering distances with the Prussian Blue array, there has been much interest in replacing Fe with other transition metals (especially early transition metals in low oxidation states). Hence, the Prussian Blue structure allows for a

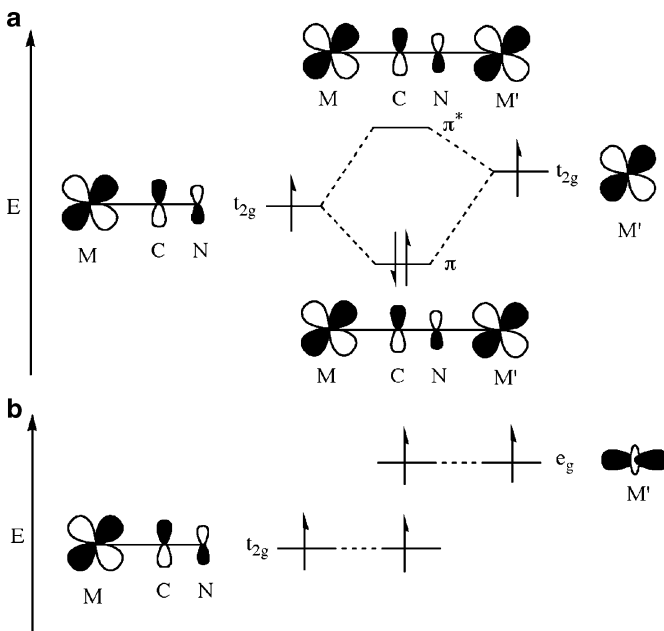
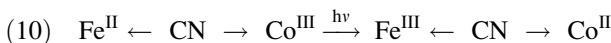


Figure 5.74. Simplified molecular orbital diagrams for an $M-CN-M'$ unit with octahedrally coordinated metal centers. Shown are (a) antiferromagnetic coupling from overlap of symmetrically aligned orbitals and (b) ferromagnetic ordering from overlap of orthogonal orbitals. Adapted with permission from Beltran, L. M. C.; Long, J. R. *Acc. Chem. Res.*, **2005**, 38, 325. Copyright 2005 American Chemical Society.

highly tunable magnetic susceptibility, since a variety of metal ions may be used in association with the cyano ligand. Not only will this affect the number of unpaired electrons that are coupled throughout the lattice, but also the type of ordering (e.g., ferro-, ferri-, antiferromagnetic) based on the metal d-orbitals that house the unpaired electrons. In particular, ferromagnetic ordering occurs when the electrons in the metal ions reside in orthogonal orbitals (e.g., $M(t_{2g})/M'(e_g)$). By contrast, antiferromagnetic coupling occurs when the electrons are housed in orbitals of comparable symmetry (e.g., $M(t_{2g})/M'(t_{2g})$), as illustrated in Figure 5.74.

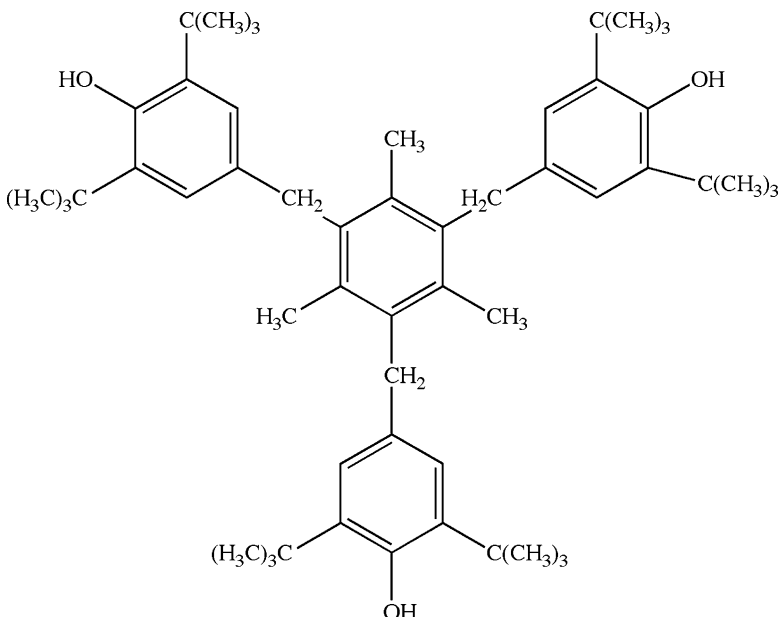
For optical storage applications, it is desirable to have a material that alters its magnetic properties in response to light. This effect is exhibited by Prussian Blue itself, wherein some low-spin Fe sites are converted to a high-spin configuration. More recently, this behavior has been demonstrated for mixed-metal systems such as $K_{0.4}Co_{1.3}[Fe(CN)₆] \cdot 5H_2O$.^[109] The light-induced redox reaction may be described by Eq. 10, where diamagnetic Fe^{II} becomes paramagnetic and may couple with other unpaired electrons throughout the solid.^[110]



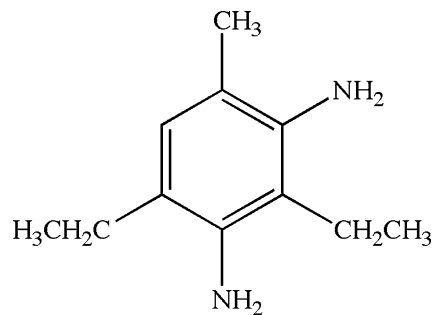
5.4. POLYMER ADDITIVES

Although the properties of polymers may be fine-tuned based on the functional groups that are present in their repeat units, all commodity polymers also contain a number of components in order to impart desired properties. Some common additives include:

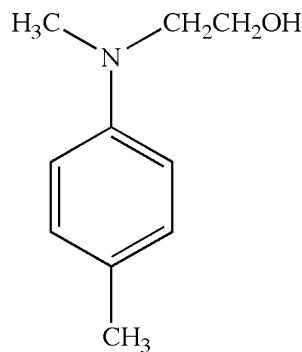
- (i) *Stabilizers* (antioxidants:^[111] e.g., 1,3,5-trimethyl-2,4,6-tris(3,5-di-tert-butyl-4-hydroxybenzyl) benzene, **XXIV**; UV-stabilizers: e.g., TiO₂; heat-stabilizers:^[112] e.g., tetrabutyltin, tetraoctyltin). Used to protect the polymer from oxidation, UV light, and heat during/after processing.



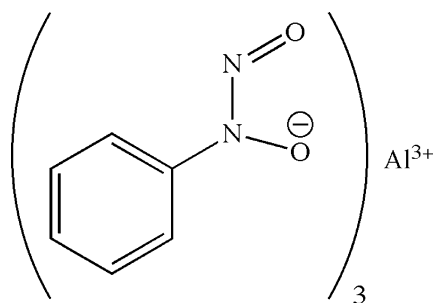
- (ii) *Nucleating/clarifying agents* (e.g., nucleation: sodium benzoate-based, nucleation/clarifying: sorbitol-based). Used to increase the crystallization rate of semi-crystalline polymers such as polypropylene, polyamide, and polyester. Clarifying agents reduce haze and significantly increase polymer transparency.
- (iii) *Curatives* (chain extenders and crosslinkers: e.g., 3,5-diethylditoluene-2,4-diamine, **XXV**,^[113] cure promoters: e.g., N-(2-hydroxyethyl)-N-methyl-para-toluidine, **XXVI**,^[114] polymerization inhibitors: e.g., tris(N-nitroso-N-phenylhydroxylamine) aluminum salt, **XXVII**^[115]). Used to promote polymer curing at lower temperatures for urethanes, epoxies, polyesters, vinyl esters, acrylates, and ureas. Also used for free radical scavenging and metal chelation to prevent unwanted polymerization during the manufacture and storage of olefinic-type resins.



xxv

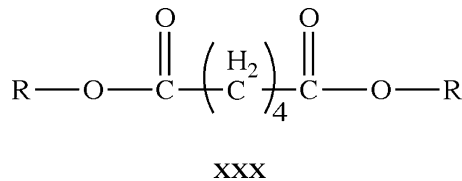
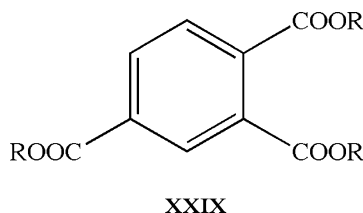
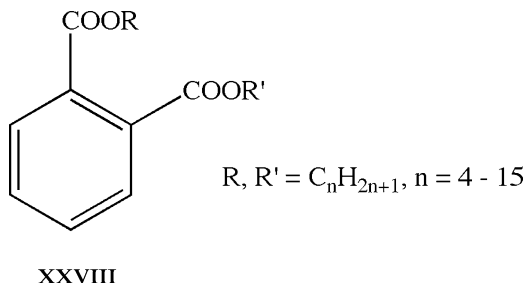


xxvi



xxvii

- (iv) *Plasticizers*^[116] or *anti-plasticizers*^[117] (e.g., phthalates – **XXVIII**,^[118] trimellitates – **XXIX**,^[119] adipates – **XXX**^[120]). Used to control the flexibility/rigidity of the polymer.



- (v) *Coloring agents* (e.g., inorganic pigments, organic dyes). Used to impart the desired color(s) to the polymer.
 (vi) *Flame retardants* (described later).

As their name implies, *plasticizers* are additives that soften a material, enhancing its flexibility. The worldwide market for plasticizers is currently over five million metric tons, with over 90% used to soften PVC. The most common plasticizers are phthalates; however, due to the relatively high vapor pressure of these compounds, plasticizers will evaporate from the polymer structure as evidenced by the “new car smell” of new cars, as well as the organic film that becomes deposited on the interior windshield surface. For these applications, it is best to use a plasticizer with a lower volatility such as trimellitates.

There are two leading theories concerning the mechanism of activity for plasticizer molecules. The ‘lubricating theory’ suggests that as the polymer is heated, the plasticizer diffuses into the polymer and disrupts the van der Waal interactions

among polymer chains. Since network formation is reduced, the T_g is lowered resulting in more flexibility/softness of the bulk polymer. By contrast, the ‘free volume theory’ suggests that the lowering of T_g is due to the polymer chains being pushed further apart by the interdiffusion of the plasticizer molecules. Since the free volume of the polymer has been increased, the chains are free to move past one another more easily resulting in greater flexibility.

The above mechanistic explanations assume that the plasticizer molecules are not permanently bound to the polymer chains. Since these interactions are relatively weak, there is likely a dynamic adsorption/desorption at various locations among neighboring polymer chains. Accordingly, the plasticizer structure may be fine-tuned to affect its solubility/miscibility with the polymer, as well as its interactions with polymer chains and with other plasticizer molecules. As the polymer–plasticizer interactions are strengthened, the T_g will increase; at low concentrations, the rigidity of the polymer is increased due to effective rigid-network formation between the plasticizer and polymer. However, as the plasticizer concentration is increased, the additive molecules themselves interact yielding the desired softening characteristics. As illustrated by **XXVIII** above, the molecular structure of a plasticizer contains both polar and nonpolar (hydrocarbon chain) units. It is usually the polar endgroups that bind reversibly with the polymer chains; the length-tunable nonpolar component affords controlled separation of neighboring polymer chains.

5.4.1. Flame Retardants

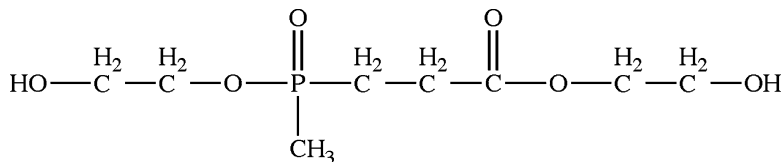
Since polymers exhibit a hydrocarbon-based structure, these materials pose a significant flammability threat. However, if one examines a room following a fire, it is obvious that some polymers withstand ignition much greater than others (Figure 5.75). In fact, these polymers are not naturally fire resistant, but rather contain additives that afford this desirable property. The largest class of flame inhibiting additives is *brominated flame-retardants* (BFRs). It is estimated that bromine-containing molecules are added to over 2.5 million tons of polymers each year, with the electronics industry accounting for the greatest consumer market. BFRs are also used in a number of other products such as electronic equipment housing, carpets, paints/stains, fabrics, and kitchen countertops/appliances. Even the “silly string” that our children plays with contains a brominated flame retardant (hexabromobenzene) to prevent the dried-up string of poly(isobutylmethacrylate) from catching fire.

Due to increasingly stringent environmental regulations, the use of BFRs is being dramatically reduced – especially in Europe. The most widely used alternative is organophosphorus-based (OP) flame-retardants (*e.g.*, **XXXI**), which are much more expensive than organohalogen additives. However, these molecules also contribute to environmental hazards, being found in air samples as far away as Antarctica and in rainwater collected across European countries. Part of the problem stems from the



Figure 5.75. Photograph of damage from a candle-ignited fire that destroyed a campus fraternity house in Amherst, MA. Flame retardants likely prevented the television and surface-treated wood cabinet from igniting. Reproduced from <http://www.buildinggreen.com>.

fact that OP flame retardants are not as active as BFRs, and must be present in much higher concentrations to be effective – often at the expense of altering the physical properties of the polymer.



XXXI

Not unlike plasticizers, the most common method used to impart flame retardancy is by simple mixing of the additives with the polymer during final processing. However, a growing area of development is the design of functionalized monomers that contain flame retardant groups (*e.g.*, halogens, organophosphorus, Figure 5.76).

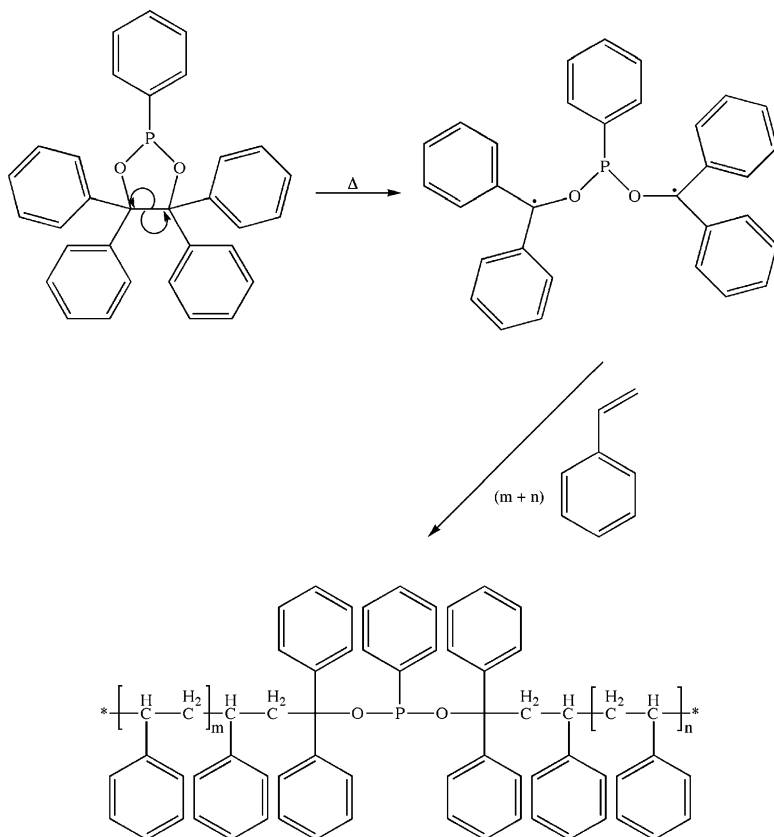
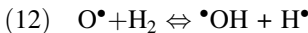
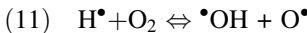


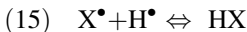
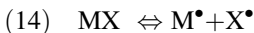
Figure 5.76. Example of the reactive flame retardant approach through incorporation of an organophosphorus unit in the polymer main chain.^[121]

These monomers are known as *reactive flame retardants*, and yield a polymer that has an inherent flame retardant characteristic – much more controllable than additives that are placed randomly within the polymer. However, this approach is not widely used due to its relatively high production cost. Further, the inclusion of functionalized monomeric units within the polymer chains may alter the physical properties of the bulk polymer.

There are two primary reactive modes for flame-retardants: either gas-phase or solid-state. Since a flame consists of a variety of gas-phase radicals and atoms (Eqs. 11 and 12), a gas-phase flame retardant is one that will scavenge the flame-propagating radicals such as $\cdot OH$ and O^\bullet . In particular, if the hydroxyl radical is suppressed, the exothermic formation of CO_2 (Eq. 13) will be prevented thereby reducing the flame temperature.



Halogenated flame-retardants are active in the gas-phase by combining with radicals. The organohalogen compound (MX) first thermally decomposes to form halogen radicals that combine with hydrogen radicals or fuel to form hydrogen halide (HX) (Eqs. 14–15). It should be noted that BFRs all possess aromatic structures since the flame temperature is sufficient to break aromatic C—Br bonds (C—Cl require higher temperatures). By comparison, aliphatic C—Br bonds are broken at temperatures lower than the flame, resulting in pre-decomposition of the organobromine compound and negligent flame retardancy. Often, antimony oxide (Sb_2O_3) is used in combination with BFRs since the side-product of SbBr_3 is sufficiently volatile, and carries a high concentration of bromine into the gas-phase.



The thermally-generated HX species may also behave as flame inhibitors by scavenging hydrogen, hydroxyl and oxygen radicals (Eqs. 16 and 17):



By contrast, solid-state flame-retardants such as organophosphorus agents act by passivating the surface of the polymer toward heat, flame, and oxygen through formation of a carbonaceous coating known as a *char*. When thermally decomposed, some phosphorus compounds generate acids that promote surface crosslinking reactions and resultant char formation. Quite often, phosphorus flame-retardants also have gas-phase reactivity, whereby PO^\bullet radicals help to scavenge flame-propagating species in the flame. Though the mechanism is not currently known, the use of nitrogen compounds (or N-containing polymers such as poly(amide)s) enhances char formation. This is most likely due to a lower number of reactive C/H/O-containing units that volatilize to fuel the flame.

Another interesting area of recent development is the synthesis of dual-action flame-retardants that contain both organophosphorus and organobromine units (Figure 5.77).^[122] Since these agents are active in both gas- and condensed phases, the activity is proposed to be much higher than current additives at much lower concentrations – in accord with environmental regulations. In addition, the synthesis of these agents is relatively inexpensive, which is also a stringent guideline in the development of alternative additives for such a large market sector.

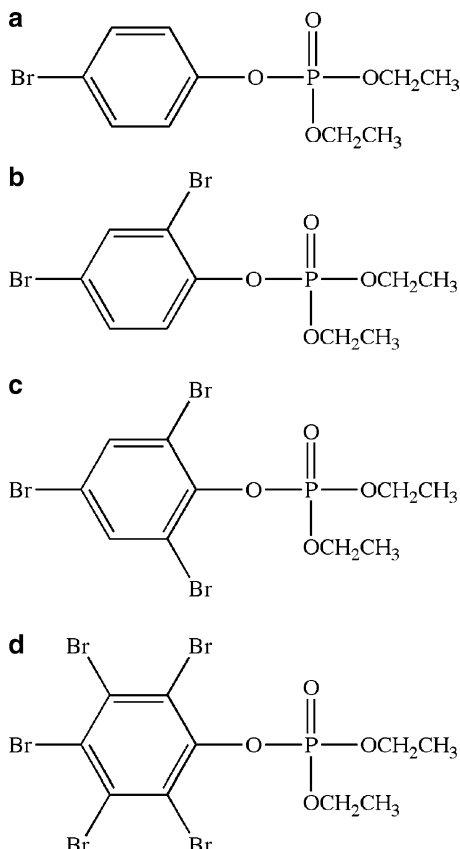


Figure 5.77. Molecular structures of dual-action brominated organophosphorus flame retardants. Shown are (a) (4-bromophenyl)diethylphosphate, (b) (2,4-dibromophenyl)diethylphosphate, (c) (2,4,6-tribromo phenyl)diethylphosphate, and (d) (2,3,4,5,6-pentabromophenyl)diethylphosphate.

IMPORTANT MATERIALS APPLICATIONS IV: SELF-HEALING POLYMERS

Imagine getting into an accident only to have your vehicle revert back to its original shape before your eyes! Though this certainly sounds like something out of a science fiction novel, these materials are fast becoming a reality. The general strategy for this activity is to have the healing agents as a part of the polymer, which become activated upon crack formation. This was first demonstrated with microcapsules of a urea-formaldehyde shell that contained a dicyclopentadiene monomer, suspended within an epoxy polymer matrix. Of course, without a polymerization catalyst, nothing would happen; hence, crystals of Grubbs' catalyst were also dispersed in

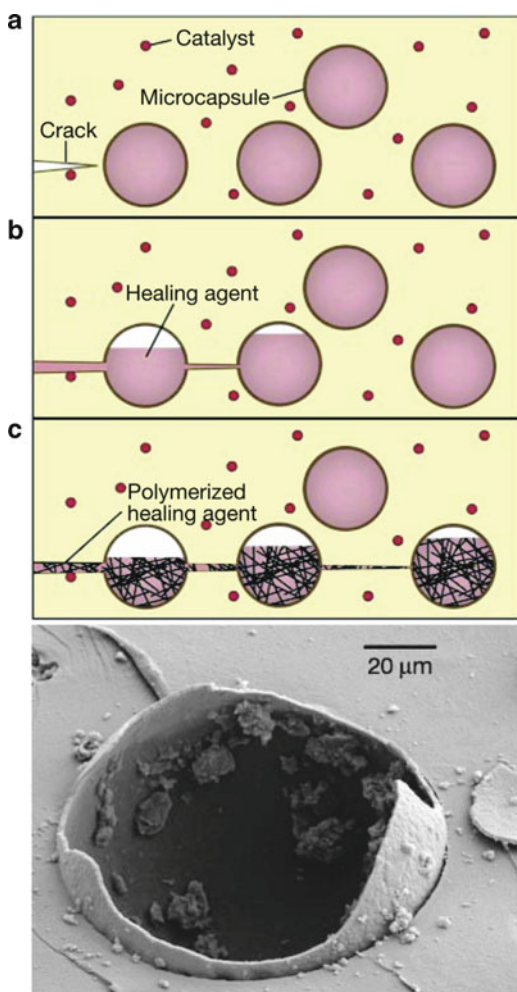


Figure 5.78. Schematic illustrating the mode of action of self-healing polymers through embedded healing-agent microcapsules that are activated by a propagating crack. Also shown is a polymeric microcapsule following rupture. Reproduced with permission from White, S. R.; Sottos, N. R.; Geubelle, P. H.; Moore, J. S.; Kessler, M. R.; Sriram, S. R.; Brown, E. N.; Viswanathan, S. *Nature*, **2001**, 409, 794. Copyright 2001 Macmillan Magazines.

the polymer (Figure 5.78). The encapsulation of the Grubbs' catalyst within a wax microsphere has been reported to improve the dispersity in the epoxy matrix and prevent side reactions between the catalyst and the amine-based epoxy curing agents.^[123]

A technique referred to as *ring-opening metathesis polymerization* (ROMP)^[124] using Grubbs' catalyst (Figure 5.79) was chosen due to rapid polymerization under

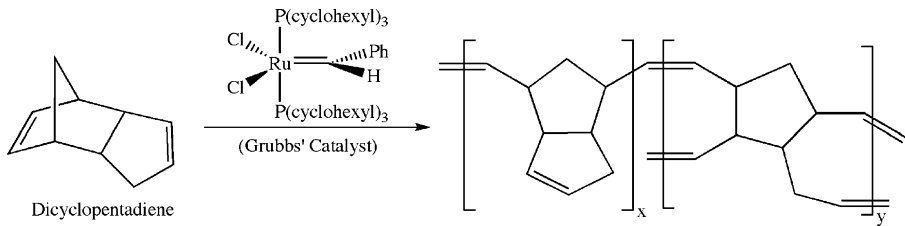


Figure 5.79. Ring-opening metathesis polymerization (ROMP) of dicyclopentadiene catalyzed by Grubbs' catalyst.

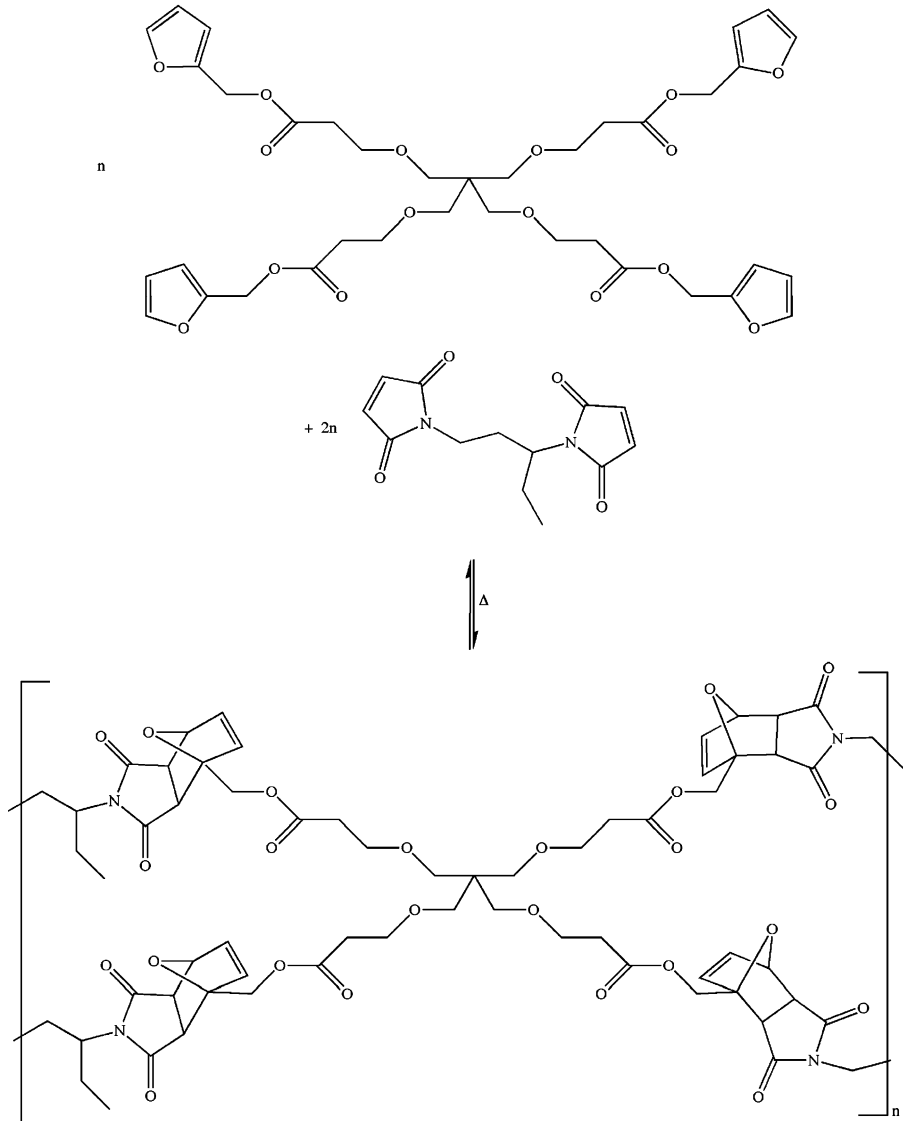


Figure 5.80. Thermally induced self-healing through a Diels-Alder reaction.^[127]

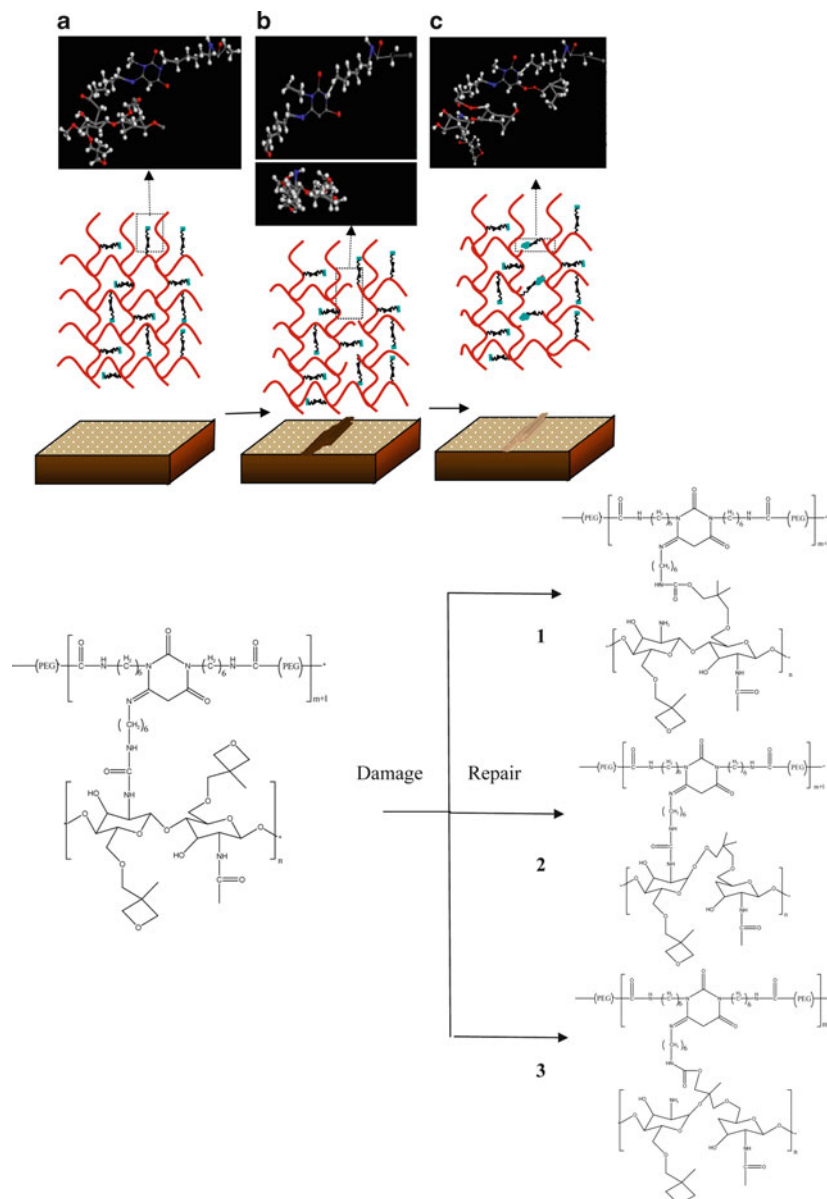


Figure 5.81. Top: proposed mechanism for the repair of oxetane-substitute chitosan polyurethane (OXE-CHI-PUR) networks. The crosslinked network is represented by red thick lines, whereas dangling OXE entities are black thinner lines. As mechanical damage is created (b), OXE rings open up. Upon exposure to UV light, crosslinking reactions of the OXE-CHI entities result in self-healing of the damaged area, (c). Bottom: illustration of chemical reactions leading to UV-induced polymer repair. Shown are (1) breaking of urea linkages as well as the ring opening of OXE and formation of urethane linkages, (2) OXE ring opening and scission of the CHI linkages and the formation of alkyl peroxide linkages, and (3) urea breakage, CHI and OXE ring opening and formation of urethane and linear —C—O—C— crosslinks. Reproduced with permission from *Science* **2009**, 323, 1458. Copyright 2009 American Association for the Advancement of Science.

ambient conditions, in the presence of oxygen and water. Further, these conditions were also suitable for low shrinkage upon polymerization – extremely important for self-healing materials. When a crack ruptured a microcapsule, the monomer became exposed to the catalyst and a strong, highly crosslinked system was formed that bonded together adjacent crack faces within minutes. This same technology is being developed for other materials such as ceramics and glasses for an unlimited number of applications.

An alternative technique that does not involve microcapsules or transition metal catalyst has recently been developed. This method features a reversible polymerization using Diels-Alder reactions of furan and imide-based monomers (Figure 5.80). When the monomers are combined, a highly crosslinked polymer is formed with properties similar to epoxy or polyester composites. However, when a crack propagates through the material, the reactions are reversed generating the monomers in the vicinity of the fracture. If this region is heated and clamped together, the monomers will polymerize to generate a self-healed material. The benefit of this approach is the ability of this material to undergo multiple fracture-healing cycles without a loss of activity. However, the area must be heated in order to undergo regeneration. Further developments in this exciting area are surfacing all the time; for instance, self-healing knee implants using encapsulated poly(methylmethacrylate) and peroxide initiators,^[125] and self-healing polyurethanes upon exposure to UV light (Figure 5.81).^[126]

References and Notes

- ¹ Mulhaupt, R. *Angew. Chem. Int. Ed.* **2004**, *43*, 1054.
- ² *Outlook for Automotive Plastics Coatings: An Analysis of the North American Market* may be accessed online at: [http://www.chemquest.com/PDF-files/Outlook%20for%20Auto%20Plastics%20Coating%20\(SA%20%20MB\)%205-99.pdf](http://www.chemquest.com/PDF-files/Outlook%20for%20Auto%20Plastics%20Coating%20(SA%20%20MB)%205-99.pdf)
- ³ http://www2.dupont.com/Automotive/en_US/applications/caseStudies/case140.html
- ⁴ http://www2.dupont.com/Automotive/en_US/applications/caseStudies/case048.html
- ⁵ http://www2.dupont.com/Automotive/en_US/applications/caseStudies/case043.html
- ⁶ http://www2.dupont.com/Automotive/en_US/applications/caseStudies/case033.html
- ⁷ http://www2.dupont.com/Automotive/en_US/applications/caseStudies/case104.html
- ⁸ <http://www.glasnovations.com/>
- ⁹ http://www2.dupont.com/Automotive/en_US/applications/caseStudies/case046.html
- ¹⁰ Note: melting points refer to the temperature required to separate molecules from one another. By contrast, the glass-transition temperature refers to the temperature required to perturb the bonds of the polymer backbone.
- ¹¹ For a very comprehensive treatise regarding epoxy-based adhesives (structure vs. properties, applications, etc.), see: Petrie, E. M. *Epoxy Adhesive Formulations*, McGraw-Hill: New York, 2006.
- ¹² Note: gel-permeation chromatography (GPC) is a subdivision of size-exclusion chromatography (SEC), in which macromolecular species are separated from one another based on their size. As its name implies, GPC employs a gel (usually cross-linked polystyrene) as the stationary phase, with detection through either light-scattering or refractive index.
- ¹³ For a recent review of living radical polymerization (LRP) involving organotellurium, organostibine, and organobismuthine mediated routes (TERP, SBRP, and BIRP, respectively), see: Yamago, S. *Chem. Rev.* **2009**, *109*, 5051.

- ¹⁴ For a recent review of transition-metal catalyzed living radical polymerization, see: Ouchi, M.; Terashima, T.; Sawamoto, M. *Chem. Rev.* **2009**, *109*, 4963.
- ¹⁵ For a review of bioapplications for RAFT polymerization, see: Boyer, C.; Bulmus, V.; Davis, T. P.; Ladimiral, V.; Liu, J.; Perrier, S. *Chem. Rev.* **2009**, *109*, 5402.
- ¹⁶ (a) Hadjikyriacou, S.; Acar, M.; Faust, R. *Macromolecules* **2004**, *37*, 7543. (b) Aoshima, S.; Segawa, Y.; Okada, Y. *J. Polym. Sci., Part A: Polym. Chem.* **2001**, *39*, 751.
- ¹⁷ For a recent review of cationic living polymerization, see: Aoshima, S.; Kanaoka, S. *Chem. Rev.* **2009**, *109*, 5245.
- ¹⁸ For a review of stereospecific living radical polymerization (LRP), see: Satoh, K.; Kamigaito, M. *Chem. Rev.* **2009**, *109*, 5120.
- ¹⁹ For a thorough classic review of homogeneously-catalyzed polymerization, see: Bikales, N. M. *Adv. in Chemistry* **1968**, *70*, 233.
- ²⁰ *Catalyst Separation, Recovery and Recycling: Chemistry and Process Design*, Cole-Hamilton, D. J.; Tooze, R. P., eds. Springer: New York, 2006.
- ²¹ For a review of homogeneous living Ziegler-Natta polymerization, see: http://images.dcheetahimages.com/www.organicdivision.org/ama/orig/Fellowship/2002_2003_Awardees/Essays/Keaton.pdf
- ²² For example, see: (a) Welborn, H. C. U.S. Patents 5,183,867, 4,808,561. (b) Bergemann, C.; Luft, G. *Chem. Eng. Technol.* **1999**, *21*, 33. (c) Broyer, J.-P.; Malinge, J.; Saudemont, T.; Spitz, R.; Verdel, N. U.S. Patent 6,239,059.
- ²³ (a) Mason, M. R.; Smith, J. M.; Bott, S. G.; Barron, A. R. *J. Am. Chem. Soc.*, **1993**, *115*, 4971. (b) Harlan, C. J.; Mason, M. R.; Barron, A. R. *Organometallics*, **1994**, *13*, 2957. (c) Landry, C. C.; Pappé, N.; Mason, M. R.; Apblett, A. W.; Barron, A. R.; *Inorganic and Organometallic Polymers*, ACS Symposium Series, Volume II, **1998**, *572*, 149. (d) Harlan, C. J.; Bott, S. G.; Barron, A. R. *J. Am. Chem. Soc.*, **1995**, *117*, 6465.
- ²⁴ (a) Watanabe, M.; McMahon, C. N.; Harlan, C. J.; Barron, A. R. *Organometallics*, **2001**, *20*, 460. (b) Koide, Y.; Bott, S. G.; Barron, A. R. *Organometallics*, **1996**, *15*, 2213. (c) Barron, A. R. *Macromol. Symp.*, **1995**, *97*, 15.
- ²⁵ Harlan, C. J.; Bott, S. G.; Barron, A. R. *J. Am. Chem. Soc.*, **1995**, *117*, 6465.
- ²⁶ Note: in general, high molecular weight polymers are typically formed from catalysts derived from early transition metals (Groups 4–6). For late transition metals, the β -hydride elimination mechanism is more preferred, leading to greater numbers of oligomers and dimers.
- ²⁷ For a recent review of hyperbranched polymer architectures, see: Voit, B. I.; Lederer, A. *Chem. Rev.* **2009**, *109*, 5924.
- ²⁸ Flory, P. J. *J. Am. Chem. Soc.*, **1952**, *74*, 2718.
- ²⁹ (a) Buhleier, E.; Wehner, W.; Vögtle, F. *Synthesis*, **1978**, 155. (b) Moors, R.; Vögtle, F. *Chem. Ber.*, **1993**, *126*, 2133. (c) Vögtle, F.; Weber, E. *Angew. Chem. Int. Ed. Engl.*, **1974**, *13*, 814.
- ³⁰ (a) Tomalia, D. A.; Baker, H.; Dewald, J.; Hall, M.; Kallos, G.; Martin, S.; Roeck, J.; Ryder, J.; Smith, P. *Polym. J.*, **1985**, *17*, 117. (b) Tomalia, D. A.; Baker, H.; Dewald, J.; Hall, M.; Kallos, G.; Martin, S.; Roeck, J.; Ryder, J.; Smith, P. *Macromolecules*, **1986**, *19*, 2466. (c) Tomalia, D. A.; Hall, M.; Hedstrand, D. *J. Am. Chem. Soc.*, **1987**, *109*, 1601. (d) Tomalia, D. A.; Berry, V.; Hall, M.; Hedstrand, D. M. *Macromolecules*, **1987**, *20*, 1164. (e) Tomalia, D. A. *et al.* US Patents 4,587,392 (1986); 4,558,120 (1985); 4,568,737 (1986); 4,599,400 (1986); 4,631,337 (1986); 4,507,466 (1985). (f) For an extensive review, see: Tomalia, D. A.; Naylor, A. M.; Goddard III, W. A. *Angew. Chem. Int. Ed. Engl.*, **1990**, *29*, 138.
- ³¹ Note: Robert Denkwalter and coworkers from Allied Corporation were granted the first patent for dendrimers (US Patent 4,410,688 – filed 11 December 1981 and published 18 October 1982: <http://www.hairlosshelp.com/html/researchframepatentus.htm>), which represents the first dendrimer-related publication. However, the term “dendrimer” can be traced back to A. J. Vogel. The generally accepted definition of dendrimers is highly branched and monodisperse polymers (particularly for convergent growth), with a degree of branching of 1.0.
- ³² (a) Newkome, G. R.; Yao, Z.; Baker, Z. R.; Gupta, V. K.; *Org. Chem.*, **1985**, *50*, 2004. (b) Newkome, G. R.; Yao, Z.; Baker, G. R.; Gupta, V. K.; Russo, P. S.; Saunders, M. J. *J. Am. Chem. Soc.*, **1986**, *108*,

849. (c) Newkome, G. R.; Baker, G. R.; Saunders, M. J.; Russo, P. S.; Gupta, V. K.; Yao, Z.; Miller, J. E.; Bouillion, K. *J. Chem. Soc., Chem. Commun.*, **1986**, 752.
- ³³ (a) Hawker, C. J.; Frechet, J. M. *J. Am. Chem. Soc.*, **1990**, *112*, 7638. (b) Hawker, C. J.; Frechet, J. M. *J. Macromolecules*, **1990**, *23*, 4726. (c) Wooley, K. L.; Hawker, C. J.; Frechet, J. M. *J. Am. Chem. Soc.*, **1991**, *113*, 4252.
- ³⁴ For a review of dendrimers and other (biohybrid) polymers that exhibit capsule properties, see: van Dongen, S. F. M.; de Hoog, H. -P. M.; Peters, R. J. R. W.; Nallani, M.; Nolte, R. J. M.; van Hest, J. C. M. *Chem. Rev.* **2009**, *109*, 6212.
- ³⁵ Matthews, B. R.; Holan, G. U.S. Patent 6,190,650.
- ³⁶ Hawker, C. J.; Hedrick, J. L.; Miller, R. D.; Volksen, W. *MRS Bull.* **2000**, *25*, 54.
- ³⁷ Bourne, N.; Stanberry, L. R.; Kern, E. R.; Holan, G.; Matthews, B.; Bernstein, D. I. *Antimicrob. Agents Chemother.* **2000**, *44*, 2471.
- ³⁸ Svenson, S.; Tomalia, D. A. *Adv. Drug Deliv. Reviews* **2005**, *57*, 2106.
- ³⁹ Li, W. -S.; Aida, T. *Chem. Rev.* **2009**, *109*, 6047.
- ⁴⁰ (a) Dvornic, P. R.; de Leuze-Jallouli, A. M.; Owen, M. J.; Perz, S. V. *Macromolecules*, **2000**, *33*, 5366. (b) Dvornic, P. R.; Li, J.; de Leuze-Jallouli, A. M.; Reeves, S. D.; Owen, M. J. *Macromolecules*, **2002**, *35*, 9323.
- ⁴¹ Sarkar, A.; Rousseau, J.; Hartmann-Thompson, C.; Maples, C.; Parker, J.; Joyce, P.; Scheide, J. I.; Dvornic, P. R. "Dendritic Polymer Networks: A New Class of Nano-Domained Environmentally Benign Antifouling Coatings", Chapter X in "New Membranes and Advanced Materials for Waste-Water Treatment", Mueller, A. and Sarkar, A., Eds., ACS Symposium Series 1022, American Chemical Society, Washington, DC, 2010.
- ⁴² De Gennes, P. G.; Hervet, H. *J. Phys. Lett.*, **1983**, *44*, 351–360.
- ⁴³ Kolb, H. C.; Finn, M. B.; Sharpless, K. B. *Angew. Chem. Int. Ed.* **2001**, *40*, 2004.
- ⁴⁴ Kolb, H. C.; Sharpless, K. B. *Drug Discov. Today* **2003**, *8*, 1128.
- ⁴⁵ (a) Iha, R. K.; Wooley, K. L.; Nystrom, A. M.; Burke, D. J.; Kade, M. J.; Hawker, C. J. *Chem. Rev.* **2009**, *109*, 5620. (b) Hawker, C. J.; Wooley, K. L. *Science* **2005**, *309*, 1200. (c) For a review of supramolecular polymerization (non-click routes), see: De Greef, T. F. A.; Smulders, M. M. J.; Wolffs, M.; Schenning, A. P. H. J.; Sijbesma, R. P.; Meijer, E. W. *Chem. Rev.* **2009**, *109*, 5687.
- ⁴⁶ J. A. Opsteen, J. A.; van Hest, J. C. M. *Chem. Commun.* **2005**, *57*.
- ⁴⁷ (a) Swanson, D. R.; Huang, B.; Abdelhady, H. G.; Tomalia, D. A. *New J. Chem.* **2007**, *31*, 1368. (b) Tomalia, D. A. *Dendritic Polymers with Enhanced Amplification and Interior Functionality*, U.S. Patent 2007/0298006 A1, published Dec. 27, 2007.
- ⁴⁸ For a history of liquid crystal displays (LCDs), see: Kawamoto, H. *Proc. IEEE* **2002**, *90*, 460.
- ⁴⁹ A comprehensive discussion regarding siloxane polymerization routes are described within the Ph.D. dissertation (J. Daum, Univ. of Akron, Dec. 2005), found online at: <http://etd.ohiolink.edu/send-pdf.cgi/Daum%20Jeremy%20L.pdf?akron1134097748>
- ⁵⁰ Some useful references related to biodegradable polymers include: (a) Steinbuchel, A. *Biopolymers: General Aspects and Special Applications*. Wiley-VCH: Weinheim (Germany), 2003. (b) Fritz, J.; Link, U.; Braun, R. *Starch* **2001**, *53*, 105. (c) Karlsson, R. R.; Albertsson, A. -C. *Polymer Eng & Sci.* **1998**, *38*, 1251. (d) Kaplan, D. J.; Mayer, J. M.; Ball, D.; McMassie, J.; Allen, A. L.; Stenhouse, P. "Fundamentals of biodegradable polymers" in *Biodegradable polymers and packaging* Ching, C., Kaplan, D. L., Thomas, E. L. eds.; Technomic publication: Basel, 1993. (e) Van de Velde, K.; Kiekens, P. *Polym. Test.* **2002**, *21*, 433. (f) Rouilly, A.; Rigal, L. J. *Macromol. Sci.-Part C. Polymer Reviews* **2002**, *C42*, 441. (g) Chandra, R.; Rustgi, R. *Prog Polym Sci* **1998**, *23*, 1273. (h) Kaplan, D.L. *Biopolymers from renewable resources*, Springer Verlag: Berlin, 1998.
- ⁵¹ For more information regarding bioabsorption/bioresorption, see: Ratner, B. D.; Hoffman, A. S.; Schoen, F. J.; Lemons, J. E. *Biomaterials Science: An Introduction to Materials in Medicine*, 2nd ed., Academic Press: New York, 2004.
- ⁵² Another common classification rationale for these polymers is by application – for either biomedical or ecological use. For instance, see: Ikada, Y.; Tsuji, H. *Macromol. Rapid. Commun.* **2000**, *21*, 117.

- ⁵³ For a review of biodegradable polymer syntheses using a bismuth catalyst, see: Kricheldorf, H. R. *Chem. Rev.* **2009**, *109*, 5579.
- ⁵⁴ The most common biodegradable polymers used for medical applications (sutures, screws, pins/rods, tacks, plates, mesh, guided tissue, etc.) are poly(*d,l*-lactide) and poly(*l*-lactide), co-polymerized with polyglycolide or poly(*l*-/*d,l*-lactide). Other important varieties are poly(dioxanone)-based.
- ⁵⁵ It should be noted that tin halides may be used to catalyze the ring-opening polymerization of lactide; however, the halide is converted to an alkoxide, which is the active catalytic species. For instance, see: Kricheldorf, H. R.; Sumbel, M. *Eur. Polym. J.* **1989**, *25*, 585.
- ⁵⁶ Mehta, R.; Kumar, V.; Bhunia, H.; Upadhyay, S. N. *Polym. Rev.* **2005**, *45*, 325, and references therein.
- ⁵⁷ Stolt, M.; Sodergard, A. *Macromolecules* **1999**, *32*, 6412.
- ⁵⁸ <https://www.almaden.ibm.com/st/chemistry/ps/catalysts/RingOpening/>
- ⁵⁹ Kobayashi, S.; Makino, A. *Chem. Rev.* **2009**, *109*, 5288.
- ⁶⁰ Note: the mechanical properties, crystallinity, molecular weight, and T_g/m.p. of the biodegradable polymer depends on various factors such as the monomer/initiator structure, synthetic and post-processing conditions, and the presence of additives. In particular, excessively high processing temperatures will shift the equilibrium toward monomer formation, which will affect the mechanical and degradation properties of the polymer.
- ⁶¹ (a) Freberg, S.; Zhu, X. X. *Int. J. Pharmaceutics* **2004**, *282*, 1. (b) Miyajima, M.; Koshika, A.; Okada, J.; Ikeda, M.; Nishimura, K. *J. Controll. Rel.* **1997**, *49*, 207. (c) <http://chemistry.creighton.edu/Opportunities/Baumann/MuszynskiBeth.pdf>
- ⁶² A nice chronology related to breast implants may be found online at: <http://www.pbs.org/wgbh/pages/frontline/implants/cron.html>
- ⁶³ Fortunately, Dow Corning was able to successfully emerge from the breast-implant controversy and now remains the global leader in silicon/silicone-based commercial products, as well as one of the world's leaders in the production of ultra-high purity Si, fabricated by Hemlock Semiconductor – a subsidiary of Dow Corning (<http://www.hscpoly.com>).
- ⁶⁴ For a review of implant materials and their carcinogenicity, see: <http://monographs.iarc.fr/ENG/Monographs/vol74/mono74-10.pdf>
- ⁶⁵ Arteriosclerosis, Thrombosis, and Vascular Biology, Vol. 22, No. 6, 2002, p. 884.
- ⁶⁶ Arterial stents may be self-expanding (spring-type), balloon-type, or thermal-expanding. Thermal-expanding varieties feature shape-memory alloys that expand in response to the application of heat.
- ⁶⁷ Lowe, H. C.; Oesterle, S. N.; Khachigian, L. M. *J. Am. Coll. Cardiol.* **2002**, *39*, 183.
- ⁶⁸ (a) Williams, M. S.; DeSimone, J. M. U.S. Patent application 2006/0121087 A1. (b) Williams, M. S.; Glenn, R. A.; Smith, J. A.; Holbrook, K. D.; DeSimone, J. M. U.S. Patent 6,887,266. (c) DeSimone, J. M.; Williams, M. S. U.S. Patent 6,932,930.
- ⁶⁹ (a) Serruys, P. W. et al. *Lancet*, **2009**, *373*, 897. (b) Ormiston, J. A. et al. *Lancet*, **2008**, *371*, 873.
- ⁷⁰ Note: in 1827, astronomer Sir John Herschel first reported the concept of making a mold of the wearer's eyes so lenses could be fabricated to perfectly conform to the eyes' surfaces. This idea was realized in 1887 by German glassblower F. A. Muller, who fabricated the first set of glass contact lenses, which were fit to adjust for nearsightedness/farsightedness by Fick and Kalt shortly thereafter. A nice summary of the history of contact lenses may be found online at: (a) <http://www.eyetopics.com/articles/18/1/The-History-of-Contact-Lenses.html> (b) http://www.revoptom.com/contactlens/pdf/clp_full.pdf
- ⁷¹ Salvatori, P. L. *The story of contact lenses*, Obrig Laboratories: New York, 1960.
- ⁷² *Clinical Anesthesia*. Barash, P. G.; Cullen, B. F.; Stoelting, R. K.; Cahalan, M.; Stock, M. C. eds, 6th ed., Lippincott Williams and Wilkins: Philadelphia, PA, 2009.
- ⁷³ Note: if the polymer contains charged monomeric units, as is common for hydrogel-based contact lenses, proteins and other charged biomolecules will be attracted resulting in biofilm formation. This will result in loss of ocular properties, as well as influence the diffusivity of oxygen through the lens, requiring immediate replacement to prevent severe irritation and infection.

- ⁷⁴ Note: PMMA is sold under a variety of trade names such as Plexiglass, Lucite, Polycast, Oroglass, Acrylite, R-Cast, Vitroflex, and many others. PMMA may be used as an alternative to glass and polycarbonate; however, it is quite brittle and has a melting point of *ca.* 130–140°C.
- ⁷⁵ It should be noted that the T_g may be varied by co-polymerization with other monomers or through simple intermixing of polymers; for example, the T_g of semi-interpenetrating networks of HEMA and polyurethane may be varied from -140 to 180°C: http://www.pu2pu.com/KNOWLEDGE/Paper/Paper_details.aspx?ID=4489
- ⁷⁶ A nice article that describes the importance of oxygen diffusion for silicone-based soft contact lenses may be found online: <http://www.clspectrum.com/article.aspx?article=12953>
- ⁷⁷ Note: if the lens contains a hydrophobic surface, it will disrupt the tear flow that results in the deposition of an albumin film on the lens. Not only will this reduce the effectiveness of the lens to correct optical aberrations, but will also cause infection/irritation. For more details regarding the lens surface and eye complications, see: Rao, J. B., Saini, J. S. "Complications of Contact Lenses" in *Contact Lenses*. Aquavella, J. V., Rao, G. N., eds. Lippincott Williams and Wilkins: Philadelphia, PA, 1987.
- ⁷⁸ Kunzler, J.; Ozark, R. *J. Appl. Polym. Sci.* **1997**, *65*, 1081.
- ⁷⁹ There is an interesting recent report that delineates the 3-D structure and interactions of calcite crystallized within an agarose hydrogel, using high-resolution electron microscopy/tomography: Li, H.; Xin, H. L.; Muller, D. A.; Estroff, L. A. *Science* **2009**, *326*, 1244.
- ⁸⁰ PureVision™ is a copolymer of tris-(trimethylsiloxy)-silyl-propylvinyl carbamate (TRIS-VC), N-vinylpyrrolidone, a vinyl carbonate functional polydimethylsiloxane (PDMS) macromer, and a vinyl carbamate derivative of alanine. For more information, see: Nicolson, P. C.; Vogt, J. *Biomaterials* **2001**, *22*, 3273.
- ⁸¹ (a) Toit, R.; Stern, B.; Sweeney, D. *Int. Cont. Lens Clinic* **2000**, *27*, 191. (b) http://www.siliconehydrogels.org/editorials/08_may.asp (c) Chen, C.; Ye, H.; Manesis, N. U.S. patent 7,572,841.
- ⁸² Benjamin, W. J.; Karkkainen, T. R. "Hydrogel Hypoxia: Where We've Been, Where We're Going" *Contact Lens Spectrum*, **1996**, September issue.
- ⁸³ <http://www.clspectrum.com/article.aspx?article=13020>
- ⁸⁴ For a summary of recent strategies for the design and development of polymeric materials for drug- and gene-delivery applications, see: *Adv. Drug Deliv. Rev.* **2008**, *60*(9), 955–1094 – thematic issue devoted to this topic. The thematic issue *Adv. Drug Deliv. Rev.* **2005**, *57*(15), 2101–2286 is devoted to dendrimers as drug-delivery agents. Lastly, the thematic issue *Adv. Drug Deliv. Rev.* **2001**, *53*(1), 1–131 also deals with polymeric materials being used for drug-delivery applications.
- ⁸⁵ The therapeutic window is defined as the drug concentration lying between minimum-effective and toxic levels, and is different for each person based on their metabolic and circulatory systems.
- ⁸⁶ Saltzman, W. M.; Olbricht, W. L. *Nat. Rev. Drug Discov.* **2002**, *1*, 177.
- ⁸⁷ Randall, C. L.; Leong, T. G.; Bassik, N.; Gracias, D. H. *Adv. Drug Delivery Rev.* **2007**, *59*, 1547.
- ⁸⁸ (a) Lehr, H. A.; Brunner, J.; Rangoonwala, R.; Kirkpatrick, C. J. *Am. J. Respir. Crit. Care Med.* **2002**, *165*, 514. (b) Martin, F. J.; Melnik, K.; West, T.; Shapiro, J.; Cohen, M.; Boiarski, A. A.; Ferrari, M. *Drugs R&D* **2005**, *6*, 71.
- ⁸⁹ Gobin, A. M.; Lee, M. H.; Halas, N. J.; James, W. D.; Drezek, R. A.; West, J. L. *Nano Lett.* **2007**, *7*, 1929.
- ⁹⁰ <http://www.starpharma.com/vivagel.asp>
- ⁹¹ Padilla De Jesus, O. L.; Ihre, H. R.; Gagne, L.; Frechet, J. M. J.; Szoka, F. C. *Bioconj. Chem.* **2002**, *13*, 453.
- ⁹² Goodwin, A. P.; Lam, S. S.; Frechet, J. M. J. *J. Am. Chem. Soc.* **2007**, *129*, 6994.
- ⁹³ (a) Williams, S. S.; Hampton, M. J.; Gowrishankar, V.; Ding, I. K.; Templeton, J. L.; Samulski, E. T.; DeSimone, J. M.; McGehee, M. D. *Chem. Mater.* **2008**, *20*, 5229. (b) Rolland, J. P.; Van Dam, R. M.; Schorzman, D. A.; Quake, S. R.; DeSimone, J. M. *J. Am. Chem. Soc.* **2004**, *126*, 2322. (c) Rolland, J. P.; Hagberg, E. C.; Denison, G. M.; Carter, K. R.; De Simone, J. M. *Angew. Chem. Int. Ed. Eng.* **2004**, *43*, 5796.
- ⁹⁴ (a) In, H. J.; Arora, W.; Buchner, T.; Jurga, S. M.; Smith, H. I.; G. Barbastathis, G. *4th IEEE Conf. on Nanotech.* **2004**, 358. (b) Kubota, K.; Fleischmann, T.; Saravanan, S.; Vaccaro, P. O.; Aida, T. *Jpn. J.*

- Appl. Phys.* **2003**, *42*, 4079. (c) Guan, J.; He, H.; Hansford, D. J.; Lee, L. J. *J. Phys. Chem., B* **2005**, *109*, 23134.
- ⁹⁵ For a recent review of conjugated polymers for organic solar cell applications, see: Cheng, Y. -J.; Yang, S. -H.; Hsu, C. -S. *Chem. Rev.* **2009**, *109*, 5868.
- ⁹⁶ For reviews of synthetic routes for conjugated polymers, see: (a) Yokozawa, T.; Yokoyama, A. *Chem. Rev.* **2009**, *109*, 5595 (chain-growth condensation polymerization) (b) Liu, J.; Lam, J. W. Y.; Tang, B. Z. *Chem. Rev.* **2009**, *109*, 5799 (synthesis, structure, and applications of acetylenic polymers).
- ⁹⁷ Interesting trivia: Rudolph Peierls was one of Heisenberg's doctoral students while he was at the Universitat Leipzig; other notable students mentored by Heisenberg included Bloch, Mulliken, Slater, Teller, Wentzel and Zener!
- ⁹⁸ Note: we already saw this in Chapter 2 (Figure 2.74) wherein the periodicity of the array gives rise to energy gaps at specific values of \mathbf{k} (*i.e.*, $\mathbf{k} = \pi/a$, where a = lattice spacing). If each of the ions in the 1-D array contributes one electron, the band will be half-filled in the ground state. If the ions "dimerize", the periodicity of the array will effectively double giving rise to new band gaps at multiples of $\mathbf{k} = \pi/2a$. Since these bands may now house electrons at a lower energy level than the original lattice, a more energetically-favorable structure will be generated.
- ⁹⁹ A bipolaron is also sometimes referred to as a *bisoliton*. For instance, see: <http://dissertations.ub.rug.nl/FILES/faculties/science/2006/m.h.van.der.veen/c1.pdf>
- ¹⁰⁰ Chen, Y. -C. *Polym. Bull.* **1990**, *23*, 411.
- ¹⁰¹ Park, S.; Jayaraman, S. *MRS Bull.* **2003**, *28*, 585.
- ¹⁰² Note: in 2,000 B.C., magnetic stones are mentioned in the oldest medical textbook ever discovered – the Yellow Emperor's Classic of Internal Medicine. Over 2,500 years ago, a shepherd named Magnes found mineral stones sticking to the metal nails in his sandals; he called the mineral *magnetite*.
- ¹⁰³ Wickman, H. H.; Trozzolo, A. M.; Williams, H. J.; Hull, G. W.; Merritt, F. R. *Phys. Rev.* **1967**, *155*, 563. For a historical review of molecular magnetism, see: Miller, J. S. *Adv. Mater.* **2002**, *14*, 1105.
- ¹⁰⁴ (a) Miller, J. S.; Calabrese, J. C.; Epstein, A. J.; Bigelow, R. W.; Zhang, J. H.; Reiff, W. M. *J. Chem. Soc., Chem. Commun.*, **1986**, 1026. (b) Miller, J. S.; Epstein, A. J. *Angew. Chem. Int. Ed. Eng.*, **1994**, *33*, 385. (c) Miller, J. S.; Epstein, A. J. *Chem. Eng. News*, **1995**, *73*(40), 30. (d) Manriquez, J. M.; Yee, G. T.; McLean, R. S.; Epstein, A. J.; Miller, J. S. *Science*, **1991**, *252*, 1415. (e) Miller, J. S.; Epstein, A. J. *J. Chem. Soc., Chem. Commun.*, **1998**, 1319. (f) Pokhodnya, K. I.; Epstein, A. J.; Miller, J. S. *Adv. Mater.*, **2000**, *12*, 410. (g) Hatlevik, O.; Buschmann, W. E.; Zhang, J.; Manson, J. L.; Miller, J. S. *Adv. Mater.*, **1999**, *11*, 914. (h) Miller, J. S. *Inorg. Chem.*, **2000**, *39*, 4392.
- ¹⁰⁵ Beltran, L. M. C.; Long, J. R. *Acc. Chem. Res.*, **2005**, *38*, 325.
- ¹⁰⁶ Vickers, E. B.; Selby, T. D.; Thorum, M. S.; Taliaferro, M. L.; Miller, J. S. *Inorg. Chem.*, **2004**, *43*, 6414.
- ¹⁰⁷ For a recent review of molecular magnetism, see: Gatteschi, D.; Bogani, L.; Cornia, A.; Mannini, M.; Sorace, L.; Sessoli, R. *Solid State Sci.* **2008**, *10*, 1701.
- ¹⁰⁸ For a good review of back-bonding, crystal/ligand field theory and the spectrochemical series, see: Shriner, D. W.; Atkins, P. *Inorganic Chemistry*, 5th ed., W. H. Freeman: New York, 2009.
- ¹⁰⁹ (a) Verdaguer, M.; Bluezen, A.; Marvaud, V.; Waissermann, J.; Seuleimann, M.; Desplanches, C.; Scuiller, A.; Train, C.; Garde, R.; Gelly, G.; Lomenech, C.; Rosenman, I.; Veillet, P.; Cartier, C.; Sato, O.; Einaga, Y.; Iyoda, T.; Fujishima, A.; Hashimoto, K. *J. Electrochem. Soc.*, **1997**, *144*, L11. (b) Einaga, Y.; Sato, O.; Ohkoshi, S.; Fujishima, A.; Hashimoto, K. *Chem. Lett.*, **1998**, 585.
- ¹¹⁰ For a very nice review on 3D cyanide-based magnets see: Miller, J. S. *MRS Bull.*, **2000**, *11*, 60.
- ¹¹¹ Examples of antioxidant additives used in polymer formulations may be found online: http://www.albemarle.com/Products_and_services/Polymer_additives/Antioxidants/Polymer/
- ¹¹² Note: heat stabilizers are used in the processing of rigid (pipe, window profiles, siding, fencing) and some flexible (packaging) PVC applications, preventing the thermal degradation of PVC resins during elevated temperature exposure. In addition, heat stabilizers extend the lifetime of finished products.

- ¹¹³ A curing agent for polyurethanes and epoxies, as well as a chain extender for polyurethane and polyurea: http://www.albemarle.com/TDS/Curatives/SC7003L_ETHACURE_100.pdf
- ¹¹⁴ An amine cure accelerator that is used to promote free-radical formation in addition polymerizations such as unsaturated polyester resin, vinyl ester, and acrylate systems: http://www.albemarle.com/TDS/Curatives/SC0006F_FIRSTCURE_MHPT.pdf
- ¹¹⁵ Used to increase the shelf life of olefinic resins, used in coatings, adhesives, photoresists, printing inks, and unsaturated polyester resins, vinyl monomers, and acrylated oligomers: http://www.albemarle.com/TDS/Curatives/SC0002F_FIRSTCURE_ST-2.pdf
- ¹¹⁶ A Plasticizer Information Center with information about various types of plasticizers may be found online at: <http://www.plasticisers.org/index.asp?page=2>
- ¹¹⁷ Anti-plasticizers are added to rigidify polymers, and may be bulky molecules that disperse in a polymer, or “sticky” molecules that induce attractive interactions between the additive and polymer. For instance, see: Dasmahapatra, A. K.; Nanavati, H.; Kumaraswamy, G. *J. Chem. Phys.* **2009**, *131*, 074905, and references therein.
- ¹¹⁸ Note: phthalates are used where good resistance to water and oils is required. For example, applications such as garden hoses, shoes, toys, food wraps, flooring materials, notebook covers, vinyl tiles, traffic cones, plastic foams, tool handles, building materials, etc.
- ¹¹⁹ Note: trimellitates have a low volatility, and are used in automobile interiors where resistance to high temperature is required.
- ¹²⁰ Note: used for low-temperature applications or those requiring resistance to UV light.
- ¹²¹ Howell, B. A. Presented in part at the 15th International Conference on Advances in Additives and Modifiers for Polymers and Blends, Las Vegas, NV, February, 2006.
- ¹²² For instance, see: (a) Howell, B. A.; Cho, Y. -J. “Brominated Aryl Phospholane Flame Retardants” in *ACS Symp. Series V – Fire and Polymers*, **2009**, 249. (b) Howell, B. A.; Wu, H. *J. Therm. Anal. Calorim.* **2006**, *83*, 79.
- ¹²³ Rule, J. D.; Brown, E. N.; Sottos, N. R.; White, S. R.; Moore, J. S. *Adv. Mater.*, **2005**, *17*, 205.
- ¹²⁴ *Controlled and Living Polymerizations: From Mechanisms to Applications*. Matyjaszewski, K.; Muller, A. H. E., eds., Wiley: New York, 2009.
- ¹²⁵ Hasenwinkel, J. M.; Lautenschlager, E. P.; Wixson, R. L.; Gilbert, J. L. *J. Biomed. Mater. Res.*, **2002**, *59*, 411.
- ¹²⁶ Ghosh, B.; Urban, M. W. *Science* **2009**, *323*, 1458.
- ¹²⁷ Chen, X.; Dam, M. A.; Ono, K.; Mal, A.; Shen, H.; Nutt, S. R.; Sheran, K.; Wudl, F. *Science*, **2002**, *295*, 1698.

Topics for Further Discussion

1. Explain the differences between a thermoplastic and thermoset.
2. What is meant by “tacticity,” and how does this influence overall polymer properties?
3. Explain the effects of the initiator concentration on the degree of polymerization (free-radical route) of styrene.
4. Why was the reported discovery of dendrimers fought with so much controversy (*i.e.*, what about the structure/route did the leading scientists not believe)?
5. What is the chemical origin of the organic film that forms on the windshield of a new car? How about the “new car smell”?
6. What is meant by the terms ‘inifer’ and ‘iniferter’ and what are some recent candidates that have been synthesized in the laboratory?
7. What is the purpose of MAO in olefin polymerizations?
8. Explain why polymers crystallize in a chain array rather than the thermodynamically favored extended chain form.
9. Earlier in this Chapter, we discussed the influence of polymer structure on the efficacy for use as contact lens applications, at the molecular level. At a more bulk level, describe the industrial techniques used to inexpensively and repeatably fabricate ‘hard’ and ‘soft’ contact lenses.

10. Examine the polymeric materials in your immediate vicinity and determine whether they were formed via condensation or addition polymerization routes.
11. What are the structures of conductive polymers, and what is the mechanism for electronic transport in the solid-state?
12. Illustrate the mechanisms for polaron, bipolaron, and soliton formation for PANI, showing the mechanism for intersoliton hopping. Why is the conductivity lower for doped PANI relative to PA?
13. Your supervisor has asked you to make a polymeric material with the following properties – what are some possible backbone and side-group structures that you would try to incorporate in the polymer?
 - (a) High-melting point, flexible
 - (b) Low-melting point, conductive
 - (c) Able to withstand strong acids or bases
 - (d) Flexible at low temperatures and becoming more rigid at elevated temperatures
 - (e) Properties of (b), and biodegradable at ambient temperatures

Further Reading

1. Wallace, G. G.; Spinks, G. M.; Kane-Maguire, L. A. P.; Teasdale, P. R. *Conductive Electroactive Polymers: Intelligent Polymer Systems*, 3rd ed., CRC Press: New York, 2008.
2. Dvornic, P. R., Owen, M. J., eds., *Silicon-Containing Dendritic Polymers*, Springer: New York, 2009.
3. Ratner, B. D.; Hoffman, A. S.; Schoen, F. J.; Lemons, J. E. *Biomaterials Science: An Introduction to Materials in Medicine*, 2nd ed., Academic Press: New York, 2004.
4. *Controlled and Living Polymerizations: From Mechanisms to Applications*. Matyjaszewski, K.; Muller, A. H. E., eds., Wiley: New York, 2009.
5. Al-Malaika, S.; Golovoy, A.; Wilkie, C. A. ed. *Chemistry and Technology of Polymer Additives*, Blackwell Science: Malden, MA, 1999.
6. Allcock, H. R.; Lampe, F. W.; Mark, J. E. *Contemporary Polymer Chemistry*, 3rd ed., Prentice-Hall: New Jersey, 2003.
7. Painter, P. C.; Coleman, M. M. *Fundamentals of Polymer Science*, 2nd ed., CRC: New York, 1997.
8. Flory, P. J. *Principles of Polymer Chemistry*, Cornell University Press: Ithaca, NY, 1953.
9. Odian, G. *Principles of Polymerization*, 3rd ed., Wiley: New York, 1991.
10. Young, R. J.; Lovell, P. A. *Introduction to Polymers*, 2nd ed., CRC: New York, 2000.
11. Stevens, M. P. *Polymer Chemistry: An Introduction*, 3rd ed., Oxford University Press: Oxford, 1998.
12. Fortin, J. B.; Lu, T. -M. *Chemical Vapor Deposition Polymerization: The Growth and Properties of Parylene Thin Films*, Springer: Berlin Heidelberg New York, 2003.
13. Hsieh, H.; Quirk, R. P. *Anionic Polymerization*, CRC: New York, 1996.